#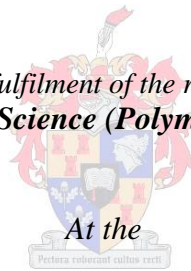 The effect of organic peroxides on the molecular composition of heterophasic ethylene-propylene impact copolymers (HECOs)

**by**

**Sifiso Magagula**

*Thesis presented in partial fulfilment of the requirements for the degree of*
***Master of Science (Polymer Science)***

*At the*

*University of Stellenbosch*

Supervisor: Prof. A.J. van Reenen                    December 2015

# Declaration

By submitting this thesis electronically, I declare that the entirety of the work contained therein is my own, original work, that I am the sole author thereof (save to the extent explicitly otherwise stated), that reproduction and publication thereof by Stellenbosch University will not infringe any third party rights and that I have not previously in its entirety or in part submitted it for obtaining any qualification.

Sifiso Magagula                                                December 2015

# Abstract

Heterophasic ethylene-propylene copolymers, also known as impact polypropylene (PP) copolymers (IPCs) or heterophasic copolymers (HECOs), are a unique group of polyolefins produced through the copolymerisation of ethylene and propylene, with the aim of improving the impact properties of the PP homopolymer at low temperatures. Therefore, this polymer comprises of a PP homopolymer matrix with a dispersed rubbery copolymer phase. Due to their unique properties, HECO polymers have become commercially important materials, with a wide range of applications. Therefore a fundamental understanding of the processes and chemistry that affects their final macroscopic properties needs to be expanded.

The main focus of this investigation was to understand why specific organic peroxides influence or interact differently with the various phases of HECO polymers, in order to utilize their properties to obtain HECO polymers with optimal and desired properties. Two HECO polymers with different ethylene contents were fractionated into three fractions (30, 100 and 130 °C), using preparative temperature rising elution fractionation (P-TREF). Each individual TREF fraction was degraded with two different types of organic peroxides, and then characterised using four different analytical tools. The changes in the molecular structures of the different fractions were investigated by Fourier transform infrared spectroscopy (FTIR) and differential scanning calorimetry (DSC). The changes in comonomer sequence distributions were investigated by carbon 13 nuclear magnetic resonance spectroscopy ($^{13}$C-NMR). Moreover, the degradation of the different fractions was investigated by high temperature size exclusion chromatography (HT-SEC).

The investigation showed that the HECO polymers with different ethylene contents were uniquely altered. It was evident that the ethylene content influenced the degradation behaviour of the HECO polymers. The ability of the peroxide to affect certain regions of the HECO polymer more than others is highly dependent upon its miscibility with certain regions of the HECO polymers. The "visbreaking" efficiency of a specific organic peroxide appears to be primarily dependent on the number of "peroxy" groups it contains in its molecular structure.

# Opsomming

Heterofase etileen-propileen ko-polimere, ook bekend as impak PP ko-polimere (IPC$_S$) of heterofase ko-polimere (HECO), is 'n unieke groep poliolefiene geproduseer deur die ko-polimerisasie van etileen en propileen, met die doel op die verbetering in die impak eienskappe van die PP homopolimeer by lae temperatur. Hierdie polimeer bestaan dus uit 'n PP homopolimeer matriks met 'n verspreide rubberagtige ko-polimeer fase. As gevolg van hul unieke eienskappe, is HECO polimere van kommersiële belang, met 'n wye verskeidenheid van toepassings. 'n Fundamentele begrip van die prosesse en chemie wat die finale makroskopiese eienskappe beïnvloed moet dus uitgebrei word.

Die hooffokus van hierdie ondersoek was om te verstaan waarom spesifieke organiese peroksiede verskillende invloede en interaksies met die verskillende fases van HECO polimere het, om sodoende van hul eienskappe gebruik te maak om HECO polimere te verkry met optimale en gewenste eienskappe. Twee HECO polimere met verskillende etileen inhoud was gefraksioneer in drie fraksies (30, 100 en 130 °C), met behulp van preparatiewe temperatuur styging eluering fraksionering (P-TREF). Elke individuele TREF fraksie was gedegradeer met twee verskillende tipes organiese peroksiede en daarna gekarakteriseer deur vier verskillende analitiese metodes. Die veranderinge in molekulêre strukture van die verskillende fraksies was geondersoek met behulp van Fourier transform infrarooi spektroskopie (FTIR) en differensiële skandering kalorimetrie (DSC). Die veranderinge in ko-monomeer volgorde distribusie was bestudeer deur middel van kern magnetiese resonans spektroskopie (KMR). Verder was die degradasie van die verskillende fraksies met behulp van hoë temperatuur grootte uitsluitingschromatografie (HT-SEC) bestudeer.

Die ondersoek het getoon dat die HECO polimere met verskillende etileen inhoud uniek gedegradeer was. Dus is dit duidelik genoeg dat die etileen inhoud die degradasie gedrag van die HECO polimere beïnvloed het. Die vermoë van die peroksied om sekere areas van die HECO polimeer meer as ander te beïnvloed is hoogs afhanklik van die mengbaarheid met sekere areas van die HECO polimere. Die "visbreking" doeltreffendheid van 'n spesifieke organiese peroksiede is meestal afhanklik van die aantal "peroksie" groepe in die molekulêre struktuur.

**Dedicated to**:

My Mother,

For her love and endless support and for giving the opportunities she did not have

# Acknowledgements

First and foremost, I would like to thank God for His protection, His grace and His guidance throughout the entire study.

The author would also like to sincere thank the following people:

A special thanks goes to my supervisor **Prof. Albert van Reenen** for his unwavering support, his encouragement, his mentorship and for giving me the opportunity to further my studies.

To Dr. Maggie Brand, Mr. Anthony Ndiripo and Mr. Mohau Phiri for their unwavering help with HT-SEC analyses.

To the olefins group for making the office a home away from home.

To Dr. Divann Robertson for his unwavering help with origion and DSC analyses, his insightful advices and for being a good friend throughout the study.

To Dr. D.J. Brand and Elsa Malherbe for all the NMR analyses.

To the technical staff at the Polymer science building: Mr. Deon Koen, Mr. Calvin Maart and Mr. Jim Motshweni.

To SASOL and NRF for their financial support.

Last but not least, to my sweet and loving mother for her love and encouragement throughout this study.

# Table of Contents

# List of Figures

# List of Tables

# List of Abbreviations

| | |
|---|---|
| $\Delta H_f$ | Enthalpy of fusion |
| $\Delta T$ | Difference in temperature |
| $^{13}C$ NMR | Carbon 13 nuclear magnetic resonance |
| AFM | Atomic force microscopy |
| ASPP | Atmosphere-switching polymerisation process |
| ASTM | American standard test method |
| ATR | Attenuated total reflectance |
| A-TREF | Analytical temperature rising elution fractionation |
| BHT | Beta-hydroxyltoluene |
| CCD | Chemical composition distribution |
| CRPP | Controlled rheology polypropylene |
| Đ | Polydispersity index |
| DSC | Differential scanning calorimetry |
| E*b*P or EPBC | Ethylene-propylene block copolymers |
| EPR | Ethylene-propylene rubber |
| EPS | Ethylene-propylene segmented copolymers |
| FTIR | Fourier transform infrared |
| GPC | Gel permeation chromatography |
| HECO | Heterophasic copolymers |
| HT-HPLC | High temperature high performance liquid chromatography |
| HT-SEC | High temperature size exclusion chromatography |
| iPP | Isotactic polypropylene |
| IR | Infra-red |
| LDPE | Low density polyethylene |

| | |
|---|---|
| LLDPE | Linear low density polyethylene |
| MFI | Melt flow index |
| MFR | Melt flow rate |
| $M_n$ | Number average molecular weight |
| MSSP | Multi-stage sequential polymerisation |
| $M_w$ | Weight average molecular weight |
| MWD | Molecular weight distribution |
| MZCR | Multizone circulating reactor |
| PE | Polyethylene |
| PP | Polypropylene |
| P-TREF | Preparative temperature rising elution fractionation |
| SEM | Scanning electron microscopy |
| T101 | Trigonox$^{®}$101 |
| T301 | Trigonox$^{®}$301 |
| $T_c$ | Crystallization temperature |
| TCB | Trichlorobenzene |
| TCE | Tetrachloroethylene |
| TEA | Triethylaluminium |
| $T_m$ | Melting temperature |
| TSP | Two-stage sequential polymerisation |
| $W_i\%$ | Weight fraction percentage |
| $X_c$ | crystallinity |
| XRD | X-ray diffraction |

# Chapter 1
# Introduction

*This chapter will give a brief introduction to heterophasic ethylene-propylene copolymers. The chapter will also present the problem statement, the main objectives and the dissertation layout of this study.*

## 1.1.    Introduction

Polyolefins constitute more than 50 % of the synthetic polymers produced annually [1] and the consumption of polypropylene has proved to be one of the fastest growing in the world. The production of propylene has been estimated to increase at an average annual growth rate of 7.0 % per annum since 1990. In 2010, the world consumption of polypropylene grew to approximately 48.5 million metric tons. [1] In 2016 the world consumption of polypropylene is predicted to increase to approximately 80 million metric tons. [2] Polypropylene has good properties that are desirable to most manufacturers. Some of its desirable properties include chemical resistance; ease of recycling and low cost of production which has led to its widespread use as a commodity in the food (and medical) packaging, automobile, furniture and toy industries. [3] Polypropylene resins commercially produced in the presence of a fourth generation Ziegler-Natta catalyst system have shown to have a relatively high molecular weight ($M_w$) and broad molecular weight distribution (MWD). These features causes them to have a high melt viscosity which makes them unsuitable for commercial end-uses such as fibre spinning, film moulding, extruded and injection-moulded thin-walled products. [4]

The rheological behaviour of the PP melt largely depends upon its MWD. Therefore, this parameter must be controlled to improve the response of the material during processing. The MWD of PP can be controlled by either improving the polymerisation technology in the reactor or by a post-reactor modification of the reactor-grade. The former technique is not efficient because it involves the use of chain terminators and transfer agents which decrease the yield and increase the costs. In the latter technique, peroxides are incorporated into the PP matrix to induce controllable degradation of PP chains which results in polymers with tailor-made properties. The PP resins prepared this way, called controlled-rheology polypropylenes (CRPP), have improved processing properties due to their lower $M_w$ and narrower MWD than the parent polymers. [5-8]

One major drawback of PP is its low fracture toughness, especially at low temperatures. [9,10] A dispersed rubbery phase is therefore incorporated into the PP matrix via either physical blending or by copolymerisation with other olefins such as ethylene to improve its fracture toughness. [9] The latter is preferred over the blending system because of the marked incompatibility of polyethylene and polypropylene. [11] The copolymerisation approach results in the formation of materials which are heterophasic in nature, consisting of a two phase

structure with an ethylene-propylene rubber (EPR) phase uniformly dispersed within a PP homopolymer phase. [12,13] These ethylene-propylene block copolymers (EPBCs), sometimes referred to as heterophasic copolymers (HECO) can also be peroxide degraded like PP homopolymers to improve their processing properties.

## 1.2.    Objectives

In 2013, Swart [1] conducted a study on the effect of controlled rheology (also called visbreaking) on the molecular characteristics of HECO polymers. It was reported that the use of chemically similar yet structurally different organic peroxides (Trigonox®101 and Trigonox®301) had different effects on the molecular make up and properties of HECO polymers. Therefore, more work is required to understand why specific organic peroxides influence or interact differently with various phases of HECO polymers and how the characteristics of the type of peroxide can be utilized to obtain a HECO polymer with optimal and desired properties. Since HECO polymers are commercially important materials, the fundamental understanding of the processes and chemistry that affects the final macroscopic properties of these materials needs to be expanded.

The main aim of this research is to determine why specific organic peroxides, Trigonox®101 and Trigonox®301, influence or interact differently with various phases of HECO polymers. The objectives of this research are as follows:

- To fractionate HECO copolymers (2 different ethylene  contents) by P-TREF (preparative temperature rising elution fraction)

- To determine the solubility of the peroxides in these fractions (30 °C, 100 °C, 130 °C).

- To develop a methodology for reaction of the peroxides with the individual fractions that represents the reactions that will occur during extrusion vis-breaking.

- To evaluate the products of reaction of the peroxides with the individual fractions of the copolymers.

- To correlate these results with the bulk vis-broken samples

In this study the HECO polymers were fractionated into three fractions (30, 100 and 130 °C) using P-TREF (preparative temperature rising elution fractionation). A methodology was then developed for the reaction of the peroxides with the individual fractions to represent reactions that occur during extrusion visbreaking. A melt flow index instrument was used to blend and react small amounts of the HECO polymers with the peroxides used in this study. Initial studies were done on the bulk materials. The effects of the peroxides on the individual fractions of the copolymers were then studied using HT-SEC, DSC, FTIR and solution state $^{13}$C-NMR spectroscopy.

## 1.3.    Dissertation layout

The dissertation is divided into the following five chapters:

**Chapter 1**

A brief introduction and background of HECO polymers is given together with an outline of the main objectives of this study. The layout of the dissertation is also given in this chapter.

**Chapter 2**

This chapter starts by emphasizing the structural complexity of heterophasic copolymers through providing information on their synthesis and morphology. It further provides a brief discussion on the P-TREF (preparative-temperature rising elution fractionation) technique, used to fractionate the heterophasic copolymers by crystallizability. Moreover, this chapter also provides a brief discussion on the Trigonox®101 and Trigonox®301 peroxides, used in this study. Furthermore, a brief discussion on peroxide-induced degradation and the analytical techniques used to investigate the structural changes induced by the degradation is provided.

**Chapter 3**

This chapter starts by providing a list of the materials used in this study, together with the places they were sourced from. It further gives the procedure and experimental conditions that were used to degrade the CMR648 and CMR348 bulk samples, together with their fractions. This chapter concludes by giving brief discussion of the analytical techniques that were used to investigate the structural changes induced by the two peroxides (Trigonox®101 and Trigonox®301) on the two samples (CMR648 and CMR348).

**Chapter 4**

This chapter gives a discussion of the results obtained from the analytical techniques discussed in Chapter 3. Some of the results obtained from the analytical techniques in Chapter 3 is presented in the addendums after Chapter 5.

**Chapter 5**

The conclusions drawn from Chapter 4 are presented in this chapter. This chapter also provides recommendations for future work in this field.

## 1.4.    References

(1)      Swart, M., PhD Thesis, University of Stellenbosch, **2013**.

(2)      Botha, L.; van Reenen, A., *European Polymer Journal* **2013**, 49, 2202.

(3)      Karger-Kocsis, J.; *Microstructural Aspects of Fracture in Polypropylene and in its Filled, Chopped Fiber and Fiber Mat Reinforced Composites* In *Polypropylene Structure, Blends and Composites*; Springer, **1995**, p 142.

(4)      Salazar, A.; Rodríguez, J. *Fracture Behaviour of Controlled-Rheology Polypropylenes*; INTECH Open Access Publisher, **2012**, p 350.

(5)      Azizi, H.; Ghasemi, I., *Polymer testing* **2004**, 23, 137.

(6)      Baik, J. J.; Tzoganakis, C., *Polymer Engineering & Science* **1998**, 38, 274.

(7)      Berzin, F.; Vergnes, B.; Delamare, L., *Journal of applied polymer science* **2001**, 80, 1243.

(8)      Ryu, S.; Gogos, C.; Xanthos, M., *Advances in Polymer Technology* **1991**, 11, 121.

(9)      Karger-Kocsis, J.; Karger-Kocsis, J.; Fakirov, S., *Nano-and Micromechanics of Polymer Blends and Composites* **2009**, 425.

(10)     Prabhat, K.; Donovan, J., *Polymer* **1985**, 26, 1963.

(11)     Teh, J.; Rudin, A.; Keung, J. C., *Advances in polymer Technology* **1994**, 13, 1.

(12)     Sun, Z.; Yu, F., *Die Makromolekulare Chemie* **1991**, 192, 1439.

(13)     Sun, Z.; Yu, F.; Qi, Y., *Polymer* **1991**, 32, 1059.

# *Chapter 2*

# Historical background and literature review

*This chapter consists of a brief introduction to heterophasic ethylene-propylene copolymers together with their synthesis and morphology. It also contains an overview of the TREF (Temperature rising elution fractionation) technique commonly used to fractionate heterophasic copolymers. It concludes with a brief overview of organic peroxides and peroxide-induced degradation, together with a brief discussion on the conventional characterization techniques used to study the chemical changes induced by peroxide induced degradation.*

## 2.1    Heterophasic ethylene-propylene copolymers (HECOs)

### 2.1.1  Introduction

Heterophasic propylene-ethylene copolymers (HECOs) are commercially important materials. Therefore the fundamental understanding of the processes and chemistry that affects their final macroscopic properties needs to be expanded. From an industrial point of view, obtaining a polymer with optimum properties is very important. [1] Based on a recent study by Swart [2], it was reported that chemically similar yet structurally different organic peroxides (Trigonox®101 and Trigonox®301) have a different effect on the molecular composition of HECOs. Based on this finding more work was recommended to understand why specific organic peroxides influence or interact differently with the different phases found in HECOs and how the characteristics of the type of peroxide can be utilized to obtain a HECO with optimum and desired properties. [2] Heterophasic propylene-ethylene copolymers sometimes referred to as polypropylene catalloys (PP-cats) [3], impact polypropylene copolymers (IPC) or ethylene-propylene block copolymers (B-PP) [4] are a unique group of polyolefins produced by improving the impact strength of the polypropylene homopolymer at low temperatures. [5-8] However, according to de Goede *et al.* [9], referring to these copolymers as ethylene-propylene block copolymers can be misleading considering the complexity of their bulk composition.

Studies performed on the molecular composition, chemical structure and micromorphology of HECOs, have revealed the existence of multiple phases in their bulk composition. [10-12] These copolymers have been reported to consist of three main phases: (1) an ethylene-propylene random copolymer phase (also called the amorphous phase), (2) a series of segmented ethylene-propylene copolymers with different ethylene and propylene sequence lengths (also referred to as the semi-crystalline phase) and (3) an isotactic polypropylene homopolymer phase (also called the highly crystalline phase). [5,6,13]

Studies on the molecular structure of HECOs revealed that the segmented ethylene-propylene copolymer phase (or semi-crystalline phase) acts as a compatibilizer between the ethylene-propylene random copolymer and polypropylene homopolymer phases. [12,14] Tian *et al.* [15] reported that an increase of the polypropylene content in the ethylene-propylene segmented copolymer phase (EPS) consequently results in a decrease in the size of the ethylene-propylene random copolymer (EPR) phase domains and therefore interfacial tension between the EPR

phase and polypropylene phase. Botha *et al*. [16] reported that the EPS phase consisted of a great variety of copolymer sequences that were proposed to be compatible with both the EPR and homopolymer phases. The propylene rich copolymer sequences in the EPS phase were reported to be more compatible with the homopolymer phase. Figure 2.1 (a) shows an AFM image of a heterophasic ethylene-propylene copolymer. A clear distinction between the polypropylene homopolymer and the EPR phases can be seen. Figure 2.1 (b) is a schematic representation of the image in Figure 2.1 (a). [20]
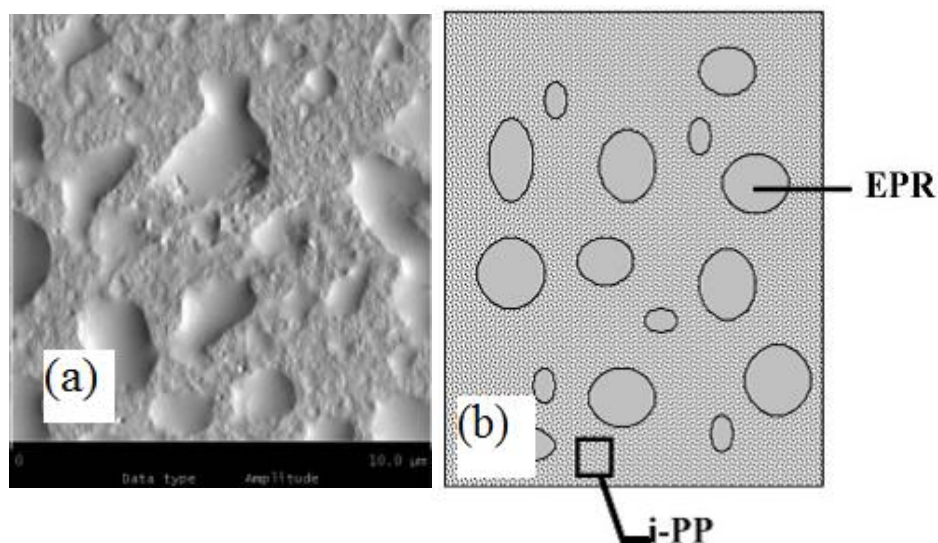
Figure 2.1          a) AFM image of a heterophasic ethylene-propylene copolymer and (b) schematic representation of the same copolymer [17]

## 2.1.2     Synthesis of heterophasic propylene-ethylene copolymers

### 2.1.2.1     In-reactor synthesis of heterophasic propylene-ethylene copolymers

In reactor heterophasic copolymers are usually synthesized via a two-step sequential polymerization procedure. In-reactor HECOs were first synthesized in the 1960s. [18] The first in-reactor heterophasic propylene-ethylene copolymer was synthesized by the incorporation of the ethylene-propylene copolymer towards the finishing steps of the polypropylene homopolymerisation stage. This therefore led to the first in-situ synthesis of rubber toughened polypropylene. Before then, the polypropylene had to be mechanically compounded with rubber in the melt to improve its toughness. [19]

HEPCs can be prepared by either a multi-stage sequential polymerization (MSSP) or a two-stage sequential polymerisation (TSP) process. The two-stage polymerization process occurs

via two stages in a sequential reaction mode. The first stage involves the polymerization of the polypropylene homopolymer in the presence of a spherical $TiCl_4/MgCl_2$-based catalyst and producing porous polypropylene particles as the end product.[20-23] In the second stage of the polymerization process, ethylene and propylene are copolymerized to produce the ethylene-propylene rubber (EPR) phase of the heterophasic copolymer which is then incorporated into the preformed polypropylene homopolymer matrix. [20-23] The final product is a continuous polypropylene homopolymer phase with a dispersed EPR phase [53]. Figure 2.2 below is a schematic representation of the two-stage polymerisation process
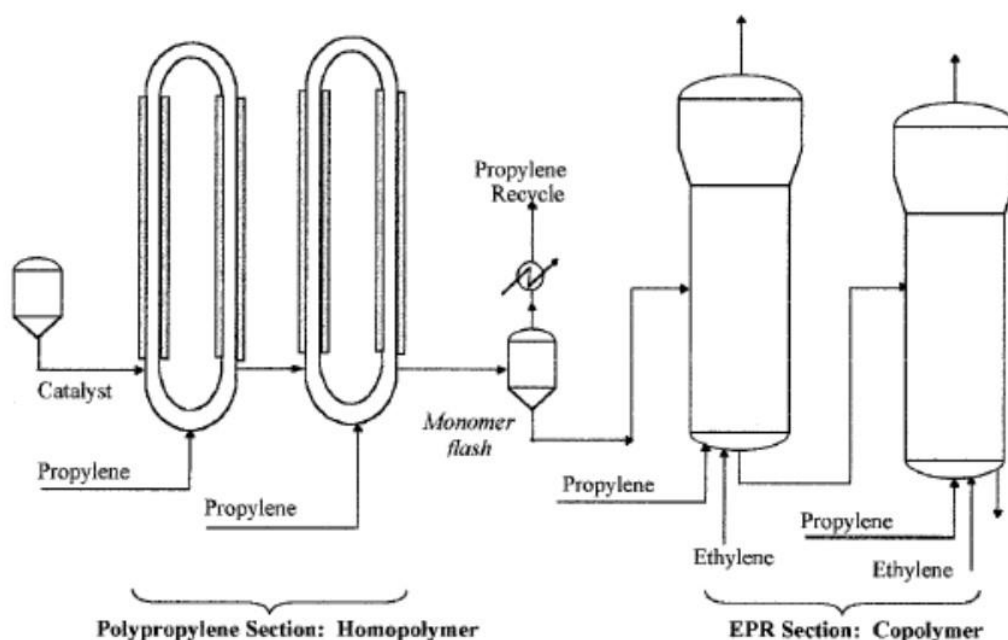


Figure 2.2          A schematic representation of the two-stage polymerisation process. [24]

The multi-stage sequential polymerization process occurs via several stages in a sequential reaction mode.[21-23,25] Before the multi-stage polymerisation process was designed, in-reactor HECOs were commonly synthesized by the conventional two-stage sequential polymerization process. [13,20] However, the two-stage polymerisation process is still common among most industries.

One of the commonly employed multi-stage processes in industry is called the Catalloy ® process and was designed by the Montell company. [19] It uses a spherical super active $TiCl_4/MgCl_2$ based catalyst to produce multiphase polypropylene in-reactor blends with a

spherical shape. [13,20] The catalloy process is also often referred to as a highly flexible gas phase multi-stage polymerisation process. [19] It involves three independent gas phase reactors arranged in a series. Each of these reactors independently produces different portions of the final end-product. In the first reactor, pure propylene is produced, in the second and third reactors different ratios of propylene/ethylene. [19] The catalloy process uses a catalyst system which allows the incorporation of multiple polymer structures within a single particle of the catalyst as it moves through the multi-stage process. [19]

Li *et al.* [23] used both the multi-stage and two-stage polymerisation processes to synthesize two heterophasic copolymers. The morphology of the two copolymers synthesized using the different methods was compared and it was found that the heterophasic copolymer prepared by the multi-stage polymerization process had more polypropylene content in its blocky copolymer fractions than the one prepared using the two-stage polymerization process. [23] It can therefore be concluded that the method used during the polymerization process contributes to the final composition of the heterophasic copolymer.

According to Li *et al*. [23], heterophasic ethylene-propylene copolymers prepared by the multi-stage polymerization process have improved mechanical properties in terms of impact strength and flexural modulus as compared to those prepared by the conventional two-stage polymerization process. Previous studies [21,25] have also shown that the multi-stage sequential polymerization process produces HECOs with an excellent stiffness-toughness balance. However, not much has been reported in literature about the structure and impact properties of HECOs synthesized via the multi-stage polymerization process [21,23,25] whereas more work has been reported on the structure and impact properties of HECOs synthesized via the two-stage polymerization process. [6,13,20,23,26-29] Figure 2.3 is an illustration of the Catalloy ® process developed by the Montell Company.
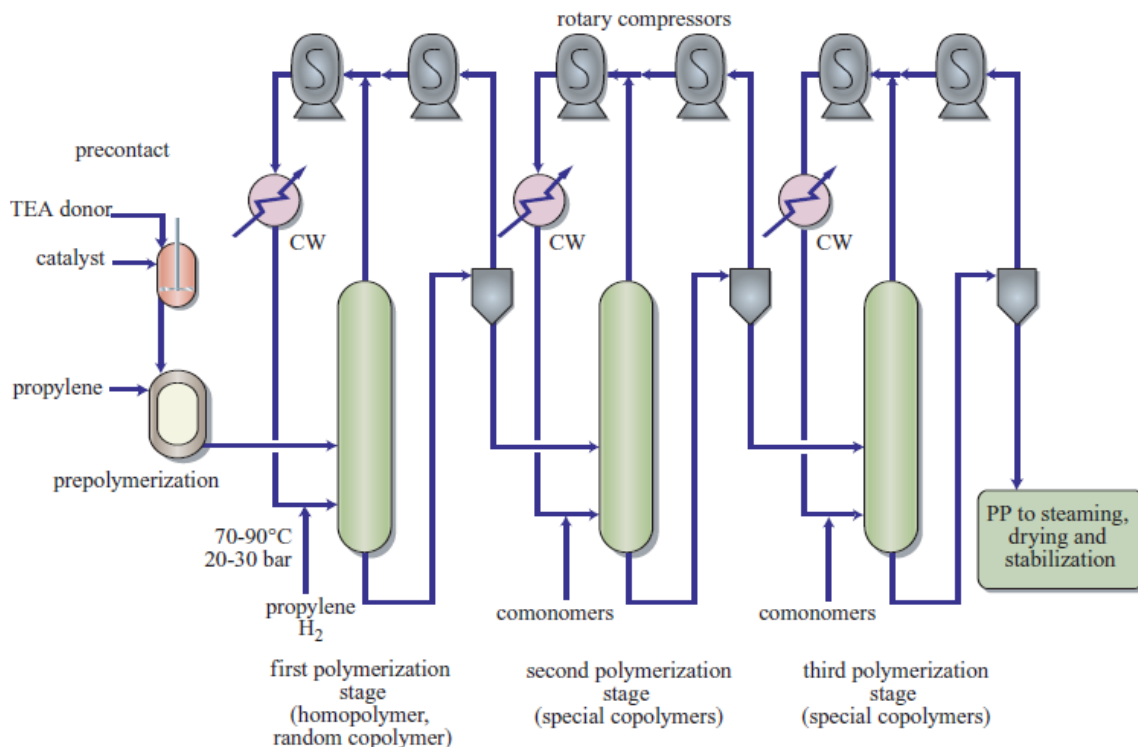
Figure 2.3       An illustration of the catalloy process by the Montell Company [19]

Recently, Basell [30,31] designed a multi-stage sequential polymerisation process called the periodic switching polymerization process (PSPP) [33] that uses a multizone circulating reactor (MZCR). This polymerisation process also involves propylene homopolymerization in the first stage, after that the polymerisation process switches to gas-phase ethylene-propylene copolymerization and gas-phase propylene homopolymerization in a circular fashion. [22,23] The propylene homopolymer is continuously and rapidly circulated between a reaction zone containing ethylene and propylene monomer gas mixtures and a reaction zone containing the propylene homopolymer. [22,23] It uses the switch frequency as a critical variable to control the composition and microstructures of the EPR (ethylene-propylene random copolymers) [33] and EPS (ethylene-propylene segmented copolymers) phases. However, ethylene is used as a variable to control the formation of the EPS and EPR phases [33] Tian *et al*. [32] reported that increasing the switching frequency between the homopolymerization and copolymerization stage not only increases the ratio between the EPS and EPR phases, but it also increases the fraction of long polypropylene and polyethylene sequences in the EPS phase.

The advantage of the MZCR over the traditional multiple-stage technologies is its flexibility to produce a wide range of polymers, from polypropylenes with a narrow and broad MWD to

ethylene/propylene rubber blends. [30] Work done by most researchers shows that the in-reactor heterophasic copolymers synthesized via the MZCR based multi-stage polymerization processes have an improved toughness-rigidity balance than heterophasic copolymers synthesized by the conventional two-stage polymerization process. [22,23]

In a recent study, Tian *et al*. [15] confirmed the capability of ASPP to produce impact polypropylene copolymers with an excellent rigidity-toughness balance. Moreover, according to a previous study by Tian *et al*. [32], ASPP does not only control the composition of the EPR and EPS phases, but it also arranges the monomer sequences in the EPS phase. Figure 2.4 below is a schematic diagram of the multi-stage polymerisation process using the MZCR technology.
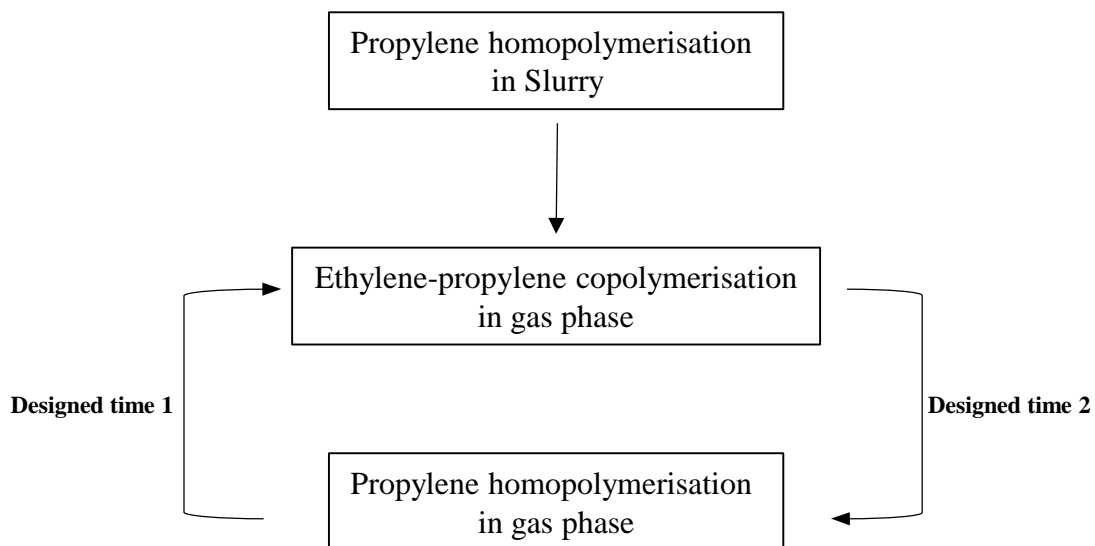


Figure 2.4    A schematic representation of the multi-stage polymerisation process using the MZCR technology

 The composition of the EPR phase in the HECOs is controlled by varying the ethylene/propylene ratio and the amount of hydrogen in the second stage of the polymerization process [2]. The ethylene/propylene comonomer ratio in mol/mol is expressed as

$$Comonomer\ ratio = {C2}/{C3} \ldots\ldots 2.1$$

and is also used to determine the composition of the EPR phase [2]. If the commoner ratio is $\geq$ 9, HECOs with a high ethylene content are produced. However, when the comonomer ratio is $\leq$ 0.1, HECOs with a low ethylene content are produced. [2]

### 2.1.3    Morphology and particle growth mechanism of heterophasic ethylene-propylene copolymers

There are two main types of models used to describe the particle growth mechanism followed by HECOs and these are: (1) the multi-grain model [34] and (2) the double grain model. [35,36] At the end of the polypropylene polymerization stage, each polypropylene particle is composed of a few secondary particles (polymer globules) which in turn consist of a few primary polypropylene particles consisting of catalyst crystallites (Figure 2.5). These catalyst crystallites consist of active sites in which the propylene chains are formed. The secondary particles are separated by macropores whilst the primary particles are separated by micropores (Figure 2.5). During the copolymerisation stage, the ethylene-propylene copolymer is formed on the catalyst active sites situated around the pores of the polypropylene homopolymer particle. [37-39]
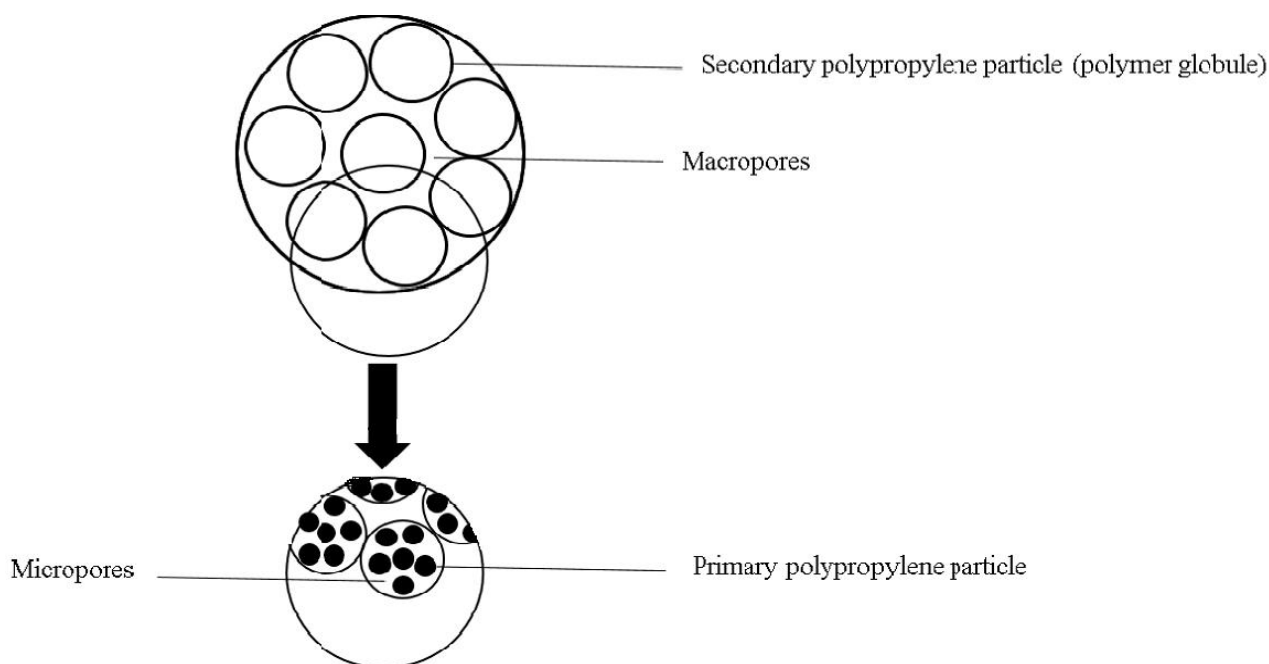


Figure 2.5    A schematic diagram showing the arrangement of primary and secondary particles and the position of macro and micro pores in the polypropylene particle.
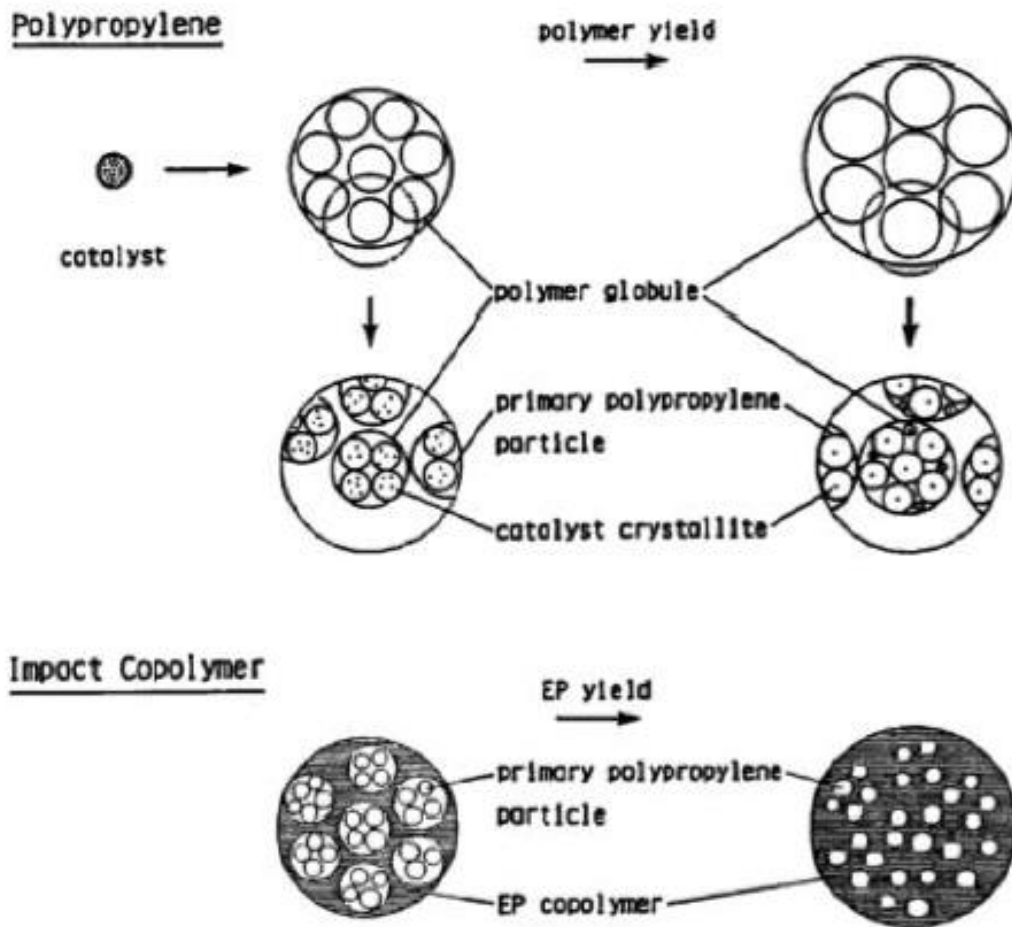
Figure 2.6        A model for propylene and HECO growth proposed by Kakugo et al. [42]
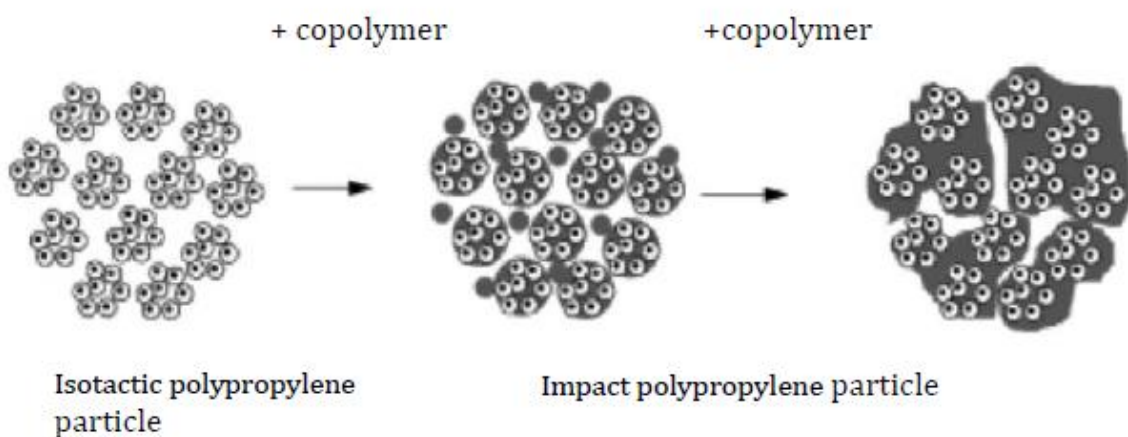


Figure 2.7        A model for impact polypropylene growth proposed by Debling and Ray [37]

The double grain model states that the copolymer phase first migrates from the macropores between the secondary particles and then into the micropores between the primary particles thus forming a continuous phase (Figure 2.5). In contrast, the multi-grain model states that the copolymer phase first expands from the micropores between the primary particles and then into the macropores seperating the secondary particles (Figure 2.6).

The "pore-filling model" is a model that is commonly used to describe the mechanism by which the EPR phase fills the micropores and macropores between the primary and secondary particles. However, although the site of formation of the EPR phase within the polypropylene homopolymer particle has been disclosed, the mechanism followed by its formation is still controversial. [17,37,40,41]

Previous studies on the morphology of HECOs using SEM (Scanning electron microscopy), TEM (Transmission electron microscopy), AFM (Atomic force microscopy), XRD (X-ray diffraction) and DSC (Differential scanning calorimetry) have shown that these heterophasic copolymers have a two phase morphological structure consisting of a dispersed rubber phase and a polypropylene homopolymer phase. [17,27,43] The "dispersed particle model" proposed by Zhang *et al.* [27] revealed that the dispersed rubber phase had a core-shell structure. The dispersed rubber phase was reported to consist of an EPR phase and some ethylene-propylene block copolymers with different sequence lengths (E*b*P) as shown in Figure 2.7 below. According to the "dispersed particle model", the EPR and the E*b*P component with crystallisable polypropylene sequences form the shell whilst the E*b*P component with crystallisable polyethylene sequences form the core of the core-shell structure.
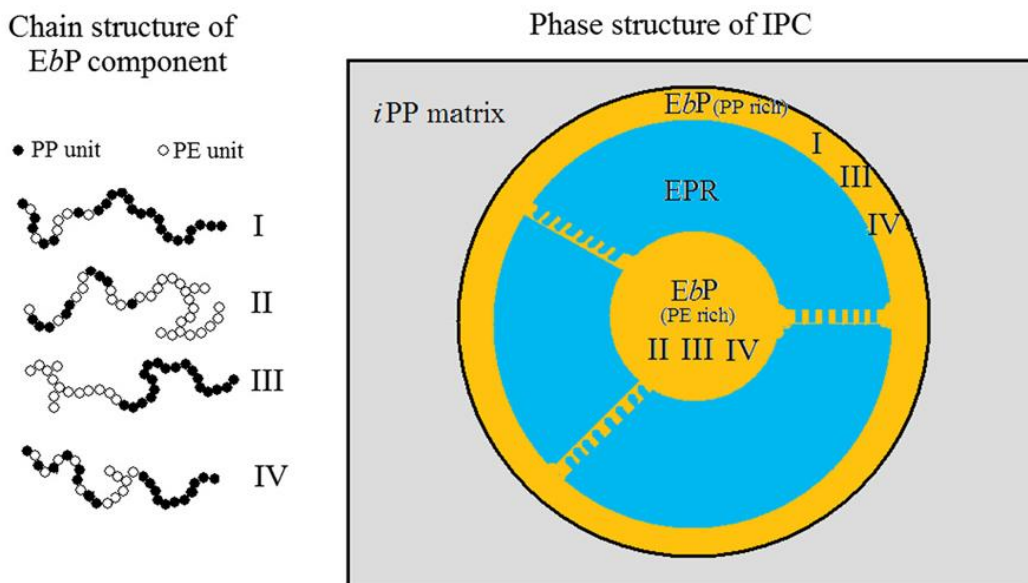
Figure 2.8          An illustration of the core-shell structure of the dispersed phase

Due to the complexity of the heterophasic ethylene-propylene copolymer, there is still a lot of work to be done to perfectly understand its particle growth mechanism. [41]

## 2.2    Crystallization of HECOs from dilute solutions

Crystallization of polymers from a dilute solution is an important process because it creates an avenue for the structural analysis of polymer crystals as these entities can be separated and studied extensively. [44] During crystallization, polymer chains fold together to form ordered regions called lamellae. These ordered regions then organise themselves into larger spheroidal structures called spherulites. [45]

For polymer crystallization to occur, the presence of a nucleation site is of fundamental importance. Nucleation is a process whereby a small amount of crystalline material is formed in the melt or dilute solution as a result of alterations in chain order due to supercooling or fluctuations in density. [46] For the crystallization process to commence, initial or primary nuclei are formed via a process called primary nucleation. After the primary nuclei are formed the crystallization process continues on the growth surface by the induction of more and more polymer chains via a process is called seconadary nucleation. Nucleation can also be classified according to the origin of the nucleation site. When no second surface or nuclei is present and the nuclei formation happens spontaneously only due to supercooling the phenomena, the

nucleation process is called homogenous nucleation. In contrast, if a second surface is present for nucleation (It may be a foreign particle or surface from the same polymer nuclei or crystal), then the process is called heterogenous nucleation. [44] However, Schulz and Wunderlich [47] introduced a third classification of the nucleation process called self-nucleation. In this type of nucleation, the nucleation is due to pre-existing or residual nuclei that survived the initial dissolution conditions. It is however very important to note that primary nucleation can either be heterogenous or homogenous whilst secondary nucleation can only be heterogenous. [44]

As mentioned in Section 2.1.1, HECOs consist of an amorphous rubber fraction, semi-crystalline ethylene-propylene copolymers and highly crystalline isotactic polypropylene regions. [27,48,49] The semi-crystalline regions consist of both crystalline and amorphous domains. More recently Phiri *et al.* [50] reported that the amorphous rubber fraction also contains a small amount of crystalline domains. This explains the reason why it crystallizes last during the TREF fractionation of HECOs. According to studies by Cheruthazhekatt *et al.* [51] on the melting and crystallization behaviour of each fraction of the heterophasic copolymers, it was reported that these fractions exhibit distinctively different melting and crystallization behaviour. The crystallization behaviour of the isotactic polypropylene homopolymer fraction was found to be affected by macromolecular chain lengths and that of the ethylene-propylene copolymer fractions was found to be affected by branching defects in the long crystallisable ethylene sequences of the ethylene rich sequences.

Crystallization of HECOs from a dilute solution is important because it creates an avenue for polymer scientists to determine the chemical composition distribution (CCD) of these complex materials. However, the chemical composition distribution analysis of these complex polymeric materials is limited by the occurrence of a process called co-crystallization during their fractionation. What happens during co-crystallization is that the components of the HECOs with similar crystallizabilities crystallize simultaneously making it difficult to perform a thorough fractionation of the bulk material. However, according to Cheruthazhekatt *et al.* [51], more alternative fractionation techniques have been introduced recently to reduce the co-crystallization effects during fractionation.

## 2.3    Fractionation of heterophasic propylene-ethylene copolymers

Heterophasic propylene-ethylene copolymers are very complex materials. Therefore a detailed analysis of such materials would provide an adequate amount of information about the contribution of each of their components to the physical and chemical properties of the bulk material. Detailed analysis of their molecular structure requires the employment of fractionation techniques. These techniques are able to separate chemically distinct components from each other consequently yielding chemically homogenous fractions which can be further analysed using ancillary techniques to obtain detailed structural information. Polymers can be fractionated according to three main areas namely: fractionation by crystallizability, fractionation by molecular weight and fractionation by chemical composition. However, in this work, emphasis will be put on fractionating by crystallizability using the temperature rising fractionation technique (TREF) as it is of relevance to the present study.

The concepts of polymer fractionation by crystallizability are based on the Flory-Huggins statistical thermodynamic treatment which takes into account the melting point depression caused by the diluent. The statistical thermodynamic theory is represented by Equation 2.3 below. [52,53] The diluent can either be a solvent or a comonomer. As the concentration of the diluent increases, the crystallization temperature decreases. [54]

$$\frac{1}{T_m} - \frac{1}{T_m^\circ} = \left(\frac{R}{\Delta H_u}\right)\left(\frac{V_u}{V_1}\right)\left[-\frac{ln(v_2)}{x} + \left(1 - \frac{1}{x}\right)v_1 - X_1 v_1^2\right] \dots\dots\dots\dots\dots\dots\dots\dots\dots 2.2\ [53]$$

Where:

| | | |
|---|---|---|
| $T_m$ (°C) | = | equilibrium melting temperature of polymer in solution |
| $T_m^0$ (°C) | = | melting temperature of pure polymer |
| $\Delta H_u$ (J/g) | = | heat of fusion per repeating unit |
| $V_1$ (cm³/mol) | = | molar volume of diluent |
| $V_u$ (cm³/mol) | = | molar volume of polymer repeating unit |
| $v_1$ | = | volume fraction of diluent |
| $v_2$ | = | volume fraction of polymer |
| $x$ | = | number of segments |
| $\chi_1$ | = | Flory-Huggins thermodynamic interaction parameter |

## 2.4    Temperature rising elution fractionation (TREF)

Shirayama *et al*. [55] were the first to use the term TREF after using the technique to fractionate low density polyethylene (LDPE) based on its degree of short chain branching. The TREF

technique can be operated via two main sequential steps namely the crystallization step and the elution step.

During the first step, the polymer is dissolved in a suitable solvent at a high temperature. After that, the polymer solution formed is then cooled at a controlled rate in a glass reactor containing an inert support like glass beads or sea sand. [54] This gives the polymer chains time to crystallize in an orderly fashion with the more crystalline chains crystallizing first and the less crystalline ones crystallizing last. According to Mirabella *et al*. [56] the polymer coats the support and consequently forms layers of different crystallinity on the support (Figure 2.8). The cooling rate is one of the significant factors in the crystallization step because it determines the quality of the fractionation.

In the second step (elution step), pure solvent is allowed to pass through a steel column containing the support and crystallized sample. [56-58] The temperature of the solvent is increased at intervals for the polymer layers to elute individually as fractions at the predetermined temperature intervals. However, the elution of the polymer layers occurs in a reverse order when compared with their crystallization on the support particle (Figure 2.9).

The TREF technique can be operated as an analytical and preparative experiment (A-TREF and P-TREF respectively). Although these two modes of TREF are based on the same principle, their differences are listed in Table 2.1.

Table 2.1          Comparison between analytical and preparative TREF

| A-TREF | P-TREF |
|---|---|
| Fastest of the two experiments but not as much polymer information is obtained. | More information can be obtained but also more time-consuming than analytical TREF. |
| Smaller columns; smaller sample size. | Larger columns; larger sample size. |
| Continuous collection of fractions. | Collection of fractions at fixed temperature intervals. |
| Polymer information obtained on-line | Polymer information obtained off-line (additional techniques used for analysis). |
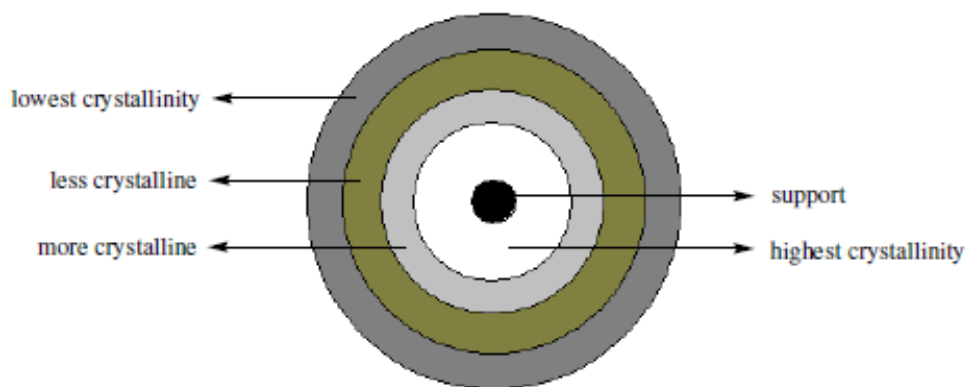
Figure 2.9         Illustration of different layers formed after the crystallization step [45]
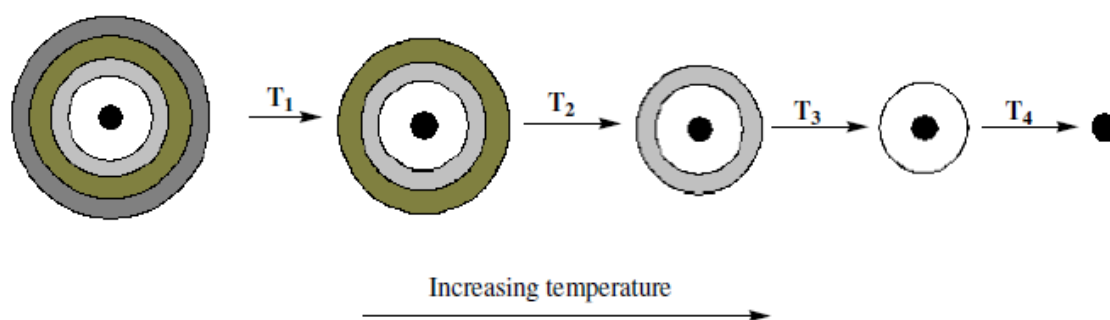


Figure 2.10        Illustration of the TREF elution step [45]

TREF is one of the best techniques for fractionating and characterizing semi-crystalline polymers. [57] It is also referred to as a standard technique for most polyolefin research laboratories. [54] A more recent study by Phiri *et al.* [50] have shown that when P-TREF is combined with other analytical tools, it can serve as a useful tool in understanding the complex chemical composition of the ethylene-propylene rubber fraction in HECOs. Major flaws of the TREF technique are its operational complexity and long analysis time. [59] The reliability of the TREF results can be affected by polyolefin molar mass, comonomer type and content, cooling rate and co-crystallization effects. [54] However, if the TREF technique is properly executed, separation occurs due to differences in crystallizability and becomes independent of polyolefin molar mass and co-crystallization influences. [57]

More information on the TREF technique can be found in literature. [57,60-62]

## 2.5    Organic peroxides

### 2.5.1    Definition

Organic peroxides are organic compounds consisting of a "peroxy" functional group (two oxygen atoms joined together –O-O-). It is this "peroxy" group that controls the usefulness and hazardousness of the peroxides. The peroxy group is unstable and can therefore decompose when the peroxide is exposed to unfavourable conditions. [63]

### 2.5.2    Properties

Organic peroxides are amongst the most hazardous substances commonly used in the laboratory. Therefore good safety precautions should be followed when working with these substances. Most organic peroxides used in the laboratory are very flammeable and highly sensitive to shock, heat, spark, friction, impact and light. They are also highly reactive towards strong oxidizing and reducing agents. Moreover, peroxides also have specific decomposition rates which depend upon the conditions they are exposed to. Changing the conditions (e.g temperature) affects their decomposition rate. For example, at extremely high temperatures their decomposition rate can auto-accelerate and this can result in an explosion. [63] Decomposition of organic peroxides can also result in the evolution of harmful and flameable gases or vapours. During the decomposition process, the O-O bond of the "peroxy" group easily breaks and forms very reactive, unstable free radicals of the form RO·.

Most organic peroxides (especially low molecular weight peroxides) are unstable at or near room temperature and therefore should be stored under cool temperatures. The normal storage temperature of peroxides is not expected to exceed 27 °C. However, this may not be the case for some peroxides. The sensitivity and instability of organic peroxides is controlled by their active oxygen content and oxygen balance increase. [64] However, the sensitivity of these substances also depends on their heat of decomposition, activation energy and reaction kinetics.[63]

### 2.5.4    Uses of organic peroxides

Organic peroxides have many uses in polymer chemistry. They are used as radical initiators for some types of polymerization [63], they are also used as cross-linking, curing and

vulcanization agents. [65,66] Organic peroxides can also be used as catalysts in some reactions. Researchers also use them in their peroxide-controlled degradation experiments to initiate chain scission reactions. [67,68]

## 2.6    Trigonox®101 peroxides

2,5-Dimethyl-2,5-di(tert-butyl peroxy)hexane (Trigonox®101 peroxide) is a bifunctional peroxide that is commonly used for the crosslinking of natural and synthetic rubbers, as well as thermoplastic polyolefins. However, Trigonox®101 peroxides are also used in the production of controlled-rheology polypropylenes (CRPPs). [67] The chemical structure of the Trigonox®101 peroxide is shown in Figure 2.12 as well as in Section 3.1.2 of Chapter 3.

The decomposition rate of a peroxide is one of the primary factors taken into account when choosing a peroxide for a specific application. The decomposition of a bifunctional peroxide like Trigonox®101 occurs via a two-step process, involving the formation of an intermediate alkoxy radical species. The lifetime of this strongly abstracting species significantly determines the decomposition rate of the peroxide. [69] Figure 2.10 gives an illustration of the decomposition mechanism followed by the Trigonox®101 peroxide.

2,5-Dimethyl-2,5-di(tert-butylperoxy)hexane (Trigonox[®]101)

Figure 2.11          Thermal decomposition of the Trigonox®101 peroxide [69]

One main disadvantage of using the Trigonox[®]101 peroxide in an industrial scale is its high cost. [70] This is why the Trigonox[®]101 peroxide is not the choice of interest in many industrial applications. According to Scorah *et al.* [67], bifunctional peroxides release di-functional radicals that promote chain extension reactions and are therefore less efficient in the reduction of the final polymer molecular weight.

## 2.7    Trigonox[®]301 peroxides

3,6,9-triethyl-3,6,9-trimethyl-1,4,7-triperoxonane  (Trigonox[®]301  peroxide)  is  a  cyclic peroxide consisting of three peroxide groups [70] and is commonly used in the production of CRPP resins in an extrusion process. Due to the presence of three "peroxy" functional groups in its chemical structure, it is therefore classified as a multifunctional peroxide. [71] Multifunctional organic peroxides are capable of generating mono or polyfunctional radicals

during thermal decomposition. [71] The chemical structure of this peroxide is shown in Section 3.1.2 of Chapter 3.

Trigonox®301 is a very cost effective, efficient and safe organic peroxide when compared to other peroxides used in CRPP production. Due to its high "visbreaking" efficiency, it is often used as a low cost alternative to other peroxides such as Trigonox®101. According to Salakhov *et al.* [70], the high "visbreaking" efficiency of the Trigonox®301 peroxide by comparison with the Trigonox®101 peroxide may be due to the presence of three peroxide groups and a high active oxygen content.

Salakhov *et al*. [70] also found out that the Trigonox®301 peroxide significantly reduces the amount of volatiles in polypropylene during the production of CRPP resins when compared with the Trigonox®101 peroxide. It was also reported that the use of the Trigonox®301 peroxide produces polypropylene grades with controllable impact strength properties and unaffected physicochemical properties.

## 2.8    Peroxide-induced degradation (controlled degradation) of HECOs

Peroxide-induced degradation or controlled degradation is a process used in the polyolefin industry to produce polyolefins with tailor-made properties for ease of processing. This type of degradation is sometimes referred to as controlled degradation because different concentrations of a suitable peroxide are used to achieve various levels of degradation. The degraded polypropylene polymer produced after the controlled rheology process is called controlled-rheology polypropylene (CRPP). The CRPP is easier to process than the original resin because it has high melt flow index (MFI), is less elastic and less sensitive to shear. Since CRPP is easier to process than the original resin, it is used in the manufacture of fibres, for film extrusion and for moulding applications. [72] During controlled rheology the polymer is blended with a suitable peroxide of known concentration (in an extruder) at the final stages of its production.  The peroxide thermally decomposes into peroxy radicals that attack the polymeric chains. During the attack by the peroxy radicals, tertiary hydrogen atoms are abstracted from the polymer chain and this consequently results in the formation of an unstable polymer radical. Finally $\beta$-scission of the polymer radical occurs resulting in the formation of a new polyolefin chain. During the peroxide-induced degradation, the larger molecular weight chains are cleaved more than the lower molecular weight chains and this results in a decrease of the average

molecular weight and narrowing of the molecular weight distribution (MWD). This is because the long polypropylene sequences are more susceptible to chain scission that the shorter sequences. [73] Figure 2.11 shows the mechanism followed by the peroxide-induced degradation process.

Peroxide decomposition and organic peroxide radical formation

$$ROOR \longrightarrow 2RO^{\cdot}$$

Radical attack, hydrogen abstraction and polymer radical formation



β-scission and new polyolefin formation
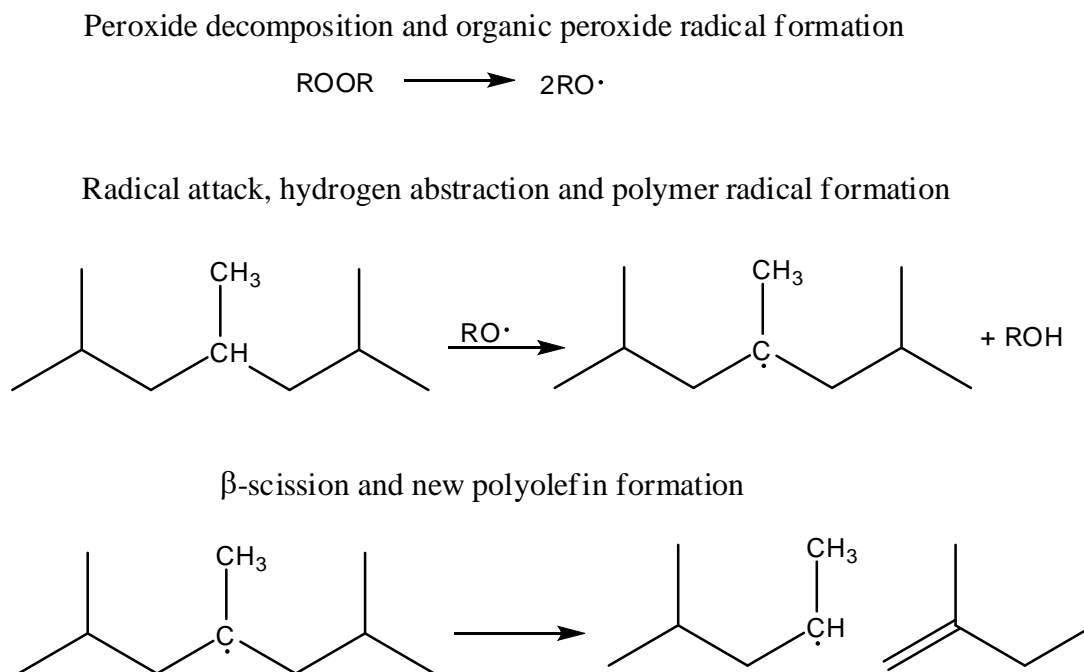


Figure 2.12        Mechanism of a peroxide-induced degradation [67]

Heterophasic propylene-ethylene copolymers have a widespread of uses in many important areas such as the automotive industry, the packaging industry and in the manufacture of office and household equipment. [74] As a type of modified polypropylene, heterophasic copolymers have gained a lot of attention in both industry and academics. [75] However, in spite of their good mechanical and thermal properties [76], heterophasic copolymers have the same poor processing properties as the PP homopolymers. Peroxide-induced degradation is therefore also used to improve the processability of these copolymers.

Peroxide-induced degradation is influenced by the following factors: the concentration of the peroxide, the type of peroxide, the residence time of the polymer and peroxide mixture in the extruder and the half-life of the peroxide. [69] Most of the research work on peroxide-induced degradation has been performed on PP homopolymers [67,73,77-80]

## 2.9    Conventional characterization techniques for studying degradation

### 2.9.1    Size exclusion chromatography

Size exclusion chromatography is a separation technique that separates molecules according to their hydrodynamic volume. It is a very common method for the determination of molecular weights (MW) and molecular weight distributions (MWD) of synthetic polymers.

When polyolefins are degraded, changes in their average molecular weights and molecular weight distributions may be observed. [79,81-84] These changes entirely depend on the type of radical reactions that occur during the degradation process. In polyethylene, an increase in molecular weight is observed as a result of crosslinking reactions [3] whilst in polypropylene, a decrease in molecular weight is observed as a result of chain scission reactions. [85] When the decrease in molecular weight of polypropylene impact copolymers was compared with that of polypropylene homopolymers, high molecular weight species were observed even at high peroxide concentrations. [82] According to literature [83] this is because of both degradation and crosslinking occurring simultaneously in the same polymer system.

The broadening of the molecular weight distribution observed in polyolefins is due to the presence of a large distribution of polymer chain lengths in the material. Moreover, a shift of the molecular weight distribution curve towards lower molecular weights indicates that chain scission is the dominant degradation mechanism. [79] Furthermore, the appearance of a bimodal molecular weight distribution curve indicates compositional heterogeneity of the degraded polyolefin sample. According to Tochacek *et al*. [85] the narrowing of the high molecular weight side and broadening of the low molecular weight side during degradation is due to a decrease of long chains and a subsequent increase of short chains.

### 2.9.2    Fourier transform infrared spectroscopy (FTIR)

Fourier transform infrared spectroscopy is a photospectroscopic technique in which infrared radiation is passed through a sample to obtain a characteristic infrared spectrum of the sample being analysed. As the infrared radiation is passed through the sample, it is either absorbed by or transmitted through the sample. Therefore, infrared spectroscopy is used to identify the spectral position (frequency) and intensity of the absorbed (or emitted) radiation caused by molecular transitions associated with vibrations and rotations of specific chemical groups. [81]

The infrared spectroscopy technique also gives quantitative and qualitative information on the changes in the chemical composition of polymers during degradation. [86,87] Kamjord and Stori [81] used FTIR to qualitatively study the grafting of maleic anhydride on the parts of heterophasic copolymers that were attacked by peroxide radicals. Degradation can either lead to the disappearance of characteristic bands or the appearance of new bands in the infrared spectra. The appearance of new bands in the spectrum indicates the presence of new functional groups in the degradation product. Saw *et al* [88] reported on the appearance of a band at 1648 cm$^{-1}$ (characteristic of the C=C functional group) after the degradation of the polymer matrix in polypropylene-ethylene copolymer-kaolin composites. The appearance of oxygenated degradation functional groups (carbonyls and hydroperoxides) in the wavelength 1550-1850 cm$^{-1}$ and 3200-3700 cm$^{-1}$ has also been reported by several authors in literature. [81-85]

Most recently, Swart reported on the disappearance of the doublet band at 720-730 cm$^{-1}$ (characteristic of long ethylene sequences) in the 100 °C TREF fraction after treatment of heterophasic copolymers with a peroxide.

### 2.9.3    Nuclear magnetic resonance spectroscopy (NMR)

Nuclear magnetic resonance spectroscopy is an analytical technique used to determine the content, purity and chemical composition of the sample being analysed. It is also used in polymer degradation studies to detect the structural changes induced by degradation. One major disadvantage of NMR spectroscopy is its inability to detect products at very low concentrations. Quaternary carbons are one of the most difficult species to detect due to their low Nuclear Overhauser Effect (NOE) and long relaxation times. [85] However, this problem can be solved by increasing the number of scans, increasing the pulse delays during analysis and using NMR tubes with large diameters.

In a more recent study on the peroxide-induced degradation of heterophasic copolymers, NMR spectroscopy was used to quantitatively trace the structural changes sustained by the polymers during the degradation process. The visbroken copolymer samples showed a decrease of long ethylene sequences (EEE) when compared to the non-visbroken ones. [89] This might be contradicting to what was observed by other literature sources mentioned before. However, it is worth noting that this is also possible when the same ethylene sequences are repeatedly "attacked" by peroxide radicals at high peroxide concentrations.

### 2.9.4    Differential scanning calorimetry (DSC)

Differential scanning calorimetry is a thermoanalytical technique used to study the thermal behaviour of a given sample. It is also a popular technique in polymer degradation studies for studying the changes in the thermal behaviour of degraded polymers. [89] The effect of degradation on the thermal behaviour of these polymers is often detected through shifts in crystallization and melting peak temperatures as well as changes in the shape of the melt endotherms. Peroxide induced degradation has been proven to affect the crystallization behaviour of heterophasic ethylene-propylene copolymers by Swart [2], Berzin *et.* [79] and Braun *et al.*. [90] Moreover, Berzin *et al.* [79] and Braun *et al.* [90] found that peroxide-induced degradation shifts the polyethylene crystallization and melting peaks in ethylene-propylene copolymers towards lower peak temperatures.

## 2.10    References

(1)      Yamahiro, M.; Mori, H.; Nitta, K.-h.; Terano, M., *Polymer* **1999**, 40, 5265.

(2)      Swart, M., PhD Thesis, University of Stellenbosch, **2013**.

(3)      Shangguan, Y.; Zhang, C.; Xie, Y.; Chen, R.; Jin, L.; Zheng, Q., *Polymer* **2010**, 51, 500.

(4)      Kanezaki, T.; Kume, K.; Sato, K.; Asakura, T., *Polymer* **1993**, 34, 3129.

(5)      Xu, J.; Feng, L.; Yang, S.; Wu, Y.; Yang, Y.; Kong, X., *Polymer* **1997**, 38, 4381.

(6)      Sun, Z.; Yu, F.; Qi, Y., *Polymer* **1991**, 32, 1059.

(7)      Feng, Y.; Hay, J., *Polymer* **1998**, 39, 6723.

(8)      Tan, H.; Li, L.; Chen, Z.; Song, Y.; Zheng, Q., *Polymer* **2005**, 46, 3522.

(9)      de Goede, E.; Mallon, P. E.; Pasch, H., *Macromolecular Materials and Engineering* **2012**, 297, 26.

(10)     Hayashi, T.; Inoue, Y.; Chûjô, R.; Asakura, T., *Polymer* **1988**, 29, 1848.

(11)     Hansen, E.; Redford, K.; Øysæd, H., *Polymer* **1996**, 37, 19.

(12)     Nitta, K.; Kawada, T.; Yamahiro, M.; Mori, H.; Terano, M., *Polymer* **2000**, 41, 6765.

(13)     Fan, Z.-q.; Zhang, Y.-q.; Xu, J.-t.; Wang, H.-t.; Feng, L.-x., *Polymer* **2001**, 42, 5559.

(14)     Pham, T.; Gahleitner, M., *Composite Interfaces* **2005**, 12, 707.

(15)     Tian, Z.; Feng, L.-F.; Fan, Z.-Q.; Hu, G.-H., *Industrial & Engineering Chemistry Research* **2014**, 53, 11345.

(16)     Botha, L.; Sinha, P.; Joubert, S.; Duveskog, H.; van Reenen, A., *European Polymer Journal* **2014**, 59, 94.

(17)     Urdampilleta, I.; González, A.; Iruin, J. J.; de La Cal, J. C.; Asua, J. M., *Macromolecules* **2005**, 38, 2795.

(18)     Ystenes, M., *Journal of Catalysis* **1991**, 129, 383.

(19)     *Encyclopaedia of Hydrocarbons: Refining and petrochemicals]*; 5th Edition ed.; Taylor & Francis Group, **2006**, p 451.

(20)     Fu, Z.-s.; Fan, Z.-q.; Zhang, Y.-q.; Feng, L.-x., *European Polymer Journal* **2003**, 39, 795.

(21)     Fu, Z.; Fan, Z.; Zhang, Y.; Xu, J., *Polymer international* **2004**, 53, 1169.

(22)     Dong, Q.; Wang, X.; Fu, Z.; Xu, J.; Fan, Z., *Polymer* **2007**, 48, 5905.

(23)     Li, Y.; Xu, J.-T.; Dong, Q.; Fu, Z.-S.; Fan, Z.-Q., *Polymer* **2009**, 50, 5134.

(24)     Kittilsen, P.; McKenna, T., *Journal of applied polymer science* **2001**, 82, 1047.

(25)     Fu, Z.; Xu, J.; Zhang, Y.; Fan, Z., *Journal of applied polymer science* **2005**, 97, 640.

(26)     Botha, L.; van Reenen, A., *European Polymer Journal* **2013**, 49, 2202.

(27)     Zhang, C.; Shangguan, Y.; Chen, R.; Wu, Y.; Chen, F.; Zheng, Q.; Hu, G., *Polymer* **2010**, 51, 4969.

(28)     Pires, M.; Mauler, R. S.; Liberman, S. A., *Journal of applied polymer science* **2004**, 92, 2155.

(29)     Randall, J., *Journal of Polymer Science Part A: Polymer Chemistry* **1998**, 36, 1527.

(30)     Santos, J. L.; Asua, J. M.; de la Cal, J. C., *Industrial & engineering chemistry research* **2006**, 45, 3081.

(31)     Covezzi, M.; Mei, G., *Chemical engineering science* **2001**, 56, 4059.

(32)     Tian, Z.; Xue-Ping, G.; Feng, L.-F.; Guo-Hua, H., *Chemical Engineering Science* **2013**, 101, 686.

(33)     Tian, Z.; Gu, X.-P.; Wu, G.-L.; Feng, L.-F.; Fan, Z.-Q.; Hu, G.-H., *Industrial & Engineering Chemistry Research* **2012**, 51, 2257.

(34)     Hutchinson, R.; Chen, C.; Ray, W., *Journal of Applied Polymer Science* **1992**, 44, 1389.

(35)    Bukatov, G.; Zaikovskii, V.; Zakharov, V.; Kryukova, G.; Fenelonov, V.; Zagrafskaya, R., *Polymer Science USSR* **1982**, 24, 599.

(36)    Skomorokhov, V.; Zakharov, V.; Kirillov, V.; Bukatov, G., *Polymer Science USSR* **1989**, 31, 1420.

(37)    Debling, J. A.; Ray, W. H., *Journal of applied polymer science* **2001**, 81, 3085.

(38)    Cecchin, G.; Marchetti, E.; Baruzzi, G., *Macromolecular Chemistry and Physics* **2001**, 202, 1987.

(39)    McKenna, T. F.; Bouzid, D.; Matsunami, S.; Sugano, T., *Polymer Reaction Engineering* **2003**, 11, 177.

(40)    Böhm, L. L., *Angewandte Chemie International Edition* **2003**, 42, 5010.

(41)    Chen, Y.; Chen, Y.; Chen, W.; Yang, D., *Polymer* **2006**, 47, 6808.

(42)    Kakugo, M.; Sadatoshi, H.; Yokoyama, M.; Kojima, K., *Macromolecules* **1989**, 22, 547.

(43)    Tanem, B.; Kamfjord, T.; Augestad, M.; Løvgren, T.; Lundquist, M., *Polymer* **2003**, 44, 4283.

(44)    Ratta, V., PhD Thesis Virginia Polytechnic Institute and State University, **1999**.

(45)    Robertson, D., Masters Thesis University of  Stellenbosch **2012**.

(46)    Gibbs, J. W., *American Journal of Science* **1878**, 441.

(47)    Schulz, E.; Wunderlich, B., *Academic, New York* **1976**, 50.

(48)    Mirabella, F. M., *Polymer* **1993**, 34, 1729.

(49)    Mahdavi, H.; Nook, M. E., *Polymer International* **2010**, 59, 1701.

(50)    Phiri, M. J.; Cheruthazhekatt, S.; Dimeska, A.; Pasch, H., *Journal of Polymer Science Part A: Polymer Chemistry* **2015**, 53, 863.

(51)    Cheruthazhekatt, S.; Mayo, N.; Monrabal, B.; Pasch, H., *Macromolecular Chemistry and Physics* **2013**, 214, 2165.

(52)    Mandelkern, L. *Crystallization of polymers*; 2nd Edition ed.; McGraw-Hill New York, **1964**, p 426.

(53)    Flory, P. J., **1953**.

(54)    Pasch, H.; Malik, M. I.; *Crystallization-Based Fractionation Techniques* In *Advanced Separation Techniques for Polyolefins*; Springer, **2014**,p 11.

(55)    Shirayama, K.; Okada, T.; Kita, S. I., *Journal of Polymer Science Part A: General Papers* **1965**, 3, 907.

(56)    Mirabella Jr, F. M., *Journal of Liquid Chromatography & Related Technologies* **1994**, 17, 3201.

(57)    Soares, J.; Hamielec, A., *Polymer* **1995**, 36, 1639.

(58)    Wild, L.; Ryle, T.; Knobeloch, D.; Peat, I., *Journal of Polymer Science: Polymer Physics Edition* **1982**, 20, 441.

(59)    Monrabal, B.; Blanco, J.; Nieto, J.; Soares, J. B., *Journal of Polymer Science Part A: Polymer Chemistry* **1999**, 37, 89.

(60)    Anantawaraskul, S.; Soares, J. B.; Wood-Adams, P. M.; *Fractionation of Semicrystalline Polymers by Crystallization Analysis Fractionationand Temperature Rising Elution Fractionation* In *Polymer Analysis Polymer Theory*; Springer, **2005**,p 1.

(61)    Aust, N.; Gahleitner, M.; Reichelt, K.; Raninger, B., *Polymer testing* **2006**, 25, 896.

(62)    Tomba, J. P.; Carella, J. M.; Pastor, J. M., *Journal of Polymer Science Part B: Polymer Physics* **2005**, 43, 3083.

(63)    Clark, D. E., *Chemical Health and Safety* **2001**, 8, 12.

(64)    Young, J. A. *Improving safety in the chemical laboratory: a practical guide*; 2nd Edition ed.; John Wiley & Sons. Inc., **1991**, p 350.

(65)    Kanthamas, T.; Piyapong, B.; Surat, A., *Open Journal of Polymer Chemistry* **2012**, 2012.

(66)    Pérez, C. J.; Cassano, G. A.; Vallés, E. M.; Failla, M. D.; Quinzani, L. M., *Polymer* **2002**, 43, 2711.

(67)    Scorah, M. J.; Zhu, S.; Psarreas, A.; McManus, N. T.; Dhib, R.; Tzoganakis, C.; Penlidis, A., *Polymer Engineering and Science* **2009**, 49, 1760.

(68)    Rocha, M. C.; Coutinho, F. M.; Balke, S. T., *Polymer testing* **1995**, 14, 369.

(69)    Ramos, V. D.; Costa, H. M. d.; Rocha, M. C. G.; Gomes, A. d. S., *Polymer Testing* **2006**, 25, 306.

(70)    Salakhov, I.; Boreiko, N.; Fatykhov, M.; Fedosova, S., *International Polymer Science and Technology* **2013**, 40, T29.

(71)    Muñoz, P. A. R.; Bettini, S. H. P., *Journal of Applied Polymer Science* **2013**, 127, 87.

(72)    Hamielec, A.; Gloor, P.; Zhu, S., *The Canadian Journal of Chemical Engineering* **1991**, 69, 611.

(73)    Azizi, H.; Ghasemi, I., *Iranian Polymer Journal* **2005**, 14, 465.

(74)    Latado, A.; Embiruçu, M.; Neto, A. G. M.; Pinto, J. C., *Polymer Testing* **2001**, 20, 419.

(75)    Gahleitner, M.; Jääskeläinen, P.; Ratajski, E.; Paulik, C.; Reussner, J.; Wolfschwenger, J.; Neißl, W., *Journal of Applied Polymer Science* **2005**, 95, 1073.

(76)    Yu, L.; Wu, T.; Chen, T.; Yang, F.; Xiang, M., *Thermochimica Acta* **2014**, 578, 43.

(77)    Krell, M.; Brandolin, A.; Vallés, E., *Polymer reaction engineering* **1994**, 2, 389.

(78)    Ryu, S.; Gogos, C.; Xanthos, M., *Advances in Polymer Technology* **1991**, 11, 121.

(79)    Berzin, F.; Vergnes, B.; Delamare, L., *Journal of applied polymer science* **2001**, 80, 1243.

(80)    Azizi, H.; Ghasemi, I., *Polymer testing* **2004**, 23, 137.

(81)    Kamfjord, T.; Stori, A., *Polymer* **2001**, 42, 2767.

(82)    Čapla, M.; Borsig, E., *European Polymer Journal* **1980**, 16, 611.

(83)    Robinson, A.; Marra, J.; Amberg, L., *Industrial & Engineering Chemistry Product Research and Development* **1962**, 1, 78.

(84)    Dionisi, R. A.; Failla, M. D.; Villar, M. A.; Quinzani, L. M.; Vallés, E. M., Macromolecular Symposia, 1998; p 127.

(85)    Tocháček, J.; Jančář, J.; Kalfus, J.; Zbořilová, P.; Buráň, Z., *Polymer Degradation and Stability* **2008**, 93, 770.

(86)    Fayolle, B.; Audouin, L.; Verdu, J., *Polymer degradation and stability* **2002**, 75, 123.

(87)    González-González, V.; Neira-Velázquez, G.; Angulo-Sánchez, J., *Polymer degradation and stability* **1998**, 60, 33.

(88)    Saw, L. T.; Rahim, N. A. A.; Viet, C. X., *Polymer Degradation and Stability* **2015**, 111, 32.

(89)    Edge, M., *Encyclopedia of Analytical Chemistry* **2006**.

(90)    Braun, D.; Richter, S.; Hellmann, G.; Rätzsch, M., *Journal of applied polymer science* **1998**, 68, 2019.

# *Chapter 3*

# **Experimental**

*This chapter begins with a list of the materials that were used for this study. It proceeds to give a brief outline of the procedure and experimental conditions that were used to degrade the polymer samples. It concludes by giving a list of the analytical techniques and experimental conditions that were used in the analysis of the degraded samples.*

## 3.1.    Materials

- Xylene (Sigma-Aldrich, 99 %) was used for polymer dissolution and elution during the P-TREF experiments.
- Deuterated 1,1,2,2-tetrachloroethane (TCE-d$_2$, Merk, 99.5 %) was used to dissolve samples in preparation for $^{13}$C NMR analysis.
- 1,2,4-trichlorobenzene (TCB) Reagent plus® (Sigma-Aldrich, ≥ 99 %) was used as a mobile phase in high temperature-size exclusion chromatography (HT-SEC).

### Stabilisers

A 2 wt% mixture of Irganox®1010/Irgafos®168, with respect to the polymer weight used, was used to prevent oxidative degradation of P-TREF samples during dissolution. 0.0125 wt% of butylated hydroxytoluene (BHT ≥ 99.0 %, Sigma-Aldrich) was added to the TCB mobile phase as a stabiliser during HT-SEC analysis.

### Heterophasic propylene-ethylene copolymer grades

The two heterophasic propylene-ethylene copolymer samples with different ethylene contents used in the present study were supplied by SASOL Polymers (Secunda, South Africa). Table 3.1 shows the ethylene content, isotacticity and molecular weight data of the two copolymers. The two samples are labelled CMR648 and CMR348 respectively.

Table 3.1          Properties of CMR648 and CMR 348 heterophasic propylene-ethylene copolymers.

| Sample | [Ethylene] [a] (mole%) | Isotacticity [a] (%mmmm) | $\overline{M}_w$ [b] (g.mol$^{-1}$) | $\overline{M}_n$ [b] (g.mol$^{-1}$) | Đ [b] |
|---|---|---|---|---|---|
| CMR648 | 18.5 | 81.5 | 364 600 | 34 000 | 10.7 |
| CMR348 | 9.4 | 90.6 | 430 100 | 82 300 | 5.2 |

[a] Ethylene content and isotacticity (%mmmm): determined from $^{13}$C-NMR

[b] $\overline{M}_w$, $\overline{M}_n$ and Đ: measured by HT-SEC

## Organic peroxides

Different concentrations of Trigonox®101 [2,5-Dimethyl-2,5-di(tert-butyl peroxy)hexane] and Trigonox®301 [3,6,9-triethyl-3,6,9-trimethyl-1,4,7-triperoxonane] (Akzo Nobel Polymer Chemicals, Amersfoort, Netherlands) peroxides were used to induce chain scission in the CMR648 and CMR348 samples. The structures of the Trigonox®301 and Trigonox®101 peroxides are illustrated in Figure 3.1.

The reactivity at various temperatures of an organic peroxide is usually determined by means of its half-life ($t_½$) at that specific temperature. Table 3.2 shows the half-lives ($t_½$) of both peroxides at 230 °C together with their molecular weights, total active oxygen contents and solubility parameters. The $t_{1/2}$ was calculated from using Equations 3.1 and 3.2 whilst the molecular weights and total active oxygen contents were obtained from literature. [1]

The solubility parameters were calculated according to the method proposed by Fedors. [2] According to the method, the deviation between the experimentally measured $\delta$ (solubility parameter) and the estimated $\delta$ (solubility parameter) is less than 5-10 %. This method is also believed to be better than Small's method based on two reasons: (1) It considers the contribution of a much larger number of functional groups and (2) only the structural formula of the compound is required for calculations.

a                                         b
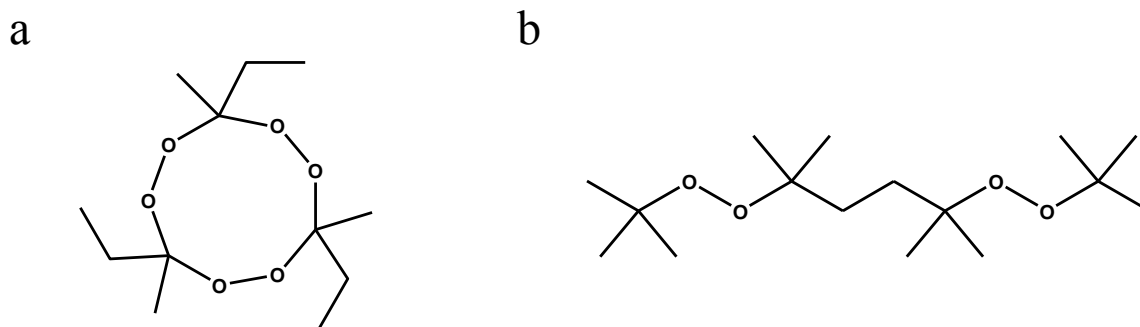


Figure 3.1        Chemical structures of (a) Trigonox®301 (T301) and (b) Trigonox®101 (T101)
                  peroxides

Table 3.2         Properties of Trigonox®101 and Trigonox®301organic peroxides.

| Organic peroxide | Half-life ($t_{1/2}$) at 230 °C (seconds) | $\overline{M}_w$ (g.mol$^{-1}$) | Solubility parameter ($\delta$) (Ca.cm$^{-3}$)$^{1/2}$ | Total active oxygen content (%) |
|---|---|---|---|---|
| Trigonox®101 | $4.28 \times 10^{-17}$ | 290.4 | 7.7 | 11.02 |
| Trigonox®301 | $7.04 \times 10^{-16}$ | 264.3 | 8.7 | 18.16 |

$$k_d = Ae^{-Ea/RT}$$

………………………..3.1

$$t_{1/2} = \frac{ln2}{k_d}$$

………………………3.2

Where,

$k_d$      =      Rate constant for the initiator dissociation (s$^{-1}$)

$t_{1/2}$      =      Half-life (s)

A      =      Arrhenius frequency factor (s$^{-1}$)

$E_a$      =      Activation energy for the initiator dissociation (J/mole)

R      =      gas constant (8.3142 J/mole.K)

T      =      temperature in K (273.15 + °C)K

## 3.2. Peroxide-induced chain scission of CMR348 and CMR648 bulk samples and their P-TREF fractions

Dry bulk copolymer samples and their TREF fractions were distinctively premixed with Trigonox®101 and Trigonox®301 peroxides in a beaker to prepare mixtures with peroxide concentrations of 0, 0.125, 0.25 and 0.5 wt% (The peroxides and bulk samples were in pellet form, whilst the Prep-TREF fractions were in powder form). The mixtures were then inserted into the MFI instrument (Section 3.3.2) with the block heated to 230 °C (Figure 3.4) for the thermal dissociation of the peroxides in the polymer melt. The polymer/peroxide mixtures were given a residence time of about 60 seconds in the heated block for the complete dissociation of the peroxides in the polymer melt. The polymer/peroxide mixtures were then extruded in the MFI instrument and the extrudates were then collected and further analysed using $^{13}$C-NMR, FTIR, HT-SEC and DSC. Various notations were used for sample identification purposes. For example, "CMR648-T101-0.25" stands for the bulk CMR648 sample mixed with 0.25 wt% of the Trigonox®101 peroxide and "CMR648-100-T101-0.25" stands for the 100°C fraction of the CMR648 sample mixed with 0.25 wt% of the Trigonox®101 peroxide.

## 3.3. Analytical techniques

### 3.3.1. Preparative-temperature rising elution fractionation (P-TREF)

A P-TREF setup (built in-house) was used for the preparative fractionation experiments. In the first step of the experiment, 3 g of each sample was mixed with a 2 wt% mixture of Irganox®1010/Irgafos®168. The mixture was then dissolved in 300 mL of xylene at 130 °C in a glass reactor (Figure 3.2a). After complete dissolution, pre-heated sea sand (white quartz, Aldrich, South Africa) was added into the solution and the reactor was transferred to an oil bath (pre-heated to 130 °C). The polymer/sand mixture inside the reactor was slowly cooled down to room temperature under controlled conditions at a rate of 1 °C/hour (Figure 3.2b). During the cooling step, the polymer segregated into layers of different composition and crystallinity on the sand particles [3,4], and these layers were separated and collected during the elution step.

In the second step of the P-TREF experiment, the polymer/sand mixture was packed into a stainless steel column and placed in a modified gas chromatograph oven. The temperature of the oven was increased in intervals at a steady rate and pre-heated xylene was pumped through

the stainless steel column. The fractions of increasing crystallizability became soluble at pre-determined temperatures (30, 100, 130 °C) and were collected at those pre-determined temperatures (Figure 3.3). After collection, the xylene was evaporated and the fractions were recovered by precipitation in acetone. Finally, the fractions were then dried to a consistent weight in a vacuum oven and stored for analysis with complementary analytical techniques ($^{13}$C-NMR, FTIR, HT-SEC and DSC).
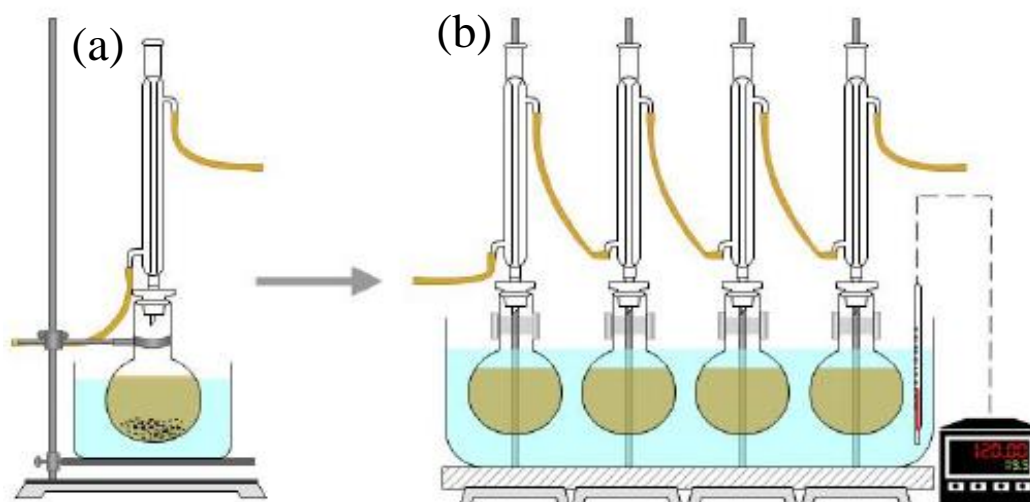


Figure 3.2    An illustration of (a) sample dissolution and (b) cooling of the sample solution during P-TREF [1]
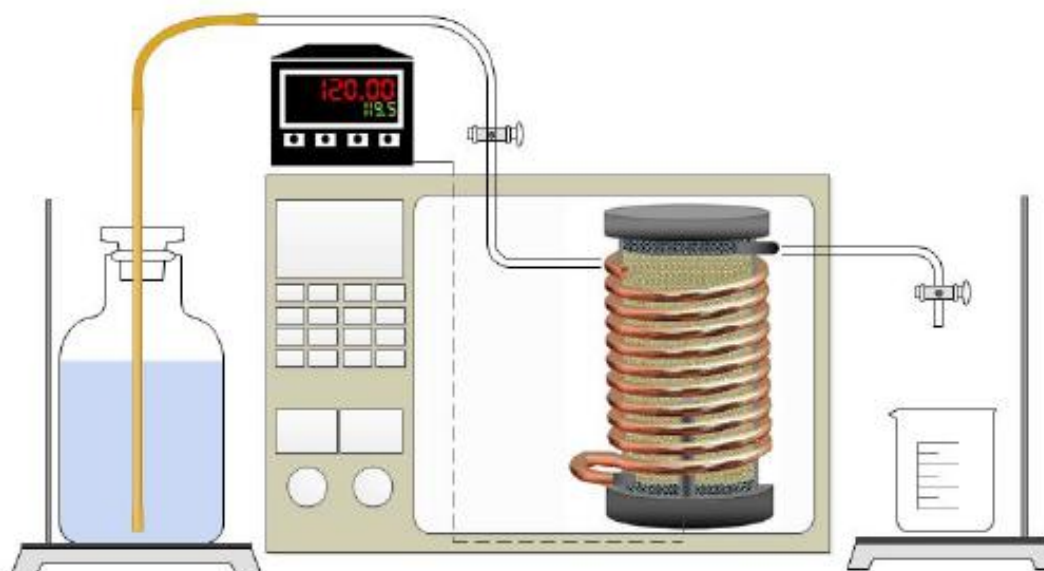


Figure 3.3        The elution setup used during P-TREF [1]

### 3.3.2.        Melt flow index (MFI)

The Melt flow index (MFI) was measured according to the ASTM D 1238 specifications using a Ceast 6542 extrusion plastometer at 230 °C/2.16 kg. Figure 3 shows a picture of the melt flow index instrument used in the present study.
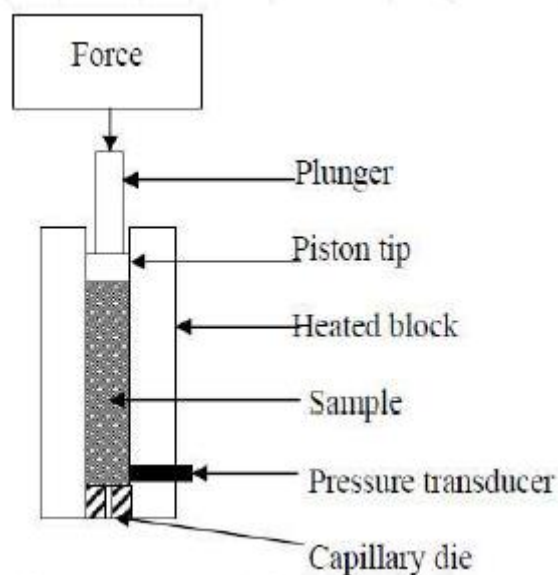


Figure 3.4        A schematic diagram of a MFI instrument [5]

### 3.3.3.        High temperature size exclusion chromatography (HT-SEC)

Molecular weight measurements for all the samples were carried out on a high temperature Polymer Laboratories PL 220 chromatograph (Polymer Laboratories, Varian Inc., Church Stretton, Shropshire, England). The injection block and column compartment were operated at 150 °C and at a flow rate of 1 ml.min$^{-1}$. The chromatographic system consisted of 300 mm ×75 mm PLgel Olexis columns (Polymer Laboratories, Varian Inc., Church Stretton, Shropshire, England) and a differential refractive index detector was used. The polymer samples were dissolved at 160 °C for two hours in 1,2,4-trichlorobenzene (TCB) Reagent plus® stabilized with butylated hydroxyltoluene (BHT) at a concentration of 2 mg/mL and 200 µl of each dissolved sample was injected into the column. Narrowly distributed polystyrene standards (Polymer standards service GmbH, Mainz, Germany) were used for calibration. Data acquisition and processing was carried out by means of a WinGPC software (Polymer standards service GmbH, Mainz, Germany).

### 3.3.4.        Differential scanning calorimetry (DSC)

The melting and crystallisation behaviour of the polymer samples were determined by means of a TA instruments Q100 calorimeter, calibrated with indium metal according to standard procedures. Approximately 6 mg of each polymer sample was weighed and heated from room temperature to 200 °C in the first cycle at a heating rate of 10 °C.min$^{-1}$ (to remove the thermal history of the samples). The temperature was then kept constant at 200 °C for 3 minutes, after which the sample was cooled to 25 °C at 10 °C.min$^{-1}$. The temperature was kept constant at 25 °C for 3 minutes and then heated to 200 °C. The data obtained from the second heating cycle were used for all the thermal analysis calculations. In all the DSC plots, the exothermic transitions were associated with the upwards curves while the endothermic transitions were associated with the downwards curves. The DSC measurements were carried out in a nitrogen atmosphere at a purge gas flow rate of 20 ml.min$^{-1}$.

### 3.3.5.        Fourier transform infrared spectroscopy (FTIR)

Attenuated total reflectance (ATR) measurements were carried out using a Nicolet iS10 FTIR spectrometer (Thermo Electron, Waltham, USA) consisting of a sensIR ATR attachment equipped with a ZnSe crystal. An incidence angle of 45° was used for all measurements. All spectra were collected at a resolution of 4 cm$^{-1}$ with 64 scans collected for each spectrum. An Automatic background subtraction was also performed for each spectrum.

### 3.3.6.        Carbon-13 nuclear magnetic resonance spectroscopy ($^{13}$C-NMR)

The samples used in the present study were dissolved in 1,1,2,2-tetrachloroethane to a final concentration of 6 wt%. High-resolution solution $^{13}$C-NMR spectra were obtained at 120 °C on a 600 MHz Varian$^{Unity}$ INOVA NMR Spectrometer. The following settings were used to obtain the solution NMR spectra: a 90° flip angle of ≈7.4 µs with inverse gated proton decoupling, an acquisition time of 1.8 s and a pulse delay of 15 s. Since only carbon atoms with $T_1$ relaxation delays of < 3 s were considered, the spectra are considered to be 99 % quantitative[6]

## 3.4.    References

(1)      Swart, M., PhD Thesis, University of Stellenbosch, **2013**.

(2)     Fedors, R. F., *Polymer Engineering & Science* **1974**, 14, 147.

(3)     Xu, J.; Feng, L., *European Polymer Journal* **2000**, 36, 867.

(4)     Monrabal, B., *Encyclopedia of Analytical Chemistry* **2000**.

(5)     Ariff, Z. M.; Ariffin, A.; Rahim, N. A. A.; Jikan, S. S. *Rheological behaviour of polypropylene through extrusion and capillary rheometry*; INTECH Open Access Publisher, **2012**, p 500

(6)     Assumption, H.; Vermeulen, J.; Jarrett, W. L.; Mathias, L. J.; Van Reenen, A., *Polymer* **2006**, 47, 67.

# *Chapter 4*
# **Results and Discussion**

*This chapter contains a brief discussion on the methodology that was developed to react the Trigonox®101 and Trigonox®301 organic peroxides with the heterophasic copolymers used in this study. A comparison between the solubility parameters of the organic peroxides and those of polyethylene and polypropylene is also provided in this chapter. Furthermore, this chapter also contains a detailed discussion on the different effects of the two peroxides on the bulk heterophasic ethylene-propylene copolymers (CMR648 and CMR348), and their fractions. Last, a brief conclusion on the degradation behaviour of the heterophasic ethylene copolymers (CMR648 and CMR348) with different ethylene contents is presented.*

## 4.1.   Introduction

Peroxide-induced chain scission of heterophasic ethylene-propylene copolymers has been reported since the 1980s. [1] Previous studies on peroxide-induced chain scission of heterophasic copolymers have shown that the various peroxides used for the degradation process induce distinctively unique structural changes to the heterophasic copolymers. However, despite this discovery, it is still unclear why the different peroxides induce different structural changes to the heterophasic copolymers. In the present study, we use chemically similar yet structurally different organic peroxides to treat heterophasic copolymers with different ethylene contents. We correlate the unique properties of the peroxides to the structural changes observed after the degradation process. We wanted to know if the distinct structural changes brought by the different peroxides are dependent on their solubility parameters, total oxygen contents and chemical structures or if the changes are primarily dependent on the ethylene content (and therefore structure) of each heterophasic copolymer.

This study was divided into three main parts. In the first part of this study, a methodology was developed that would represent extrusion visbreaking using peroxides (a detailed experimental procedure of the methodology is available in Chapter 3). The validity and reliability of our methodology was tested by repeating the degradation experiments three times and calculating the melt flow index (MFI) at each peroxide concentration. It is worth mentioning that the methodology was tested on the bulk polymer samples. Part two of the research involved fractionation of the treated copolymer samples into three distinct fractions. In part three of the study, the three fractions of each copolymer were treated using two peroxides and analysed by means of high temperature-size exclusion chromatography (HT-SEC), Fourier transform infrared spectroscopy (FTIR), differential scanning calorimetry (DSC) and carbon-13 nuclear magnetic resonance spectroscopy ($^{13}$C NMR).

## 4.2.  Development of a methodology for the reaction of Trigonox®101 and Trigonox®301 with the three fractions of CMR648 and CMR348 copolymers

Preliminary studies were performed on the bulk CMR648 and CMR348 samples to test the validity and reliability of the methodology. The MFI of the two heterophasic copolymers was determined about 8 times at each peroxide concentration in order to monitor the progress of the molecular weight breakdown with increasing peroxide concentration. Figures 4.1 and 4.2 show the MFI error bars and the influence of peroxide dosage (Trigonox®101 and Trigonox®301) on the MFI of CMR648 and CMR348 copolymers. The MFI value of both the CMR648 and CMR348 samples increased linearly with increasing peroxide concentration, indicating that the samples were successfully visbroken using our methodology. The linear relationship between the MFI value and the peroxide concentration was also reported by Salakhov *et al.* [2] Moreover, the samples treated with Trigonox®101 had a higher MFI value at each peroxide concentration than those treated with Trigonox®301.
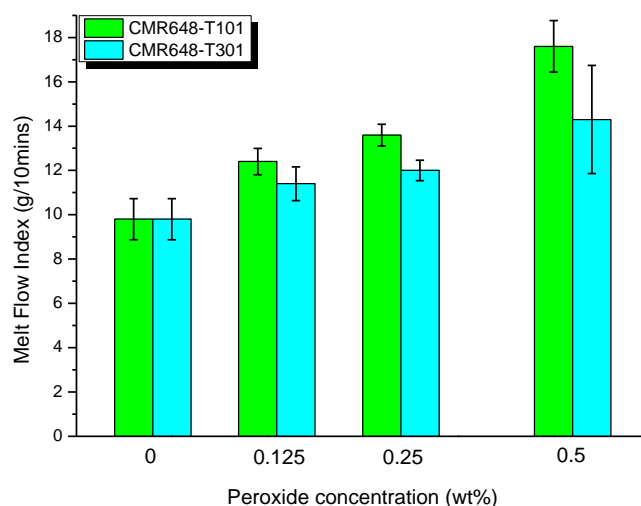


Figure 4.1    The effect of peroxide dosage (Trigonox®101 and Trigonox®301) on the melt flow index (MFI) of the CMR648 sample
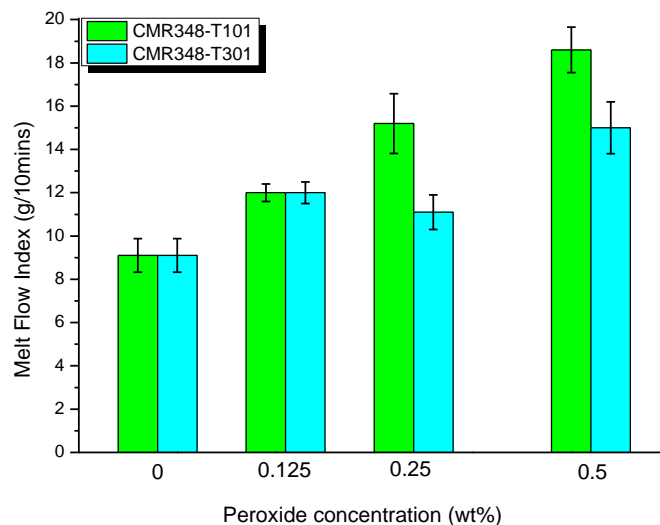
Figure 4.2        The effect of peroxide dosage (Trigonox®101 and Trigonox®301) on the melt flow index (MFI) of the CMR348 sample

HT-SEC analysis were also performed on the virgin CMR648 sample and the extruded one (without peroxide) to find out if there were any contributions from mechanical and thermal degradation in our methodology. Figure 4.3 compares the molecular weight distributions of the virgin CMR648 and the extruded CMR648 sample. A shift of the molecular weight distribution belonging to the virgin CMR648 sample, towards lower molecular weights after extruding it through the MFI instrument. Moreover, the molecular weight of the virgin CMR648 sample was decreased from about 523 700 to 390 000 after the extrusion process, indicating that mechanical and thermal degradation also contributed to the peroxide induced degradation of the sample. However, this is also expected to happen during extrusion visbreaking.
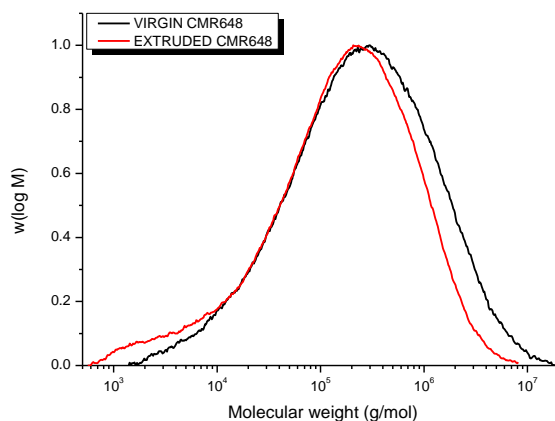
Figure 4.3    The molecular weight distributions (MWDs) of the virgin and extruded CMR648 samples

## 4.3.    Characterization of the peroxide-treated and untreated bulk CMR348 and CMR648 samples

### 4.3.1.    HT-SEC analysis

Size exclusion chromatography was performed on the bulk heterophasic copolymer samples to monitor the progress of their molecular weight decrease with increasing peroxide concentration. The molecular weight distributions of the CMR648 and CMR348 copolymers treated with Trigonox®101 and Trigonox®301 are shown in Figure 4.4 and Figure 4.5.

The untreated CMR648 and CMR348 samples exhibit a very slight shoulder at the low molecular weight side. This might be due to compositional heterogeneity of the samples. When the CMR648 sample was treated with either Trigonox®101 or Trigonox®301, there was a slight decrease of the shoulder. Narrowing of the molecular weight distribution curve, together with a shift of the peak maxima towards lower molecular weights was also observed with increasing Trigonox®101 peroxide dosage. In the case of the CMR648 sample treated with Trigonox®301, a narrowing of the molecular weight distribution curve was observed at 0.125 wt% and a slight broadening of the distribution curve on the high molecular weight side was observed at higher concentrations (0.25 and 0.5 wt%). A shift of the peak maxima was also observed with increasing peroxide concentration. The information shown by the HT-SEC curves was confirmed by the HT-SEC data tables shown in Appendix B (Table B − 1 and Table − 2). From

the HT-SEC data tables, it was shown that the weight average molecular weight of the CMR648 sample treated with Trigonox$^{®}$101 decreased from about 364 600 to about 302 000, at 0.5 wt% peroxide concentration. When the same sample was treated with Trigonox$^{®}$301, the molecular weight decreased to about 360 400, at 0.5 wt% peroxide concentration. The narrowing of the HT-SEC peaks indicates a lowering of dispersity (Đ) and the broadening of the peaks indicates an increase of dispersity.

When the CMR348 sample was treated with either of the peroxides, there was a significant shift and a broadening of the molecular weight distribution curve towards lower molecular weights with increasing peroxide dosage. The shift and broadening of the HT-SEC peaks is reflected by the HT-SEC data tables shown in Appendix B (Table B – 3 and Table B – 4). The broadening of the HT-SEC peaks reflect the increase in the dispersity with treatment of the samples with either of the peroxides, and the shift of the HT-SEC peaks is reflected in the decrease in molecular weight with increasing peroxide dosage. The HT-SEC data tables show that the molecular weight of the CMR348 sample treated with 0.5 wt% Trigonox$^{®}$101, decreased from about 430 100 to about 331 300, and when the same sample was treated with 0.5 wt% Trigonox$^{®}$301, the molecular weight decreased to about 336 100.. Since the CMR348 sample has a low ethylene content, the decrease in molecular weight might mostly be due to the chain scission of PP sequences.

From the HT-SEC data tables, the increase of the dispersity and therefore the broadening of the molecular weight distribution after visbreaking might be contradicting what was observed in literature. A possible explanation for this could be based on the compositional complexity of these materials. Due to complexity of these materials, a more heterogenous distribution of polymer sequences is achieved as a result of the peroxides "attacking" particular sequences more than others

The decrease in molecular weight appeared to be more significant for the samples treated with Trigonox$^{®}$101 relative to those treated with Trigonox$^{®}$301, indicating that the Trigonox$^{®}$101 peroxide might be more "active" with respect to a particular sequence. It is also observed that the decrease in molecular weight for both samples is lower than might be expected when we consider the changes in chemical composition after visbreaking (see Section 4.7.4), the possibility for this might also be that the peroxides are "attacking" specific sequences and

leaving out others. However, considering the complexity of the samples, crosslinking reactions might also be a contributing factor towards this.
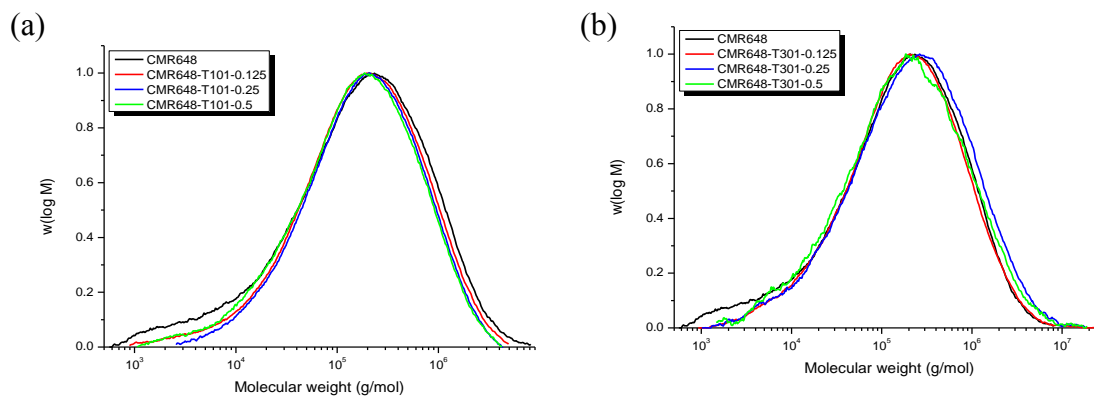


Figure 4.4    Molecular weight distributions (MWDs) of CMR648 samples before and after degradation with (a) Trigonox®101 and (b) Trigonox®301 peroxides
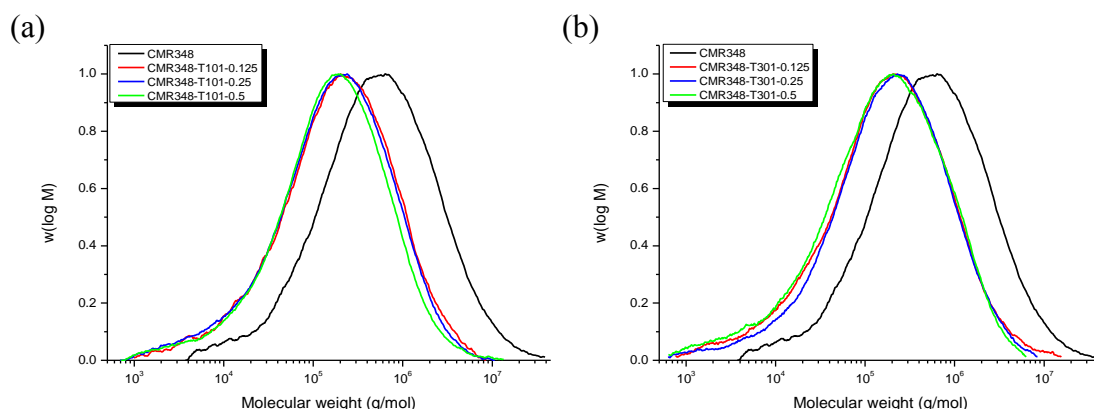


Figure 4.5    Molecular weight distributions (MWDs) of CMR348 samples before and after degradation with (a) Trigonox®101 and (b) Trigonox®301 peroxides

The tables showing the change in molecular weights with dosage of the peroxides are shown in Appendix B (Table B-1 to Table B-4)

### 4.3.2.    FTIR analysis

FTIR analyses were also performed on the bulk CMR648 and CMR348 copolymers to track down any structural changes sustained during the reaction. Figures 4.6 and 4.7 show the FTIR

spectra of the CMR648 and CMR348 samples before and after treatment with Trigonox®101 and Trigonox®301 peroxides.

Visible changes of the bands at 808, 1044, 1100 and 1216 cm$^{-1}$ were observed in both samples with increasing peroxide dosage. The band at 808 cm$^{-1}$ is assigned to PP helix segments with at least 7 propylene units, and the PP band at 1100 cm$^{-1}$ is associated with PP helix segments with at least 6 propylene units, respectively. Other bands of interest would be those at 720-730, 841, 998 and 973 cm$^{-1}$. The doublet band at 720-730 cm$^{-1}$ is a PE band in which the band at 720 cm$^{-1}$ is associated with 5 or more methyl rocking vibrations (2 or more continuous ethylene sequences) and the shoulder band at 730 cm$^{-1}$ indicates the presence of crystalline ethylene sequences, respectively. [3] The bands at 841, 998 and 973 cm$^{-1}$ are associated with PP helical lengths of at least 12, 10 and 3 to 4 propylene units, respectively. [4] No changes in these bands are visible in the FTIR spectra for the bulk polymer treated with peroxides. The visible changes of the PP bands at 808, 1044, 1100 and 1216 cm$^{-1}$ clearly indicate that the peroxides affected the short PP sequences more relative to the long PP sequences in these bulk samples.

In the CMR648 sample, we see a decrease of the PP bands at 808, 1044, 1100 and 1216 cm$^{-1}$, relative to the PP bands at 841, 998, 1163 cm$^{-1}$ at low concentrations (0.125 and 0.25 wt%) of the Trigonox®301 peroxide as shown by Figure 4.6 (a). This might be due to the peroxide "attacking" polymer sequences with at least 6, 7 or less propylene repeating units at those concentrations. The 1163 cm$^{-1}$ PP band is associated with at least 6 propylene units, respectively. [4] At 0.5 wt% of Trigonox®301, we see a slight decrease of the PP band at 1100 cm$^{-1}$ relative to the PP band at 1163 cm$^{-1}$, indicating that this peroxide was "attacking" polymer sequences with at least 6 propylene units at this concentration.

In the CMR648 sample treated with 0.125 wt% of Trigonox®101, we see that the decrease of the PP bands at 808, 1044, 1100 and 1216 cm$^{-1}$ was more, relative to the sample treated with Trigonox®301, at the same concentration (Figure 4.6 b). This might be due to the Trigonox®101 peroxide being more "active" with respect to a particular sequence. Since the PP bands at 1100 and 1163 cm$^{-1}$ are both associated with at least 6 propylene repeat units, their intensities were compared to relate this comparison to the polydispersity indices obtained from HT-SEC results. At 0.25 wt%, we see that the bands at 1163 and 1100 cm$^{-1}$ have similar intensities and that the intensities of the other PP bands at 808 and 1163 cm$^{-1}$ relative to those in the untreated sample,

are similar. This, together with the polydispersity index at this concentration (shown in Table B − 1), indicates that the Trigonox®101 peroxide at this concentration "attacks" the polymer sequences in this sample in such a way that the sample composition approaches a homogenous distribution of polymer sequences.
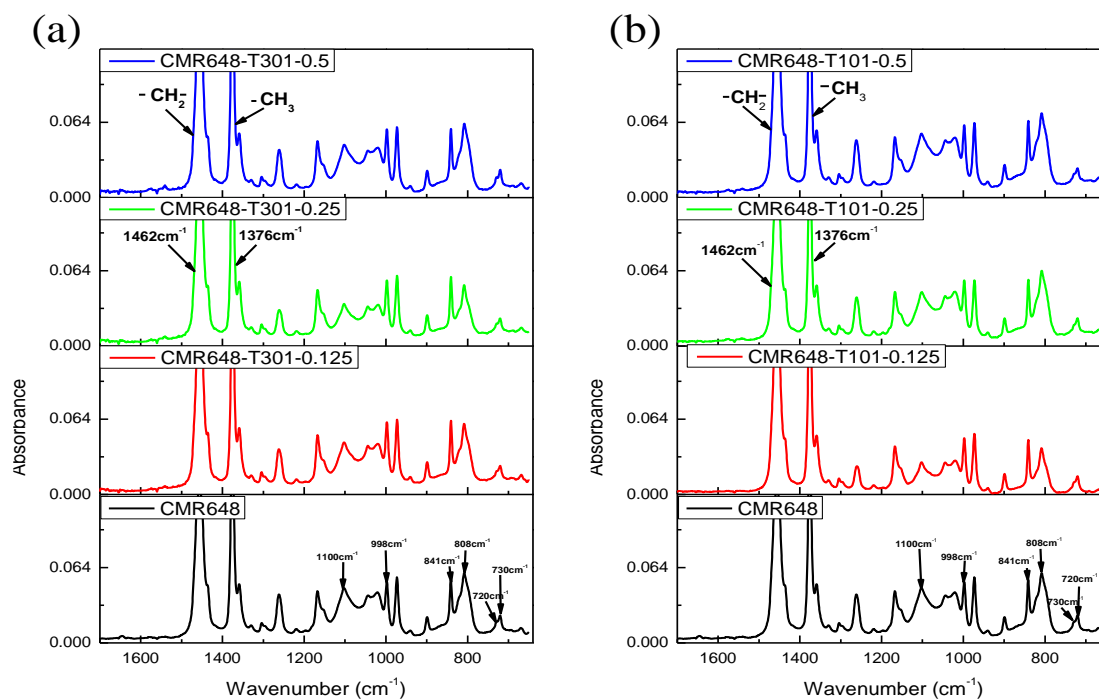


Figure 4.6     FTIR spectra of the CMR648 sample before and after degradation with (a) Trigonox®101 and (b) Trigonox®301 peroxides

In the CMR348 sample, we see a decrease of the PP bands at 808, 1044, 1100 and 1216 cm$^{-1}$, relative to the PP bands at 841, 998, 1163 cm$^{-1}$ at low concentrations (0.125 and 0.25 wt%), for both peroxides. This is suspected to be due to the scission of short propylene sequences (containing 6, 7 or less propylene units). An increase of the short propylene sequences was observed at 0.5 wt%, indicating that the peroxides might have been "attacking" certain sequences in the polymer matrix and thus allowing for the "release" of these PP sequences. The Trigonox®101 peroxide has more of an effect in this regard than the Trigonox®301 peroxide.
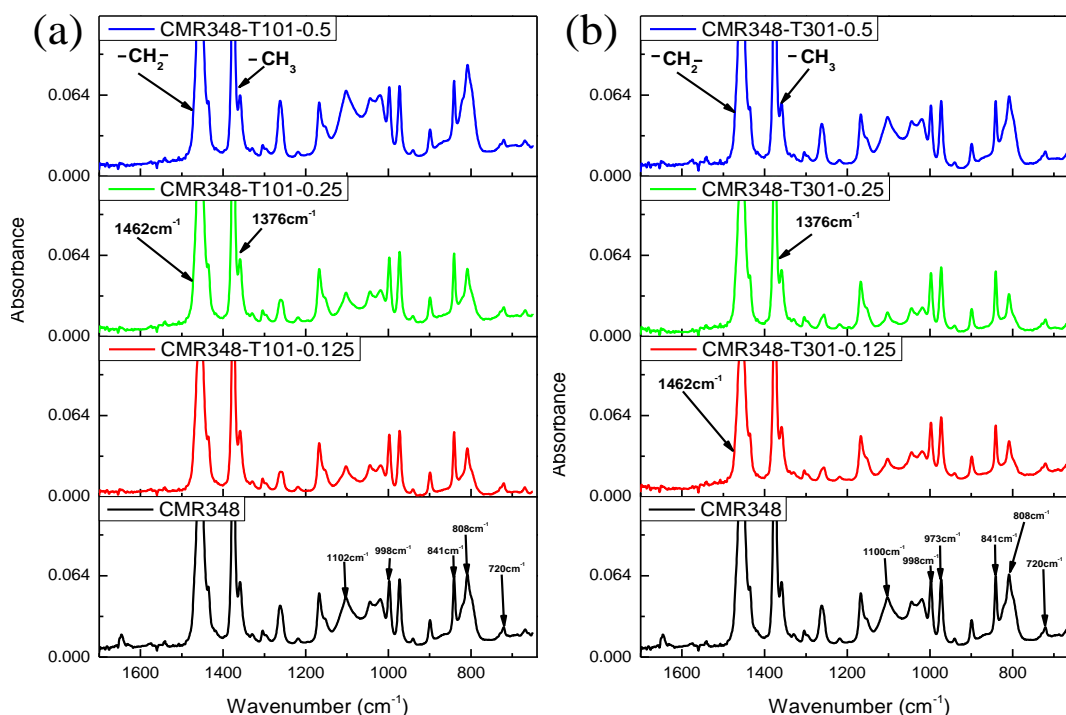
Figure 4.7    FTIR spectra of the CMR348 sample before and after degradation with (a) Trigonox®101 and (b) Trigonox®301 peroxides

## 4.3.3.        DSC analysis

Differential scanning calorimetry was performed on the bulk copolymer samples before and after reaction to monitor changes in their thermal properties as a result of the treatment. Figure 4.8 (a and b) and Figure 4.9 (a and b) show the DSC curves of the CMR648 sample before and after treatment with Trigonox®101 and Trigonox®301. Table 4.1 and Table 4.2 gives a tabular representation of the thermal properties represented by the DSC curves. Interestingly, there was no shift of the crystallisation and melting peaks belonging to the CMR648 and CMR348 samples with increasing Trigonox®101 and Trigonox®301 dosage. The lack of change in the melting and crystallization temperatures indicates that the isotactic PP fraction of the samples appears not to be affected by the peroxides. However, from Table 4.1, a slight decrease of the heat of fusion ($\Delta H_{melt}$ (J/g) at 0.25 wt% and a slight increase at 0.5 wt% was observed after treating the CMR648 sample with either Trigonox®101 or Trigonox®301 peroxides. In contrast, a slight decrease of the heat of fusion was observed at 0.125 wt% after treating the

CMR348 sample with Trigonox®101. When the same sample was degraded with the Trigonox®301 peroxide, an increase of the heat of fusion was observed with increase in peroxide concentration (Table 4.2). These results can be an indication that there were increasing chain irregularities with increase in peroxide dosage. [5]
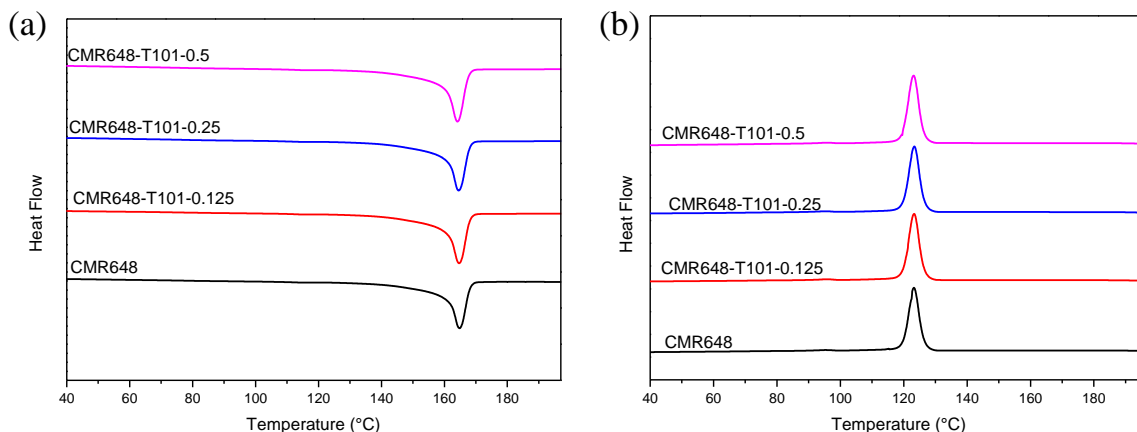


Figure 4.8    DSC (a) melting and (b) crystallisation curves of the CMR648 sample before and after degradation with Trigonox®101
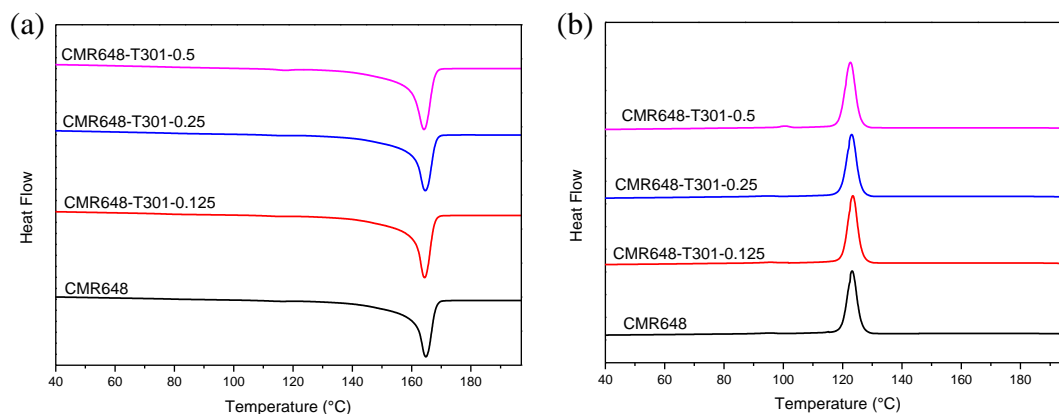


Figure 4.9    DSC (a) melting and (b) crystallisation curves of the CMR648 sample before and after degradation with Trigonox®301

DSC curves of the CMR348 sample before and after treatment with peroxides are shown in Appendix C (Figure C-1 and Figure C-2)

Table 4.1    Thermal properties of the CMR648 sample before and after degradation with Trigonox®101 and Trigonox®301 peroxides

| SAMPLE | $T_m$ (°C) | $T_c$ (°C) | $\Delta H_{melt}$ (J/g) |
|---|---|---|---|
| CMR648 | 164.8 | 123.2 | 74.0 |
| CMR648-T101-0.125 | 164.6 | 123.3 | 74.9 |
| CMR648-T101-0.25 | 164.5 | 123.3 | 73.2 |
| CMR648-T101-0.5 | 164.1 | 123.1 | 74.8 |
| CMR648-T301-0.125 | 164.4 | 123.5 | 74.1 |
| CMR648-T301-0.25 | 164.6 | 123.1 | 69.0 |
| CMR648-T301-0.5 | 164.1 | 122.6 | 74.9 |

Table 4.2    Thermal properties of the CMR348 sample before and after degradation with Trigonox®101 and Trigonox®301 peroxides

| SAMPLE | $T_m$ (°C) | $T_c$ (°C) | $\Delta H_{melt}$ (J/g) |
|---|---|---|---|
| CMR348 | 165.5 | 124.0 | 77.0 |
| CMR348-T101-0.125 | 165.5 | 124.1 | 74.5 |
| CMR348-T101-0.25 | 165.3 | 123.6 | 76.8 |
| CMR348-T101-0.5 | 164.8 | 123.7 | 75.4 |
| CMR348-T301-0.125 | 165.0 | 124.5 | 83.7 |
| CMR348-T301-0.25 | 165.4 | 124.2 | 86.9 |
| CMR348-T301-0.5 | 164.6 | 124.3 | 89.4 |

Up to this point, it has been observed that the Trigonox®101 and Trigonox®301 peroxides did induce chemical changes in the bulk CMR648 and CMR348 samples. It has also been observed

that the bulk CMR648 and CMR348 samples were affected by both peroxides. However, we were still uncertain about how each phase of the heterophasic copolymers is uniquely affected by the peroxides and how each of the structural changes in these phases contribute to the overall changes that were observed in the bulk.

## 4.4.    Fractionation of CMR648 and CMR348 copolymers using P-TREF

The bulk CMR648 and CMR348 samples were fractionated into three fractions (30, 100 and 130 °C) representing the three main parts of heterophasic copolymers. The fractionation was performed to achieve a thorough characterization of the individual parts of the heterophasic copolymers before and after degradation. Figure 4.10 (a and b) compares the percentage weights of the different fractions belonging to the undegraded CMR648 and CMR348 samples after four elutions of a single P-TREF experiment. The content of the 30 and 100 °C fractions was found to be higher in the CMR648 sample than the CMR348 sample. This might be due to a higher ethylene content in the CMR648 sample than in the CMR348 sample. Both the CMR648 and CMR348 samples exhibit a high content of the 130 °C fraction. This shows that the bulk of these materials is made up of crystalline iPP.
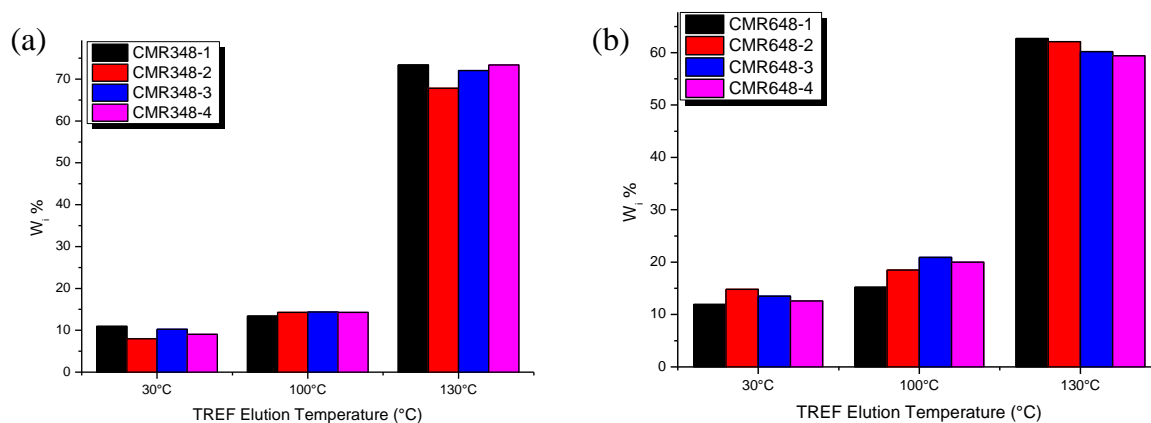


Figure 4.10    Weight percentages of the P-TREF fractions obtained from (a) CMR648 and (b) CMR348 samples after 4 consequitive fractionations

## 4.5.    Evaluation of the solubility of Trigonox®101 and Trigonox®301 peroxides in the CMR648 and CMR348 copolymers

Solubility parameters of the Trigonox®101 and Trigonox®301 peroxides were calculated to ascertain their miscibility with the polypropylene (PP) rich and polyethylene (PE) rich phases of the CMR648 and CMR348 samples. Figure 4.11 compares the solubility parameters of the peroxides to those of PE and PP. The structures and annotations of the peroxides are given in Figure 3.1.

A comparison of the solubility parameters of the different peroxides and polyolefins, suggests that a peroxide like Trigonox®101 (T101) is more miscible with ethylene rich copolymers than with the homopolymeric PP-phase, whereas an opposite distribution is expected for the Trigonox®301 (T301) peroxide.
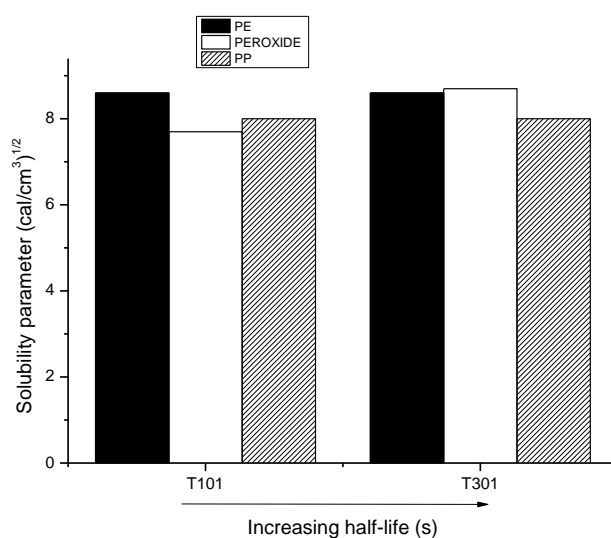


Figure 4.11    A comparison of the solubility parameters of PE and PP with those of the Trigonox®101 and Trigonox®301 peroxides

## 4.6.    Characterization of untreated TREF fractions of the CMR348 and CMR648 copolymers

The 30, 100 and 130 °C fractions of the untreated CMR648 and CMR348 samples were analysed using HT-SEC, FTIR, DSC and $^{13}$C NMR to ascertain their chemical composition.

These results will be compared with those of the degraded copolymers and this will assist in monitoring the structural changes induced by the different peroxides during degradation.

### 4.7.1. HT-SEC analysis

Figure 4.12 (a and b) compares the molecular weight distributions of the 30, 100 and 130 °C fractions belonging to the CMR648 and CMR348 samples. In both the CMR648 and CMR348 samples, the 100 °C fraction exhibits a bi-modal distribution whereas the 130 °C fraction shows a mono-modal distribution. Similar results were also shown by Tochacek *et al.* [6] The 30 °C fraction also shows a mono-modal distribution, together with a slight shoulder in the low molecular weight region of the distribution. This is similar to what was shown by De Goede *et al.* [7] The appearance of a bi-modal distribution indicates compositional heterogeneity, which is often caused by the co-elution of non-identical products. This is commonly seen in the mid-temperature elution fractions of heterophasic copolymers. [8,9] The low and the high molecular weight components of the bi-modal distribution were found to consist mainly of PP homopolymer and ethylene-propylene copolymer sequences. [10]
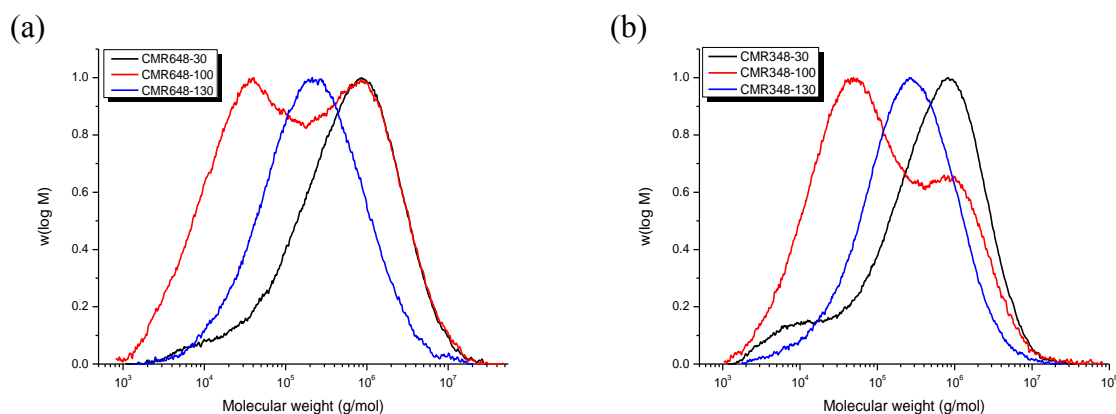


Figure 4.12     A comparison of the MWD curves of the 30, 100, 130 °C fractions in the (a) CMR648 and (b) CMR348 samples

### 4.7.2. FTIR analysis

Figure 4.13 (a) and (b) compares the FTIR spectra of the 30, 100 and 130 °C fractions in both CMR648 and CMR348 samples. The spectrum of the 100 and 130 °C fractions in both samples, show bands at 720-730, 998 and 841, 1303 cm$^{-1}$, which are assigned to PE and PP crystalline

parts respectively [11]. Moreover, the bands at 841, 998 and 1303 cm$^{-1}$ belong to helix segments for iPP with at least 11, 14 and 13 propylene units, respectively. [11] The band at 720 cm$^{-1}$ is due to 5 or more $CH_2$ rocking vibrations (2 or more continuous E sequences). The appearance of the shoulder band at 730 cm$^{-1}$ indicates the presence of crystalline PE sequences. [3] In the 30 °C fraction, the band at 730 cm$^{-1}$ is not observed, indicating the absence of long (crystallisable) ethylene sequences in this fraction. In addition to that, we also see an absence of the PP bands at 841, 998 and 1303 cm$^{-1}$ in the 30 °C fraction, indicating the absence of long crystallisable PP sequences in this fraction. Therefore, since it has no bands assigned to crystalline PE and PP, the 30 °C fraction is thought to be composed of ethylene-propylene random copolymers. The 100 °C fraction appears to be a complex mixture of partially crystalline (co)polymers that contain crystallisable ethylene and / or propylene sequences. In contrast to the compositional complexity of the 30 and 100°C, the composition of the 130 °C fraction is simple. This fraction is composed mainly of isotactic PP since there are no bands at 720 and 730 cm$^{-1}$ which are assigned to PE.
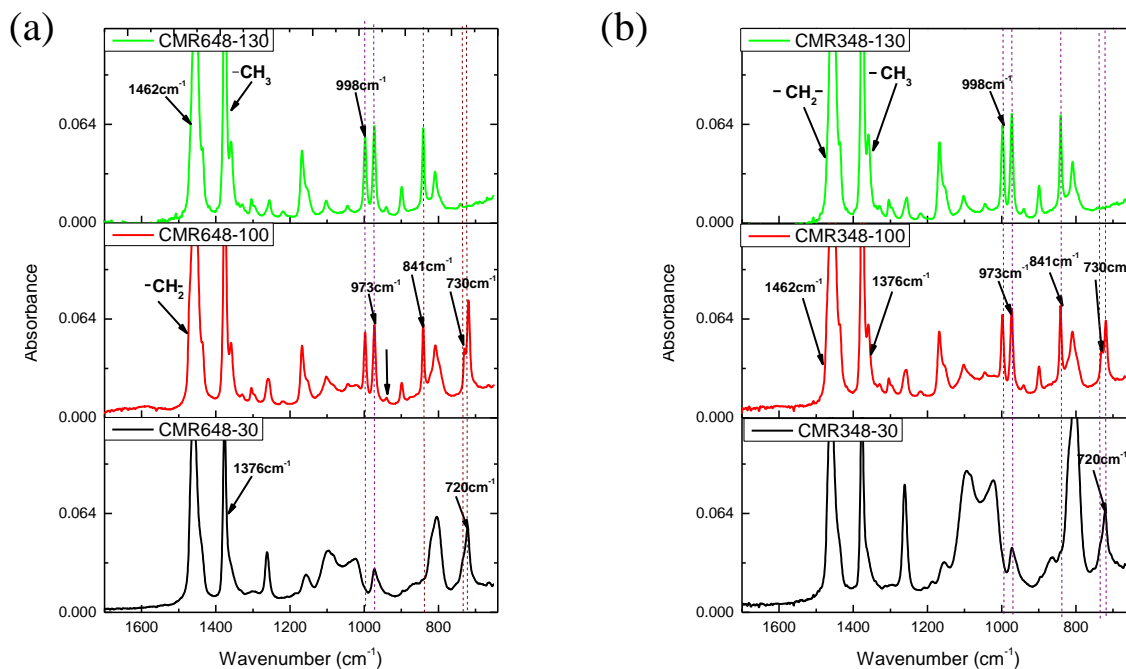


Figure 4.13    A comparison of the FTIR spectra of the 30, 100, 130 °C fractions in the (a) CMR648 and (b) CMR348 samples

### 4.7.3.        DSC analysis

The melting and crystallisation behaviour of the 30, 100 and 130 °C fractions in both CMR648 and CMR348 samples was evaluated using differential scanning calorimetry.

Figure 4.14 (a and b) and Figure 4.15 (a and b) shows the melting and crystallisation behaviour of the fractions in both samples. In the 130 °C fraction, a clear melting peak is observed around 160 °C, indicating that this fraction consists mainly of isotactic PP, as confirmed by the FTIR results. The appearance of the slight shoulder in this fraction might be due to the presence of some copolymer or disrupted PP sequences.

Due to the appearance of a flat DSC curve in the 30 °C fraction, it is concluded that this fraction consists of amorphous polymeric material. In the case of the 100 °C fraction, a weak melting peak is observed around 120 °C in the CMR648 sample (Figure 4.14 a) and around 114.3 °C in the CMR348 sample (Figure 4.15 a), which is attributed to the presence of PE in the fraction (or maybe a copolymer). This is confirmed by the absence of this peak in the 130 °C fraction and the presence of the PE doublet band in the FTIR spectra of this fraction. In addition, two melting peaks are also observed around 156 and 160 °C, which are due to the melting of less perfect crystals. These less perfect crystals are formed as a result of ethylene insertion into PP chains during polymerisation. These ethylene units disturb the order in the PP chains, consequently causing defective crystals. These less perfect crystals melt, re-crystallise and melt at higher temperatures, where they have more mobility, and this gives rise to the second melting peak. The deformed crystals formed upon recrystallization have shorter chains. [12]

Figure 4.14 (a and b) and Figure 4.15 (a and b) shows that upon cooling, all the fractions show one clear crystallisation peak at the same temperature, which indicates that, for the current thermal conditions, crystallisation of their matrix component occurs at the same temperatures.[13] A weak exotherm is also observed around 100 °C in the 100 °C fraction of both samples, and is suspected to be due to the crystallisation of PE (or maybe a copolymer). This shows that the 100 °C is a blend of crystalline PP and PE sequences.
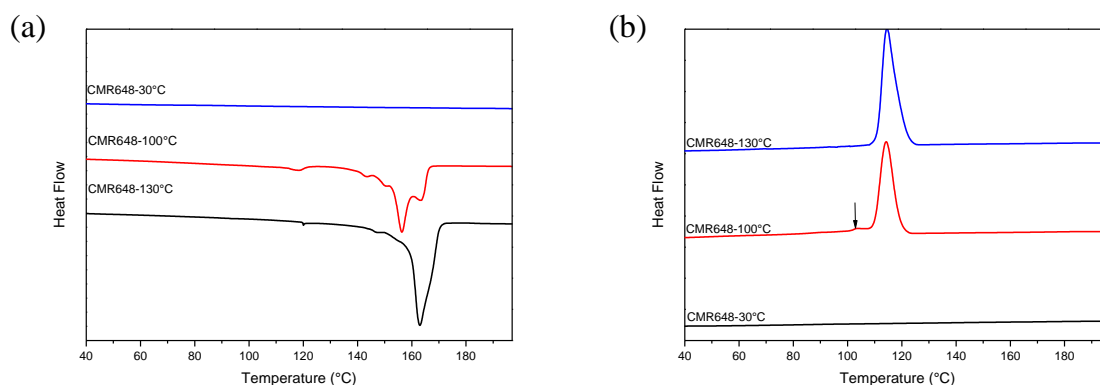
Figure 4.14    A comparison of the DSC (a) melting and (b) crystallisation curves of the 30, 100, 130 °C fractions in the CMR648 sample
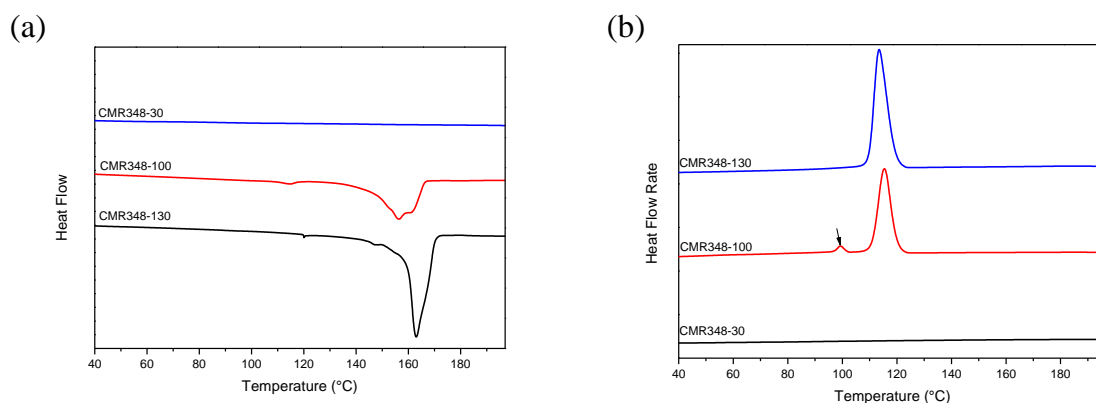


Figure 4.15    A comparison of the DSC (a) melting and (b) crystallisation curves of the 30, 100, 130 °C fractions in the CMR348 sample

The melting and crystallisation temperatures of the different TREF fractions in both sample are shown in Appendix C (Table C - 5 and Table C – 6).

### 4.7.4.        $^{13}$C NMR analysis

$^{13}$C NMR was used to determine the ethylene content and monomer sequence distributions of all the TREF fractions. The ethylene content was calculated according to relationships established by Nakatani et al. [14], whereas the monomer sequence distributions were calculated according to relationships developed by Ray et al. [15] and Randall. [16] Figure 4.17 (a and b) compares the spectrum of each fraction in CMR648 and CMR348 samples. The notation used to assign the peaks in the spectra is represented in Figure 4.16. Moreover Table 4.3 and Table 4.4 show the triad distribution measurements and ethylene sequence lengths in the

different fractions. It is observed that the ethylene content decreases with increasing elution temperature. The "blocky" E (PEE triads) and P (PPE triads), together with the isolated E (PEP triads) and P (EPE triads), seem to decrease with increasing elution temperature. However. In the case of the PPP triads, an increase is observed with increasing elution temperature. There is also an initial increase of the EEE triads in the 100 °C fraction and a subsequent decrease at the 130°C fraction.

The high amount of "blocky" E and P triads, isolated E and P triads and the low content of PPP, EEE triads in this fraction, confirms that the 30 °C fraction is composed of random ethylene-propylene copolymers. The presence of the PE and PP melting peaks, the presence of the 720 and 730 cm$^{-1}$ and the high content of EEE and PPP is a confirmation that the 100 °C consists of a blend of ethylene and propylene rich polymers. [14] The high content of PPP triads, the presence of a clear melting peak around 160 °C and the absence of the bands at 720 and 730 cm$^{-1}$, confirm that the 130 °C fraction consist mainly of homo-isotactic PP.
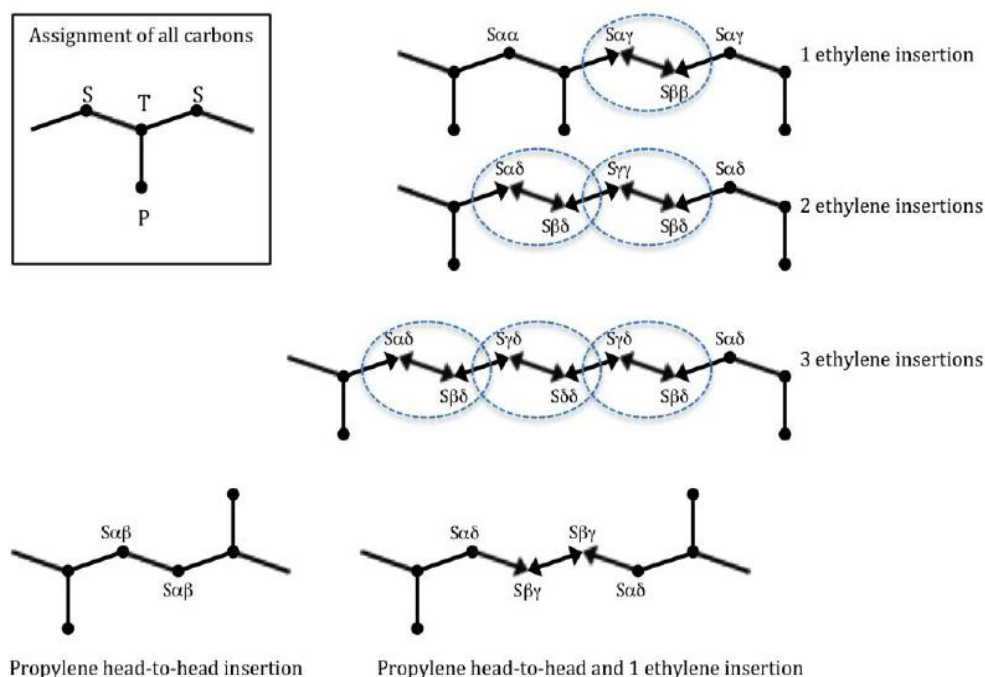


Figure 4.16    Carbon assignment used for $^{13}$C solution NMR adapted from Carman and Wilkes [17] and Ray *et al.* [15]

In Figure 4.17 (a) and (b), we see three major peaks, namely $S_{\alpha\alpha}$ (CH$_2$), $T_{\beta\beta}$ (CH) and $P_{\beta\beta}$ (CH$_3$), which are associated with the three carbons in the constitutional base unit of PP.

Moreover, the $S_{\delta\delta}$ resonance peak observed in the 30 and 100 °C fractions is associated with the CH$_2$'s in PE. The minor peaks ($S_{\alpha\gamma}$; $S_{\alpha\delta}$; $S_{\beta\delta}$; $S_{\gamma\delta}$; $T_{\delta\delta}$; $P_{\beta\delta}$; $P_{\delta\delta}$) in the 30 and 100 °C fractions indicate the presence of triad sequences such as PEP, EPE, PPE, EEP, as junctions between longer ethylene and propylene segments. [18] The absence of the $S_{\alpha\beta}$ resonance peak in the spectrum indicates the absence of inverted propylene units.

(a)



(b)
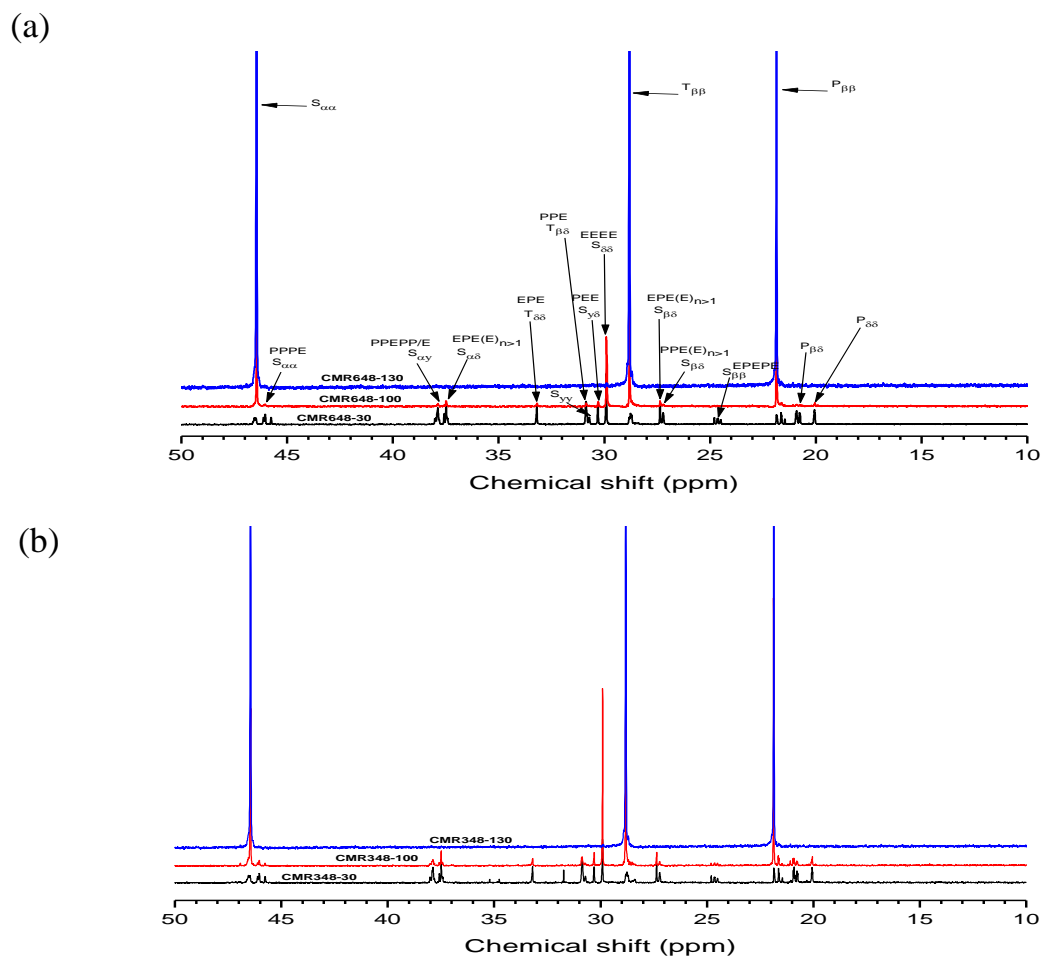


Figure 4.17    A comparison of the ^{13}C NMR spectra of the 30, 100, 130 °C fractions in the (a) CMR648 and (b) CMR348 sample

Table 4.3     Monomer sequence distribution data for the 30, 100, 130 °C TREF fractions in CMR648

| CMR648 fraction (°C) | PPP | Triad sequence distribution[a] (mol %) | | | | EEE | Ethylene content[b] (mol %) |
|---|---|---|---|---|---|---|---|
| | | PPE | EPE | PEP | PEE | | |
| 30 | 12.5 | 17.1 | 8.1 | 14.2 | 26.6 | 21.8 | 62.6 |
| 100 | 60.7 | 2.0 | 2.9 | 1.3 | 5.2 | 26.7 | 33.2 |
| 130 | 100.0 | 0.0 | 0.0 | 0.0 | 0.0 | 0.0 | 0.0 |

[a] P, propylene unit; E, ethylene unit.

[b] Ethylene content = PEP+PEE+EEE

Table 4.4     Monomer sequence distribution data for the 30, 100, 130 °C TREF fractions in CMR348

| CMR348 fraction (°C) | PPP | Triad sequence distribution (mol %) | | | | EEE | Ethylene content (mol %) |
|---|---|---|---|---|---|---|---|
| | | PPE | EPE | PEP | PEE | | |
| 30 | 15.4 | 18.0 | 8.4 | 14.1 | 21.4 | 18.8 | 54.3 |
| 100 | 61.2 | 5.2 | 2.2 | 2.3 | 4.6 | 24.2 | 31.1 |
| 130 | 100.0 | 0.0 | 0.0 | 0.0 | 0.0 | 0.0 | 0.0 |

## 4.7.     Comparison of the effects that both the Trigonox®101 and Trigonox®301 peroxides have on each P-TREF fraction of the CMR348 and CMR648 sample

All the fractions in the CMR648 and CMR348 samples were treated with the same peroxide concentration (0.25 wt%), and the structural changes induced by each peroxide were studied by HT-SEC, FTIR, DSC and $^{13}$C NMR.

### 4.8.1.        HT-SEC analysis

The effect of the Trigonox$^{®}$101 and Trigonox$^{®}$301 peroxides on the molecular weight distributions of all the TREF fractions was investigated using high temperature size exclusion chromatography. Figure 4.18 (a-f) compares the effect of both peroxides on the TREF fractions of both samples.

In the 30 °C fraction of the CMR648 sample (Figure 4.18 a), we see a shift, towards lower molecular weights, of the peak maxima and a narrowing of the HT-SEC curves belonging to the treated fractions. The narrowing of the HT-SEC curves shows that the distribution of sequences in the treated fractions is homogenous relative to that of the untreated fraction, and the shift of the peak maxima shows that there was a scission of particular sequences in the treated fractions. However, the fraction treated with Trigonox$^{®}$301 had more of an effect in this regard than the one treated with Trigonox$^{®}$101. Since the 30 °C fraction consists of mainly ethylene-propylene copolymers (as confirmed by FTIR and $^{13}$C NMR), this indicates that the Trigonox$^{®}$301 peroxide has more of an effect with respect to a particular sequence in this fraction.

In the case of the 30 °C fraction belonging to the CMR348 sample (Figure 4.18 d), not only do we observe a slight shift of the peak maxima and narrowing of the HT-SEC curves, but there is also a decrease of the low molecular weight shoulder, respectively. This shows that the peroxides "attack" particular sequences in the treated fractions in such a way that a homogenous distribution of sequences is achieved relative to the untreated fractions. Once again, the Trigonox$^{®}$301 peroxide has more of an effect in this regard.

In the case of the 100 °C fraction belonging to the CMR648 sample (Figure 4.18 b), a significant decrease of the high molecular weight distribution is observed for the fraction treated with Trigonox$^{®}$301, whereas the phase separation between the low and high molecular weight distributions becomes distinct when the fraction is treated with Trigonox$^{®}$101. This indicates that the Trigonox$^{®}$301 peroxide might be "attacking" a particular sequence more, in the ethylene-propylene copolymers, relative to the PP homopolymer sequences, and that the Trigonox$^{®}$101 might be "attacking" both the PP homopolymer and ethylene-propylene sequences in such a way that there is an even distribution of the two.
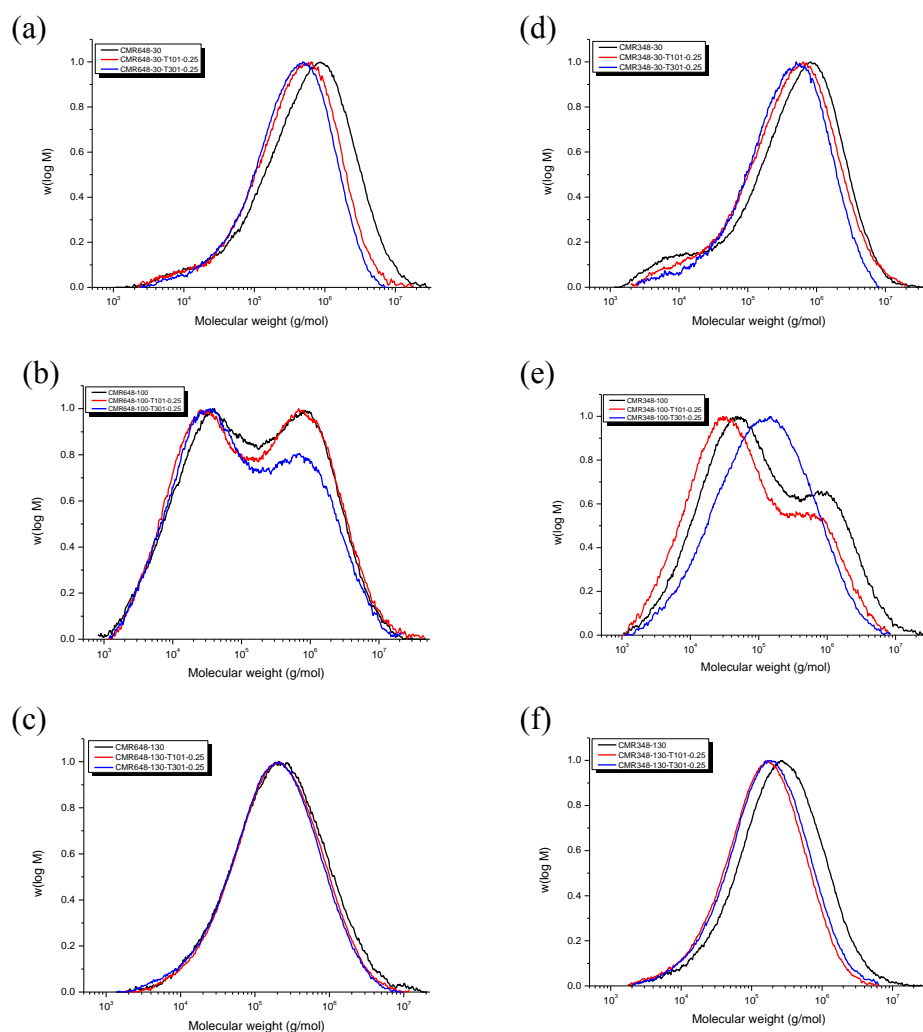
Figure 4.18    A comparison of the MWD curves of the untreated and treated 30, 100, 130 °C TREF fractions belonging to the CMR648 (a-c) and CMR348 (d-f) samples

In the case of the CMR348 sample (Figure 4.18 e), a shift of the molecular weight distribution curve towards lower molecular weights and a slight decrease of the high molecular weight distribution is observed in the 100 °C fraction treated with Trigonox®101, whereas in the fraction treated with Trigonox®301, a narrow mono-modal peak is obtained. This might be due to the Trigonox®101 peroxide "cutting down" longer sequences and "cutting down" a particular sequence in the ethylene-propylene copolymers and PP homopolymers. Moreover, the observations made in relation to the Trigonox®301 peroxide, might be due to the peroxide "attacking" the PP homopolymer and ethylene-propylene copolymers in such a way that a homogenous distribution of sequences is achieved, relative to the untreated fraction.

The reproducibility of the result in Figure 4.18 (e) is complemented by the DSC result obtained in Figure 4.20 (d) which indicates that a more crystalline material is obtained as the fraction is treated with Trigonox®301.

The shift, towards lower molecular weights of the molecular weight distribution belonging to the treated 130 °C fractions of the CMR648 is almost insignificant (Figure 4.18 c). However, in the CMR348 sample, the shift was profound (Figure 4.18 f). However, the shift is more significant in the 130 °C fraction degraded with Trigonox®101, respectively. Since the 130 °C fraction, consists mostly of homo-isotactic PP, this might be due to the Trigonox®101 peroxide being miscible with PP (as confirmed by the solubility parameter results).

### 4.8.2.      FTIR analysis

Fourier transform infrared spectroscopy was used to investigate about the different structural changes induced by the Trigonox®101 and Trigonox®301 peroxides on the 30, 100 and 130 °C fractions. Figure 4.19 (a-f) shows the FTIR spectra of all the TREF fractions belonging to the CMR648 and CMR348 samples.

In the 30 °C fraction of the CMR648 sample (Figure 4.19 a), we see the appearance of a new band around 1190 cm$^{-1}$ for both peroxides. This does not happen with the CMR348 sample, indicating that this change is dependent on the chemical nature of the fraction. This is most likely due to molecular weight differences as well. The Trigonox®101 peroxide has more of an effect in this regard than the Trigonox®301 peroxide. This means that in this particular case, the Trigonox®101 peroxide is more "active'' with respect to a particular sequence. This observation is further enhanced by the observation of the band at 973 cm$^{-1}$. This band is due to methyl rocking vibrations of atactic (amorphous) polypropylene. [19] The 973 cm$^{-1}$ band is also associated with helix segments with at least 3 to 4 propylene repeat units, respectively. [4] With increase of the PP band at 973 cm$^{-1}$, we see a splitting of the band at 1100 cm$^{-1}$ .This band is usually associated with helix segments with at least 6 propylene units, respectively. [4] This band is greatly influenced by the conformational environment of polymer chains. The splitting might be due to the presence of short P sequences with different conformational environments, as a result of chain scission, confirmed by the HT-SEC results shown in Figure 4.18 (a). The

increase in the intensity of the band at 973 cm$^{-1}$ might be due to a "release" of short PP sequences, as a result of chain scissions.

In the case of the 30 °C fraction belonging to the CMR348 sample (Figure 4.19 d), we see a slight increase in intensity of the band at 1100 cm$^{-1}$. Based on the HT-SEC results, this might also be due to a "release" of short PP sequences, as a result of chain scission. No "new" band is seen around 1190 cm$^{-1}$ and no splitting is observed at 1100 cm$^{-1}$ for both peroxides. This must be due to the difference in chemical composition, with the CMR348 having a lower ethylene content.

In the 100 °C fraction of the CMR648 sample, we see a decrease of the PE doublet band around 730-720 cm$^{-1}$ for both peroxides, and a splitting of the band around 1100 cm$^{-1}$ together with an appearance of a weak band around 1193 cm$^{-1}$. The Trigonox$^{®}$301 peroxide has more of an effect in this regard than the Trigonox$^{®}$101 peroxide. It is clear from the FTIR spectra that the Trigonox$^{®}$101 peroxide had a similar effect on the PP bands (808, 841, 973, 998 and 1163 cm$^{-1}$) as on the PE doublet band, and this is seen when comparing the ratios of this bands relative to the untreated fraction. Moreover, the Trigonox$^{®}$301 peroxide affected the PE doublet band more relative to the PP bands. Based on the solubility parameter results (Figure 4.11), this might be due to the Trigonox$^{®}$301 peroxide being highly miscible with the PE rich phase. The observations made in this fraction correlate well with the HT-SEC results shown in Figure 4.18 (b). Based on these HT-SEC curves and the FTIR spectra shown in Figure 4.19 (b), it is clear that the Trigonox$^{®}$101 peroxide affected the PP homopolymer and ethylene-propylene copolymer sequences similarly, and that the Trigonox$^{®}$301 peroxide affected the the ethylene-propylene copolymer sequences more than the PP homopolymer sequences. The weak band appearing at 1190 cm$^{-1}$ might be due to short PP sequences that were "released" as a result of of the peroxide "acting" on neighbouring E sequences, since this band is not distinct in the fraction treated with Trigonox$^{®}$101. The splitting of the 1100 cm$^{-1}$ band becomes more distinct with the decrease in the PE doublet band and since the PP bands at 841, 973, 998 and 1163 cm$^{-1}$ seem to be unaffected by the Trigonox$^{®}$301 peroxide, the splitting of the band might be due to a change in the conformational environment of the short PP sequences, as a result of the peroxide affecting neighbouring ethylene sequences.

In the case of the 100 °C fraction belonging to the CMR348 sample, we see an increase of the PP bands at 808, 1044, 1100, 1193, 1216 and 1260 cm$^{-1}$ with the decrease of the PP bands at 841, 973, 998, 1163 and 1303 cm$^{-1}$, for the Trigonox®101 peroxide, indicating an increase of short PP sequences with a decrease of long P sequences. It is also observed that the Trigonox®101 peroxide affected the bands associated with long PP sequences more relative to the Trigonox®301 peroxide, indicating that the Trigonox®101 peroxide attacks the long P sequences more than the Trigonox®301 peroxide. We see a splitting of the PP band at 841 cm$^{-1}$ for both peroxides, indicating the presence of two long PP sequences with different chemical environments as a result of chain scissions. Moreover, this effect is more pronounced in the fraction treated with Trigonox®101. The shifting of HT-SEC curve, towards lower molecular weights as shown in Figure 4.18 (e), confirms that the Trigonox®101 peroxide attacks long PP sequences more relative to the Trigonox®301 peroxide. The slight decrease of the high molecular weight side of the HT-SEC curve shown in Figure 4.18 (e), and the slight decrease of the doublet band around 730-720 cm$^{-1}$, show that the Trigonox®101 peroxide also attacked ethylene-propylene copolymer and long E sequences.

The CMR348 sample like the CMR648 sample also shows a splitting of the band at 1100 cm$^{-1}$. This time, it is really clear that the splitting of this band might be dependent on the decrease of the PE doublet band, and therefore the attack of E sequences. Based on the FTIR spectrum shown in Figure 4.19 (a) and the HT-SEC curve shown in Figure 4.18 (e), it is suspected that the Trigonox®301 peroxide might be "cutting" the polymer sequences (i.e. long P and E sequences, ethylene-propylene copolymer sequences with varying E and P sequences) present in this fraction until a homogenous distribution of sequences is obtained.

In the 130 °C fraction of the CMR648 sample, we see a decrease of the PP bands at 841, 973, 998, 1163 and 1303 cm$^{-1}$ with an increase of the PP bands at 808, 1044, 1100, 1193, 1216 and 1260 cm$^{-1}$ for both peroxides, indicating that there was a decrease of long P sequences and an increase of short P sequences, as a result of the peroxides "attacking" the the PP sequences. We also see a splitting of the PP band at 1100 °cm$^{-1}$, indicating the presence of short PP sequences with different conformational environments, as a result of the peroxide "attacking" the long PP sequences.

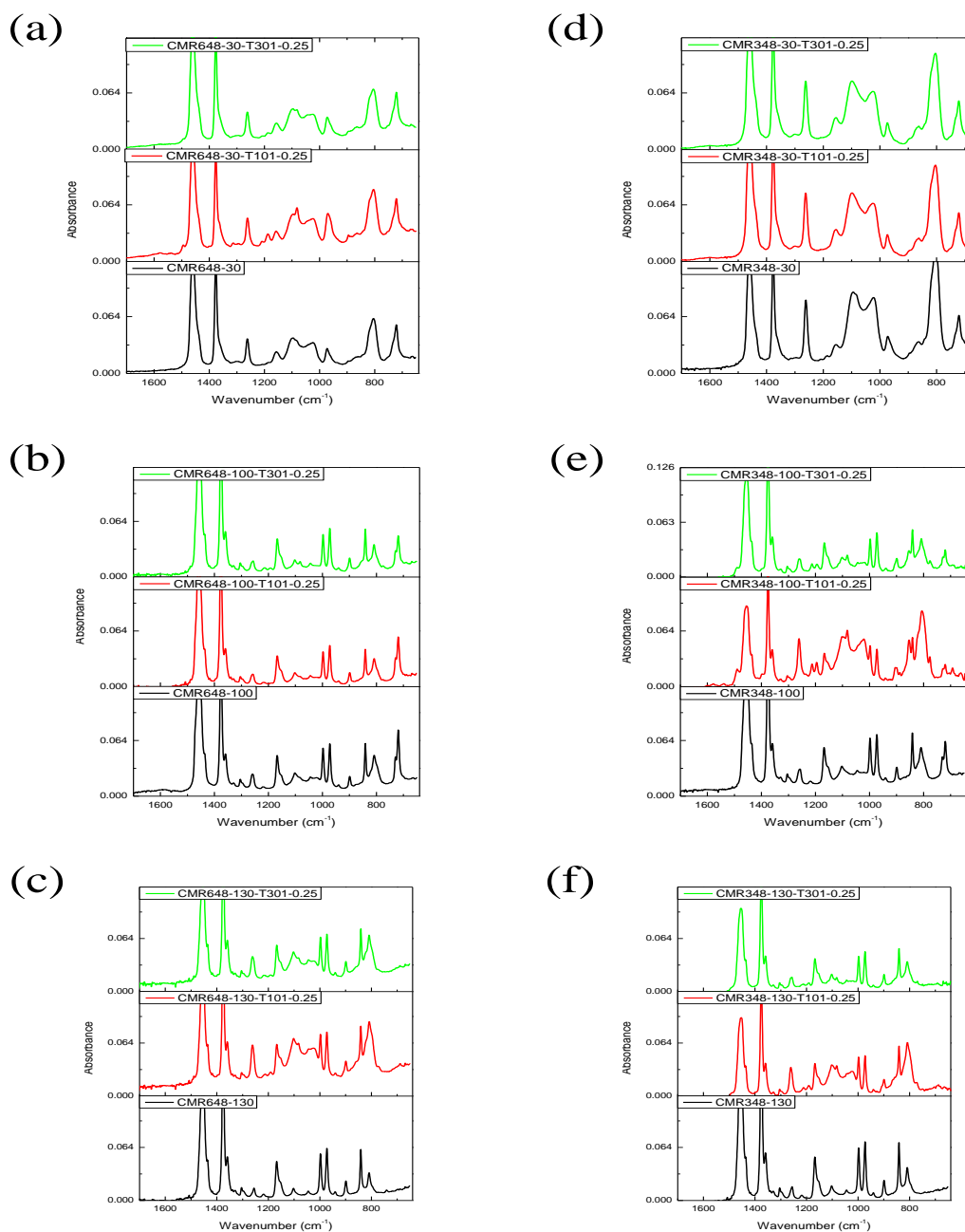Figure 4.19    Comparing the FTIR spectra of the untreated and treated TREF fractions belonging to the CMR648 (a-c) and CMR348 (d-f) samples

The PP bands at 841, 973, 998, 1163 $°cm^{-1}$ in the untreated 130 °C fraction appear to be stronger than those observed in the CMR648 sample, which might be the reason why the HT-SEC curves in the treated 130 °C fractions of the CMR348 sample show a more significant

shift towards lower molecular weights, when comparing Figure 4.18 (c) with Figure 4.18 (f). The FTIR spectra of both samples show that the Trigonox[®]101 peroxide affected this fraction more relative to the Trigonox[®]301 peroxide. This correlates well with the solubility parameter results shown in Figure 4.11 and discussed in Section 4.6.

### 4.8.3.       DSC analysis

Differential scanning calorimetry was used to study the melting and crystallisation behaviour of all the fractions treated with peroxide in the CMR648 and CMR348 samples. Figure 4.20 (a-d) shows the differences in melting behaviour of the individual fractions treated with Trigonox[®]101 and Trigonox[®]301.

The melting behaviour of the treated 30 and 130°C fractions is the same in both the CMR648 and CMR348 samples. As expected, the treated 30°C fractions (just like the untreated 30°C fractions) also show flat DSC curves. Moreover, the treated 130°C fractions show a slightly broad melting curve around 160°C, indicating the presence of heterogenous crystallisable sequence distributions, respectively. A few differences are noted in the melting curves of the treated 100°C fractions in both the CMR648 and CMR348 samples. In the treated 100°C fractions of the CMR648 and CMR348 samples (Figure 4.20 b and c), we see a decrease of the lower melting peak around 156 °C of the double melt endotherm. This melting peak is suspected to be due to the melting of PP crystals with longer chains. In the CMR648 sample (Figure 4.20 b), we see that the decrease of this melting peak is accompanied by an increase of the weak band around 120 °C. This might be due to the peroxides "attacking" the longer PP sequences and thus causing a "release" of copolymer sequences with crystallisable ethylene sequences.

In the case of the 100°C fraction treated with Trigonox[®]301, of the CMR348 sample (Figure 4.20 c), we see a disappearance of the melting peaks around 114.3 and 156 °C and an appearance of a broad single melting peak around 160°C. This might be due to the Trigonox[®]301 peroxide "cutting down" all the sequences present in the fraction in such a way that a homogenous distribution of sequence lengths is achieved.
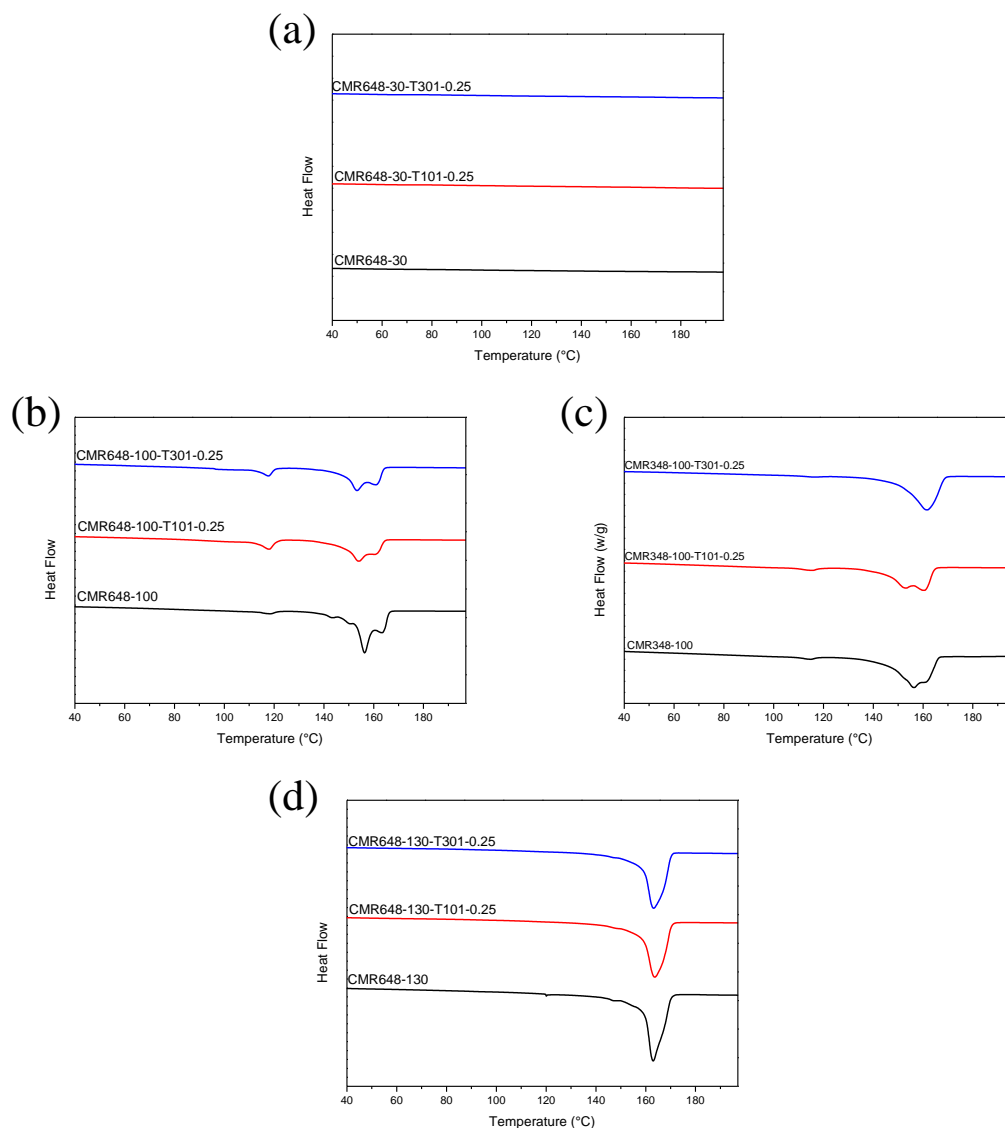
Figure 4.20    DSC melting curves for the undegraded and degraded 30, 100, 130°C fractions (a,b,d) belonging to the CMR648 sample and the undegraded and degraded 100°C (c) fraction belonging to the CMR348 sample

Figure 4.21 (a-d) shows the crystallisation behaviour of all the treated TREF fractions in the CMR348 and CMR648 samples. Once again, the cooling curves of the treated 30 and 130 °C fractions in the CMR648 and CMR348 samples are similar (Figure 4.20 a and d). However, the cooling curves of the treated 100 °C fractions in the CMR648 and CMR348 samples are also different (Figure 4.20 a and d). In both samples, we see a clear crystallisation peak at the same temperature (around 115 °C) in all the treated 100 °C fractions, indicating that they have a matrix component that crystallises at the same temperature.
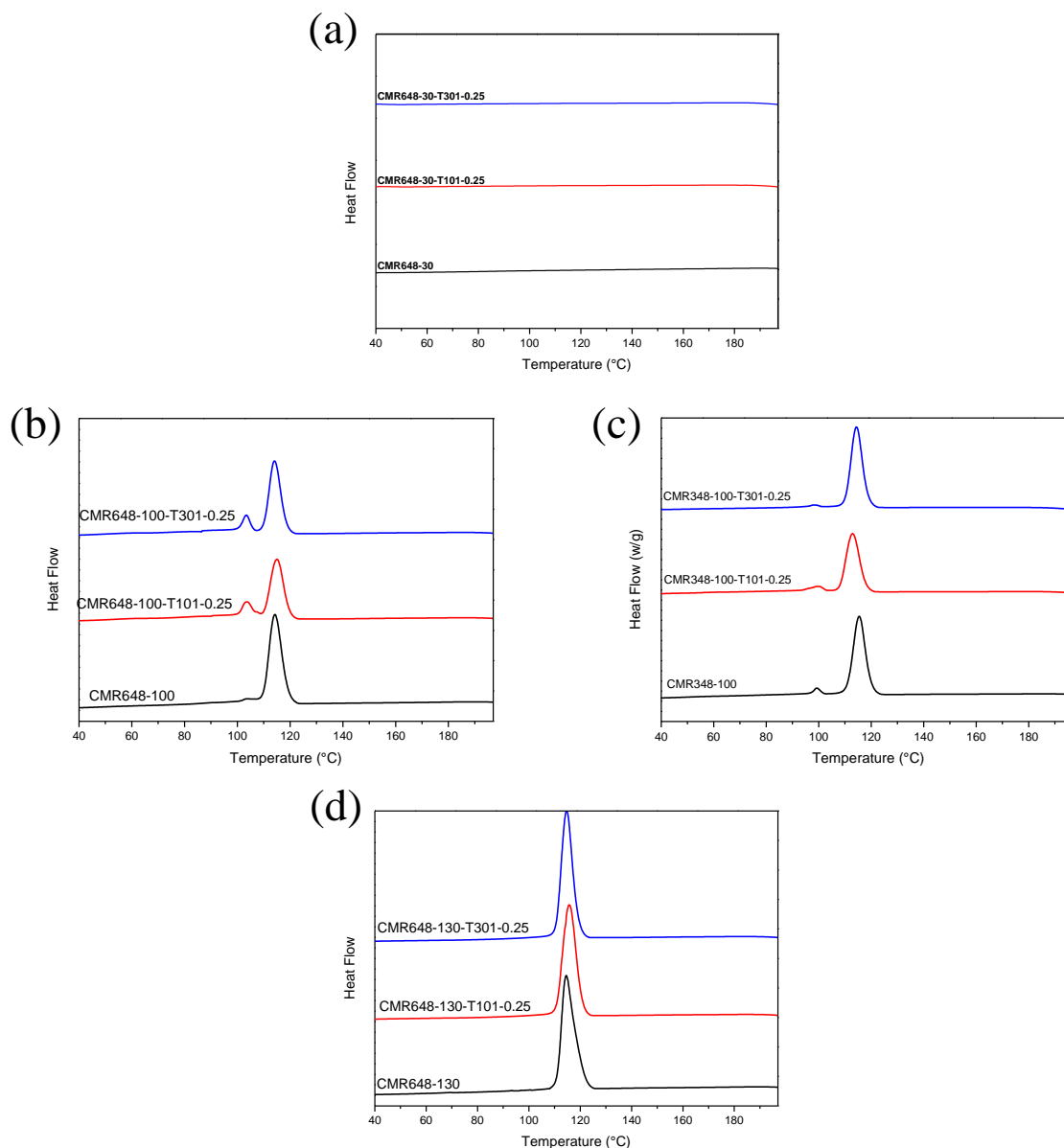
Figure 4.21    DSC crystallisation curves of the undegraded and degraded 30, 100, 130 °C fractions
(a,b,d) belonging to the CMR648 sample and the undegraded and degraded 100°C
fraction (c) belonging to the CMR348 sample

In the CMR648 sample (Figure 4.21 b), the weak crystallisation peak around 100 °C becomes

distinct with treatment of 100°C fractions with peroxide, and this is a confirmation of what is

observed in the melt endotherms.

In the CMR348 sample (Figure 4.21 c), the 100 °C fraction treated with Trigonox[®]301 shows

a very weak crystallisation peak around 100 °C, indicating that this fraction still contains a

small amount of copolymers containing crystallisable ethylene sequences (as confirmed by the FTIR spectra).

Tables showing the changes in crystallization and melting temperatures of the 100 and 130 °C fractions after treatment with both peroxides are shown in Appendix C (Table C - 1 to Table C - 4).

### 4.8.4.        $^{13}$C NMR analysis

Carbon-13 nuclear magnetic resonance spectroscopy was used to determine the concentrations of monomer sequence distributions of all the treated and untreated fractions in the CMR648 and CMR348 samples. Table 4.8-4.9 shows the monomer sequence distributions of all the untreated and treated fractions.

In the treated 30 °C fractions of the CMR648 sample (Table 4.5), we see a decrease of the EE diads and EEE triads. However, the Trigonox®101 peroxide has more of an effect in this regard than the Trigonox®301 peroxide. The decrease of the EEE triads and EE diads might be due to the peroxides "attacking" between ethylene units. Moreover, we also see a slight decrease of the EEP triads in the fraction treated with Trigonox®101. However, the concentration of these triads was constant in the fraction treated with Trigonox®301. Since the concentration of PE diads was constant, whilst the concentration of EE diads decreased in the 30 °C fraction treated with Trigonox®101, this confirms that the Trigonox®101 peroxide might be "attacking" at the junctions between ethylene units.

The 30 °C fraction treated with Trigonox®301, shows a slight decrease of the PE diads, EE diads and PEP triads, indicating that this peroxide might be attacking at the EP juntions and at the junctions between ethylene units. Furthermore, we see a decrease of the PPP triads in the fraction treated with Trigonox®101 and an increase of these triad sequences in the fraction treated with Trigonox®301. The decrease of the PPP triads together with an increase of the PP diads and P units, indicate that the Trigonox®101 peroxide might also be "attacking" at the junction between two propylene units in this fraction. According to Swart *et. al.* [19] the increase in the PPP triad sequences is due to molecular weight (chain end) effects as crystalline PP

sequences are "broken down" by the Trigonox®301 peroxide (this is confirmed by the increase of the PP diads and P units).

In the 30 °C fraction treated with Trigonox®301, we see a constant concentration of EPP and EEP triads wherelse an increase of the EPP and a slight decrease of the EEP is observed in the fraction treated with Trigonox®101. This indicates that the Trigonox®101 peroxide has an effect on the "blocky" triad sequences, in this fraction relative to Trigonox®301 peroxide. The increase of the EPP, EPE and PEP in the fraction treated with Trigonox®101 and the increase of EPE in the fraction treated with Trigonox®301 might be due to the peroxide "attacking" at the junctions between ethylene units or propylene units of crystalline PP and PE sequences, thus causing a "release" of these triad sequences.

In the treated 30 °C fractions of the CMR348 sample (Table 4.6), we see a slight decrease of the PP triads in the fraction treated with Trigonox®101. However, the concentration of these triad sequences is constant in the fraction treated with Trigonox®301. The decrease of the PP triads might be due to the Trigonox®101 peroxide "attacking" at the junctions between propylene units. We also see a decrease of the EE triads in the treated 30 °C fractions. This is an indication that the Trigonox®101 peroxide does not only "attack" between propylene units but it also "attacks" between ethylene units. Moreover, the treated 30 °C fractions also show a slight decrease of the PPE triads. Due to the increase of the PE diads in the fraction treated with Trigonox®101, the decrease of the PPE diads might be due to the peroxide "attacking" at the junctions between the P units in these diads.

The 30 °C fraction treated with Trigonox®301, shows a decrease of the PEP triads, whilst the concentration of these triads remains constant in the fraction treated with Trigonox®101. This might be due to the Trigonox®301 peroxide "attacking" at the EP junctions of the PEP triads. Therefore, the increase of the PE diads in the 30 °C fraction treated with Trigonox®301 might be due to the peroxide "attacking" at the EP junctions of the PEP triads and thus leading to a release of the EP diads.

Table 4.5        Monomer sequence distribution data of the 30°C fraction belonging to the CMR648 sample before and after treatment with Trigonox®101 and Trigonox®301 peroxides

| Monomer sequence distribution (%) | CMR648-30 | CMR648-30-T101-0.25 | CMR648-30-T301-0.25 |
|---|---|---|---|
| P | 37.7 | 42.3 | 40.2 |
| E | 62.3 | 57.7 | 59.8 |
| PP | 10.5 | 14.6 | 13.4 |
| PE/ EP | 55.0 | 55.4 | 53.5 |
| EE | 34.9 | 30.7 | 33.0 |
| PPP | 12.5 | 11.8 | 13.2 |
| EPP/ PPE | 17.1 | 20.5 | 17.7 |
| EPE | 8.1 | 10.0 | 9.4 |
| EEE | 21.8 | 19.8 | 19.9 |
| EEP/ PEE | 26.6 | 24.8 | 26.1 |
| PEP | 14.2 | 15.3 | 13.7 |

The increase of the EEP triads in the treated 30 °C fractions correlates well with the increase of the $S_{\gamma\gamma}$ peak (30.75 ppm) relative to the $T_{\beta\delta}$ peak in the NMR spectra shown in Appendix D (Figure D – 4). This peak is associated with a carbon between two ethylene units in a sequence with two ethylene insertions between propylene units (see Figure 4.16). Therefore, the increase of the EEP triads might be due to the peroxides "attacking" at the EP junctions of PEEP sequences and thus causing a "release" of the EEP or PEE triads. Moreover, the increase of the EEE and PPP triads in the treated fractions is suspected to be due to molecular weight (chain end) effects as crystalline PP and PE sequences are "broken down" by the peroxides. Furthermore, since the EPE triads are associated with the $T_{\delta\delta}$ peak in the NMR spectra, which

is a tertiary carbon between ethylene units in a sequence with three ethylene insertions between propylene units (refere to Figure 4.16), the increase of the EPE triads might be due to the peroxides "attacking" between ethylene units, thus leading to a "release" of these triad sequences.

Table 4.6        Monomer sequence distribution data of the 30 °C fraction belonging to the CMR348 sample before and after treatment with Trigonox®101 and Trigonox®301 peroxides

| Monomer sequence distribution (%) | CMR348-30 | CMR348-30-T101-0.25 | CMR348-30-T301-0.25 |
|---|---|---|---|
| P | 41.8 | 42.7 | 42.8 |
| E | 58.2 | 57.3 | 57.2 |
| PP | 17.0 | 16.8 | 17.1 |
| PE/ EP | 49.6 | 51.7 | 51.4 |
| EE | 32.1 | 27.8 | 31.5 |
| PPP | 15.4 | 16.0 | 17.2 |
| EPP/ PPE | 18.0 | 17.6 | 15.8 |
| EPE | 8.4 | 9.1 | 9.9 |
| EEE | 18.8 | 19.2 | 19.4 |
| EEP/ PEE | 21.4 | 22.5 | 24.6 |
| PEP | 14.1 | 14.6 | 13.4 |

In the treated 100 °C fractions of the CMR648 sample (Table 4.7), we see a decrease of the PP diads and PPP triads for both peroxides. However, the Trigonox®101 peroxide has more of an effect in this regard than the Trigonox®301 peroxide. This might be due to the Trigonox®101 peroxide being highly miscible with the propylene rich phase of the copolymer, as confirmed by the solubility parameter results (Figure 4.11). We also see an increase of the EEE triads in

the treated fractions for both peroxides. This might be due to molecular weight (chain end) effects as the crystalline PE sequences are broken down by the peroxides. This is confirmed by the increase of the EE diads. The increase of the EE is more significant for the fraction treated with Trigonox$^®$301 than for the one treated with Trigonox$^®$101. This might be due to this peroxide being highly miscible with the ethylene rich phase of the copolymer, as confirmed by the solubility parameter results (Figure 4.11). In NMR spectra of the 100 °C fraction treated with Trigonox$^®$301, shown in Appendix D (Figure D – 2), we see an increase of the $S_{\gamma\gamma}$ peak around 30.75 ppm relative to the $T_{\beta\delta}$ peak. This peak is associated with PEEP sequences according to Figure 4.16 of Section 4.7.4. Due to the decrease of the PP diads and PPP triads in the treated fractions, this might be due to the peroxide "attacking" at PP junctions in crystalline PP sequences and thus causing a "release" of the PEEP sequences. In the NMR spectra of the fraction treated with Trigonox$^®$101, the $S_{\beta\beta}$ peak becomes more distinct. This correlates well with the increase of the PEP triads in this fraction, as this peak according to Figure 4.16 of Section 4.7.4 indicates a single ethylene insertion between propylene units. Since the transition segments such as PEP, EPE, PPE, EEP are present as junctions between longer ethylene and propylene segments [18], the increase of these transition segments in the treated fractions might be due to the peroxides "breaking down" crystalline PP and PE sequences and causing a "release" of these sequences. The appearance of the peak around 31 ppm in the NMR spectrum of the fraction treated with Trigonox$^®$101 (Figure D – 2 of Appendix D), might be confirming the increase of these triad sequences.

In the treated 100 °C fractions of the CMR348 sample (Table 4.8), we see a decrease of the PE, EPE, EEP and PEP sequences in the fraction treated with Trigonox$^®$301, whilst in the fraction treated with Trigonox$^®$101, the concentration of these sequences is constant. This is suspected to be due to the Trigonox$^®$301 peroxide "attacking" at the EP junctions of theses sequences. The treated 100 °C fractions also show a decrease of the EE diads and EEE triads for both peroxides. However, the Trigonox$^®$301 peroxide has more of an effect in this regard than the Trigonox$^®$101 peroxide, indicating that the Trigonox$^®$301 peroxide, relative to the Trigonox$^®$101, is "active" towards the ethylene sequences. Furthermore, we see a decrease of the EPP triads in the fraction treated with Trigonox$^®$301 and an increase of the same triad sequences in the fraction treated with Trigonox$^®$101.

The decrease of the EPP triads and the significant increase of the PP diads, in the fraction treated with Trigonox®301 might be due to the Trigonox®301 peroxide "attacking" at the EP junctions of the EPP triads and thus contributing to the increase of the PP diads. The increase of the EPP triads might be due to Trigonox®101 peroxide "attacking" somewhere else. The increase of the PPP triads is due to molecular weight (chain end) effects as the peroxides "break down" longer PP sequences [19], as confirmed by the increase of the PP diads and P units.

Table 4.7        Monomer sequence distribution data of the 100 °C fraction belonging to the CMR648 sample before and after treatment with Trigonox®101 and Trigonox®301 peroxides

| Monomer sequence distribution (%) | CMR648-100 | CMR648-100-T101-0.25 | CMR648-100-T301-0.25 |
|---|---|---|---|
| P | 65.6 | 54.7 | 55.5 |
| E | 34.4 | 45.3 | 44.5 |
| PP | 61.7 | 46.5 | 51.0 |
| PE/ EP | 7.8 | 16.3 | 9.3 |
| EE | 30.1 | 37.0 | 39.5 |
| PPP | 60.7 | 43.0 | 44.7 |
| EPP/ PPE | 2.0 | 8.1 | 7.0 |
| EPE | 2.9 | 3.5 | 3.8 |
| EEE | 26.7 | 32.2 | 35.9 |
| EEP/ PEE | 5.2 | 9.1 | 6.0 |
| PEP | 1.3 | 3.6 | 1.7 |

Table 4.8        Monomer sequence distribution data of the 100 °C fraction belonging to the CMR348 sample before and after treatment with Trigonox®101 and Trigonox®301 peroxides

| Monomer sequence distribution (%) | CMR348-100 | CMR348-100-T101-0.25 | CMR348-100-T301-0.25 |
|---|---|---|---|
| P | 68.5 | 74.8 | 90.9 |
| E | 31.5 | 25.2 | 9.1 |
| PP | 63.9 | 69.9 | 89.5 |
| PE/ EP | 9.26 | 9.88 | 2.82 |
| EE | 26.7 | 20.2 | 7.85 |
| PPP | 61.2 | 66.0 | 86.6 |
| EPP/ PPE | 5.2 | 6.1 | 4.1 |
| EPE | 2.2 | 2.6 | 0.1 |
| EEE | 24.2 | 17.5 | 7.5 |
| EEP/ PEE | 4.6 | 4.9 | 1.5 |
| PEP | 2.3 | 2.5 | 0.7 |

As expected in the treated 130 °C fractions (Figure 4.9), we see a decrease of the PPP triads. The Trigonox®101 peroxide has more of an effect in this regard than the Trigonox®301 peroxide. This might be due to the Trigonox®101 peroxide being highly miscible with the propylene rich phase of the copolymer, as confirmed by the solubility parameter results shown in Figure 4.11 of Section 4.6.

Table 4.9         Monomer sequence distribution data of the 130 °C fraction belonging to the CMR648
                  sample before and after treatment with Trigonox®101 and Trigonox®301 peroxides

| Monomer sequence distribution (%) | CMR648-130 | CMR648-130-T101-0.25 | CMR648-130-T301-0.25 |
|:---:|:---:|:---:|:---:|
| P | 100.0 | 100.0 | 100.0 |
| E | 0.0 | 0.0 | 0.0 |
| PP | 100.0 | 100.0 | 100.0 |
| PE/ EP | 0.0 | 0.0 | 0.0 |
| EE | 0.0 | 0.0 | 0.0 |
| PPP | 100.0 | 86.1 | 90.9 |
| EPP/ PPE | 0.0 | 13.9 | 9.13 |
| EPE | 0.0 | 0.0 | 0.0 |
| EEE | 0.0 | 0.0 | 0.0 |
| EEP/ PEE | 0.0 | 0.0 | 0.0 |
| PEP | 0.0 | 0.0 | 0.0 |

In conclusion, it is worth noting that the decrease in the overall molecular weight of each sample is not individually reflected by the changes observed in each fraction. Each fraction gives us an idea of each peroxide affects it, which constitutes the main aim of the study. Therefore, the "attacking" of the peroxide radicals at specific junctions do possibly result in a chain-breaking event. However, considering the complexity of the materials, especially in the 100 °C fraction, there is also a possibility of crosslinking reactions.

The appearance of carbonyl peaks around 205 ppm, which are indicative of the presence of ketones confirms the occurrence of chain-breaking events in the fractions (Figure D-1 to Figure D-5).

The NMR spectra of the TREF fractions treated with the Trigonox®101 and Trigonox®301 peroxides are shown in Appendix D (Figure D-1 to Figure D-5)

## 4.8.    Effect of the organic peroxides on the two heterophasic copolymers with different ethylene contents (CMR648 and CMR348 copolymers)

From the HT-SEC, FTIR, DSC and C NMR results shown in Section 4.8 for both CMR648 and CMR348 samples, we see that the chemical structures of the two copolymers were affected differently by the peroxides. Therefore, it can be concluded that the effect of the organic peroxides on these copolymers was not only determined by the type of peroxide but their chemical composition (ethylene content) was also a contributing factor. It can also be concluded that the two peroxides affect copolymers with different ethylene contents differently.

## 4.9.    Conclusions

The decrease of the high molecular weight component and of the PE doublet band (720-730 cm$^{-1}$) relative to the crystalline PP bands (841 and 998 cm$^{-1}$), in the FTIR and HT-SEC results of the 100 °C fraction of the CMR648 sample treated with Trigonox®301 peroxide, indicates that the Trigonox®301 peroxide affects the ethylene rich sequences more than the PP rich sequences in this fraction.

The HT-SEC results of the 100 °C fraction belonging to the CMR648 sample treated with Trigonox®101 shows a distinct phase separation between the low and high molecular weight distribution components. The FTIR results show that the ratio of the PE doublet band and crystalline PP bands is constant relative the ratio of these bands in the untreated fraction. This is suspected to be due to the Trigonox®101 peroxide affecting the ethylene rich and propylene rich sequences, in this fraction, similarly and thus causing an even distribution of these sequences in this fraction.

The HT-SEC curve of the 100 C fraction treated with Trigonox®301 (belonging to the CMR348 sample) show mono-modal distribution relative to the untreated fraction. This indicates the

presence of a homogenous distribution of sequences in the fraction. Due to the chemical nature of the sample (low ethylene content), this might be due to the peroxide "breaking down" the ethylene rich sequences more than the propylene rich sequences (as confirmed by the NMR sequence distribution data) until a homogenous distribution is achieved. It is possible that the sequences present in this distribution are mostly propylene rich, as confirmed by the appearance of a single melt endotherm around 160 °C in the DSC results.

Taking into consideration the chemical nature of the CMR348 sample, the shift towards lower molecular weights of the HT-SEC curve belonging to the 100 °C fraction treated with Trigonox®101, is suspected to be due to the peroxide "breaking down" the longer PP sequences, as confirmed by the FTIR results.

The NMR results of the treated 130 °C fraction, show that the Trigonox®101 peroxide affects the crystalline PP sequences more than the Trigonox®301 peroxide.

From the results obtained, it is clearly evident that the Trigonox®101 peroxide mostly affected the PP rich phase, whilst the Trigonox®301 peroxide mostly affected the PE rich phase of the heterophasic ethylene-propylene copolymers. This was also confirmed by the solubility parameter results by indicating that the Trigonox®101 peroxide is highly miscible with the PP rich phase, whilst the Trigonox®301 peroxide is more miscible with PE rich phase.

## 4.10.  References

(1)     Čapla, M.; Borsig, E., *European Polymer Journal* **1980**, 16, 611.

(2)     Salakhov, I.; Boreiko, N.; Fatykhov, M.; Fedosova, S., *International Polymer Science and Technology* **2013**, 40, T29.

(3)     Xue, Y.; Fan, Y.; Bo, S.; Ji, X., *European Polymer Journal* **2011**, 47, 1646.

(4)     Geng, Y.; Wang, G.; Cong, Y.; Bai, L.; Li, L.; Yang, C., *Macromolecules* **2009**, 42, 4751.

(5)     Ramos, V. D.; Costa, H. M. d.; Rocha, M. C. G.; Gomes, A. d. S., *Polymer Testing* **2006**, 25, 306.

(6)     Tocháček, J.; Jančář, J.; Kalfus, J.; Zbořilová, P.; Buráň, Z., *Polymer Degradation and Stability* **2008**, 93, 770.

(7)     de Goede, E.; Mallon, P.; Pasch, H., *Macromolecular Materials and Engineering* **2010**, 295, 366.

(8)     Zacur, R.; Goizueta, G.; Capiati, N., *Polymer Engineering & Science* **1999**, 39, 921.

(9)     Zacur, R.; Goizueta, G.; Capiati, N., *Polymer Engineering & Science* **2000**, 40, 1921.

(10)    Swart, M., PhD Thesis, University of Stellenbosch, **2013**.

(11)    Boudou, L.; Guastavino, J., *Journal of Physics D: Applied Physics* **2002**, 35, 1555.

(12)    De Goede, E., PhD Thesis University of Stellenbosch, **2009**.

(13)    van Drongelen, M.; Gahleitner, M.; Spoelstra, A. B.; Govaert, L. E.; Peters, G. W., *Journal of Applied Polymer Science* **2015**, 132.

(14)    Nakatani, H.; Manabe, N.; Yokota, Y.; Minami, H.; Suzuki, S.; Yamaguchi, F.; Terano, M., *Polymer international* **2007**, 56, 1152.

(15)    Ray, G. J.; Johnson, P. E.; Knox, J. R., *Macromolecules* **1977**, 10, 773.

(16)    Randall, J. C., *Macromolecules* **1978**, 11, 33.

(17)    Carman, C.; Wilkes, C., *Rubber Chemistry and Technology* **1971**, 44, 781.

(18)    Paxson, J. R.; Randall, J. C., *Analytical Chemistry* **1978**, 50, 1777.

(19)    Swart, M.; Van Reenen, A. J., *Journal of Applied Polymer Science* **2015**, 132.

# *Chapter 5*

# Conclusions and Future work

*This chapter contains conclusions from the results discussed in Chapter 4. It also contains propositions for future work in this field of study.*

## 5.1.    Summary

The main aim of this study was to investigate the reason why specific organic peroxides influence or interact differently with the various phases of heterophasic copolymers (HECOs). An understanding of the problem statement mentioned above will help us to know how we can utilize the properties of the type of peroxide used during controlled rheology, to obtain a HECO polymer with optimal and desired properties.

## 5.2.    Conclusions

From P-TREF results, it was observed that the CMR648 sample contained more of the 30 and 100°C fractions than the CMR348 sample, confirming that the CMR648 sample had more ethylene content. However, both the CMR648 and CMR348 samples had a higher content of the 130°C fraction, as compared to the other fractions, indicating that the 130°C forms the base matrix in these two polymers.

Solubility parameter results, showed that the solubility parameter of the Trigonox$^{®}$101 [7.7 (cal.cm$^{-3}$)$^{1/2}$] peroxide was closer to that of PP [8.0 (cal.cm$^{-3}$)$^{1/2}$], indicating that the two are miscible. However, the solubility parameter of the Trigonox$^{®}$301 peroxide [8.7 (cal.cm$^{-3}$)$^{1/2}$] was closer to that of PE [8.6 (cal.cm$^{-3}$)$^{1/2}$], again indicating the miscibility of the two.

When the 30, 100 and 130°C fractions of the CMR648 sample were degraded with the Trigonox$^{®}$101 and Trigonox$^{®}$301 peroxides, several interesting phenomena were observed.

HT-SEC results of the treated 30 °C fractions revealed that the shift of the MWD curve was more dominant in the fraction treated with Trigonox$^{®}$301 than the one treated with Trigonox$^{®}$101. This might be due to decrease in the concentration of the PE diads, EE diads and EEE triads, since the 30 °C has higher concentration of these sequences (as confirmed by the NMR monomer sequence distribution data). This indicates that the Trigonox$^{®}$301 peroxide might be "attacking" EP and EE junctions in this fraction.

The bi-modal MWD curve of the 100°C fraction was affected differently by the peroxides. This might be due the peroxides being "active" with respect to a particular sequence. The distinct phase separation between the low and high molecular weight components in the 100°C fraction treated with Trigonox$^{®}$101 might be due to the peroxide "breaking down" the propylene rich

sequences and ethylene rich sequences (as confirmed by NMR analysis) in such a way that there is an even distribution of PP homopolymer sequences and ethylene-propylene sequences. This is also confirmed by the FTIR results, which showed a decrease of the PE doublet band (720-730 cm$^{-1}$) and crystalline PP bands (841 and 998 cm$^{-1}$), whilst the ratio of these bands remained constant relative to the intensities and ratio of these bands in the untreated fraction. The decrease of the high molecular weight component in the 100 °C fraction treated with Trigonox$^®$301 might be due the Trigonox$^®$301 peroxide "breaking down" the ethylene rich sequences in the fraction. This is confirmed by the decrease of the PE doublet band relative to the crystalline PP bands in the FTIR spectrum.

The DSC melting and crystallization curves of the treated 100 °C fraction, show a distinct peak around 120 and 100 °C, indicating that the scission of particular sequences in this fraction might have led to "release" of ethylene rich sequences that could melt or crystallise at these temperatures. Therefore the DSC melting and crystallisation curves of the 100°C fraction revealed that the structural composition of this fraction was affected by the peroxides.

Each of the 30, 100 and 130°C P-TREF fractions belonging to the CMR348 sample were also treated with Trigonox$^®$101 and Trigonox$^®$301, and interesting results were obtained.

The shifting towards lower molecular weights of the HT-SEC curve in the 100 °C fraction treated with Trigonox$^®$101 might be due to the peroxide "breaking down" the long PP sequences, as confirmed by the FTIR results. Moreover, the appearance of a mono-modal HT-SEC curve in the 100 °C fraction treated with Trigonox$^®$301, might be due to the peroxides "breaking down" the ethylene rich sequences (as confirmed by the NMR results) until a homogenous distribution of sequences is achieved. Most of these sequences will most likely be propylene rich, as confirmed by the melting peak appearing around 160 °C in the DSC results.

The 130 °C fraction seemed to be mostly affected by the Trigonox$^®$101 peroxide relative to the Trigonox$^®$301 peroxide. This is confirmed by the HT-SEC, FTIR and NMR results.

Based on the results obtained from the treated fractions and considering the chemical composition of the sample (low ethylene content), the significant shift of the HT-SEC curves

belonging to the CMR348 sample with peroxide dosage, might be due to the peroxides "breaking down" the long PP sequences in this sample.

Based on the results obtained, it can be concluded that the CMR648 and CMR348 samples were affected differently by the peroxides, indicating that the ethylene content of polymer also affects the behaviour of the peroxides towards a particular sample. Moreover, it was also established that the propylene rich phases of the polymer were mostly affected by the Trigonox®101 peroxide, whilst the ethylene rich phases were mostly affected by the Trigonox®301 peroxide. This correlated well with the results obtained from the solubility parameters of the peroxides.

## 5.3.    Future work

The concentrations of the two organic peroxides (Trigonox®101 and Trigonox®301) will be increased to higher concentrations, to investigate their effects on the various phases of the polymers (CMR648 and CMR348).

High temperature high performance liquid chromatography (HT-HPLC) will also be used in addition to HT-SEC, FTIR, DSC and $^{13}$C NMR, in order to investigate any changes in chemical composition and microstructure of the various phases, that were induced by the peroxides.

Each of the three fractions (30, 100 and 130°C) of the CMR648 and CMR348 samples, will be degraded with the peroxides (Trigonox®101 and Trigonox®301) and re-blended with the other undegraded fractions. These blends will be characterised and mechanical tests will be carried out on them. This will help in the investigation of how each of the degraded fractions affect the chemical composition and mechanical properties of the overall sample.

# Appendix

*This chapter contains supplementary information to the results discussed in Chapter 4.*

# Appendix A        TREF data

Table A.1        Elution data of the CMR648 TREF fractions after 4 elutions

| Fraction (°C) | CMR648-1 | | CMR648-2 | | CMR648-3 | | CMR648-4 | |
|---|---|---|---|---|---|---|---|---|
| | $W_i$ (g) | $W_i$ (%) | $W_i$ (g) | $W_i$ (%) | $W_i$ (g) | $W_i$ (%) | $W_i$ (g) | $W_i$ (%) |
| 30 | 0.36 | 11.9 | 0.44 | 14.8 | 0.40 | 13.5 | 0.38 | 12.6 |
| 100 | 0.47 | 15.2 | 0.56 | 18.5 | 0.63 | 20.9 | 0.6 | 20.0 |
| 130 | 1.89 | 62.7 | 1.86 | 62.1 | 1.81 | 60.2 | 1.79 | 59.4 |

Table A.2        Elution data of the CMR648 TREF fractions after 4 elutions

| Fraction (°C) | CMR348-1 | | CMR348-2 | | CMR348-3 | | CMR348-4 | |
|---|---|---|---|---|---|---|---|---|
| | $W_i$ (g) | $W_i$ (%) | $W_i$ (g) | $W_i$ (%) | $W_i$ (g) | $W_i$ (%) | $W_i$ (g) | $W_i$ (%) |
| 30 | 0.33 | 11.0 | 0.24 | 8.0 | 0.31 | 10.2 | 0.27 | 9.1 |
| 100 | 0.40 | 13.4 | 0.43 | 14.3 | 0.43 | 14.4 | 0.43 | 14.3 |
| 130 | 2.21 | 73.4 | 2.04 | 67.8 | 2.17 | 72.1 | 2.21 | 73.4 |

# Appendix B          HT-SEC data

Table B.1     HT-SEC data of the CMR648 bulk samples treated with Trigonox®101 at different concentrations

| Sample | $M_w$ (g/mol) | $M_n$ (g/mol) | Đ |
|--------|---------------|---------------|---|
| CMR648 | 364 600 | 34 000 | 10.7 |
| CMR648-T101-0.125 | 336 600 | 52 800 | 6.4 |
| CMR648-T101-0.25 | 321 800 | 70 400 | 4.6 |
| CMR648-T101-0.5 | 302 000 | 50 900 | 5.9 |

Table B.2     HT-SEC Data of the CMR648 bulk samples treated with Trigonox®301 at different concentrations

| Sample | $M_w$ (g/mol) | $M_n$ (g/mol) | Đ |
|--------|---------------|---------------|---|
| CMR648 | 364 600 | 34 000 | 10.7 |
| CMR648-T301-0.125 | 344 100 | 47 600 | 7.2 |
| CMR648-T301-0.25 | 349 700 | 33 600 | 10.4 |
| CMR648-T301-0.5 | 360 400 | 34 100 | 10.5 |

Table B.3　　HT-SEC data of the CMR348 bulk samples treated with Trigonox®101 at different concentrations

| Sample | $M_w$ (g/mol) | $M_n$ (g/mol) | Đ |
|---|---|---|---|
| CMR348 | 430 100 | 82 300 | 5.2 |
| CMR348-T101-0.125 | 388 200 | 50 700 | 7.7 |
| CMR348-T101-0.25 | 360 800 | 44 000 | 8.1 |
| CMR348-T101-0.5 | 331 300 | 45 100 | 7.3 |

Table B.4　　HT-SEC data of the CMR348 bulk samples treated with Trigonox®301 at different concentrations

| Sample | $M_w$ (g/mol) | $M_n$ (g/mol) | Đ |
|---|---|---|---|
| CMR348 | 430 100 | 82 300 | 5.2 |
| CMR348-T301-0.125 | 432 600 | 41 000 | 10.5 |
| CMR348-T301-0.25 | 400 800 | 43 500 | 9.2 |
| CMR348-T301-0.5 | 336 100 | 43 100 | 7.8 |

# Appendix C        DSC data

(a)



(b)
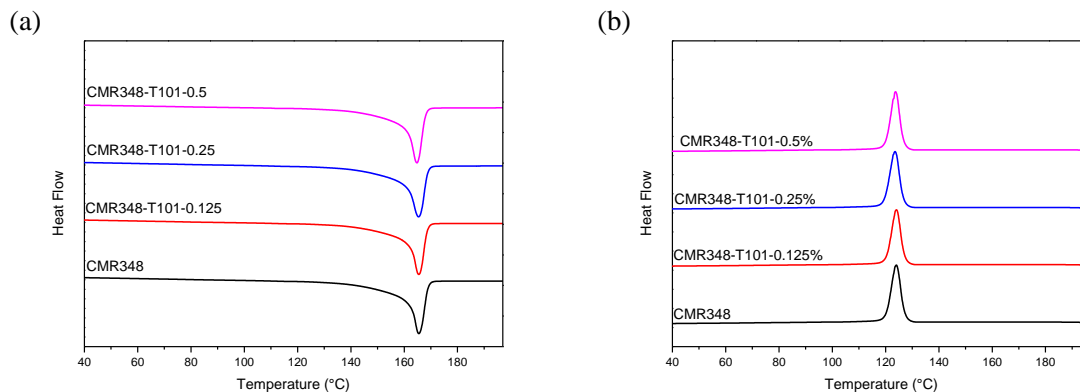


Figure C.1    DSC curves of the CMR348 bulk samples treated with Trigonox®101 at different concentrations

(a)



(b)
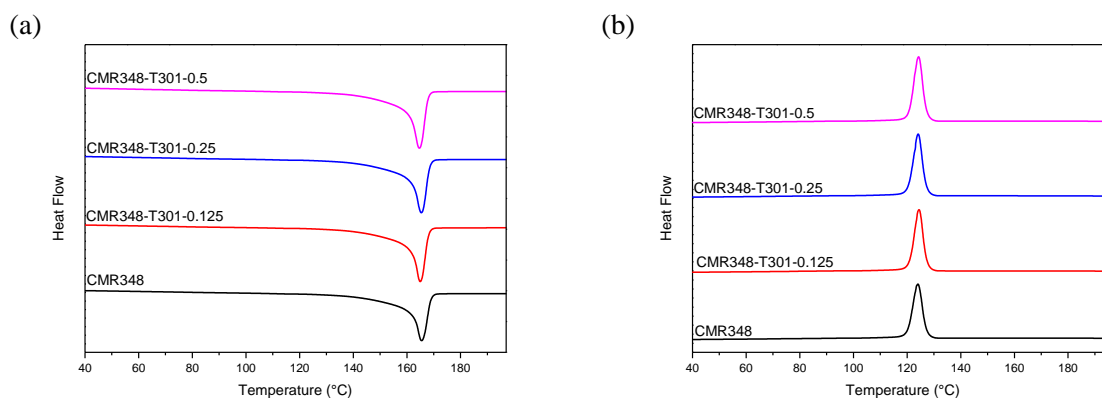


Figure C.2    DSC curves of the CMR348bulk samples treated with Trigonox®301 at different concentrations

Table C.1    DSC data of 100 °C TREF fraction belonging to the CMR648 sample, before and after treatment with Trigonox®101 and Trigonox®301

| Sample | $T_c$ (°C) | $T_m$ (°C) |
|---|---|---|
| CMR648-100 | 103 / 114. | 120 / 156 / 163 |
| CMR648-100-T101-0.25 | 103 / 114 | 118 / 153 / 161 |
| CMR648-100-T301-0.25 | 104 / 114 | 119 / 154 / 161 |

Table C.2    DSC data of the 130 °C fraction belonging to the CMR648 sample, before and after treatment with Trigonox®101 and Trigonox®301

| Sample | $T_c$ (°C) | $T_m$ (°C) |
|---|---|---|
| CMR648-130 | 115 | 163 |
| CMR648-130-T101-0.25 | 115 | 163 |
| CMR648-130-T301-0.25 | 116 | 163 |

Table C.3    DSC data of the 100 °C fraction belonging to the CMR348 sample, before and after treatment with Trigonox®101 and Trigonox®301

| Sample | $T_c$ (°C) | $T_m$ (°C) |
|---|---|---|
| CMR348-100 | 99 / 115 | 114 / 156 / 161 |
| CMR348-100-T101-0.25 | 100 / 113 | 116 / 153 / 160 |
| CMR348-100-T301-0.25 | 98 / 114 | 117 / 162 |

Table C.4    DSC data of the 130 °C fraction belonging to the CMR348 sample, before and after treatment with Trigonox®101 and Trigonox®301

| Sample | $T_c$ (°C) | $T_m$ (°C) |
|---|---|---|
| CMR348-130 | 114 | 163 |
| CMR348-130-T101-0.25 | 115 | 162 |
| CMR348-130-T301-0.25 | 115 | 164 |

Table C.5        DSC data of untreated TREF fractions belonging to the CMR648 sample

| Sample | $T_c$ (°C) | $T_m$ (°C) |
|---|---|---|
| CMR648-30 | - | - |
| CMR648-100 | 103/ 114 | 120/ 156/ 163 |
| CMR648-130 | 115 | 163 |

Table C.6        DSC data of untreated TREF fractions belonging to the CMR348 sample

| Sample | $T_c$ (°C) | $T_m$ (°C) |
|---|---|---|
| CMR348-30 | - | - |
| CMR348-100 | 99 / 115 | 114 / 156 / 161 |
| CMR348-130 | 114 | 163 |

# Appendix D        NMR data
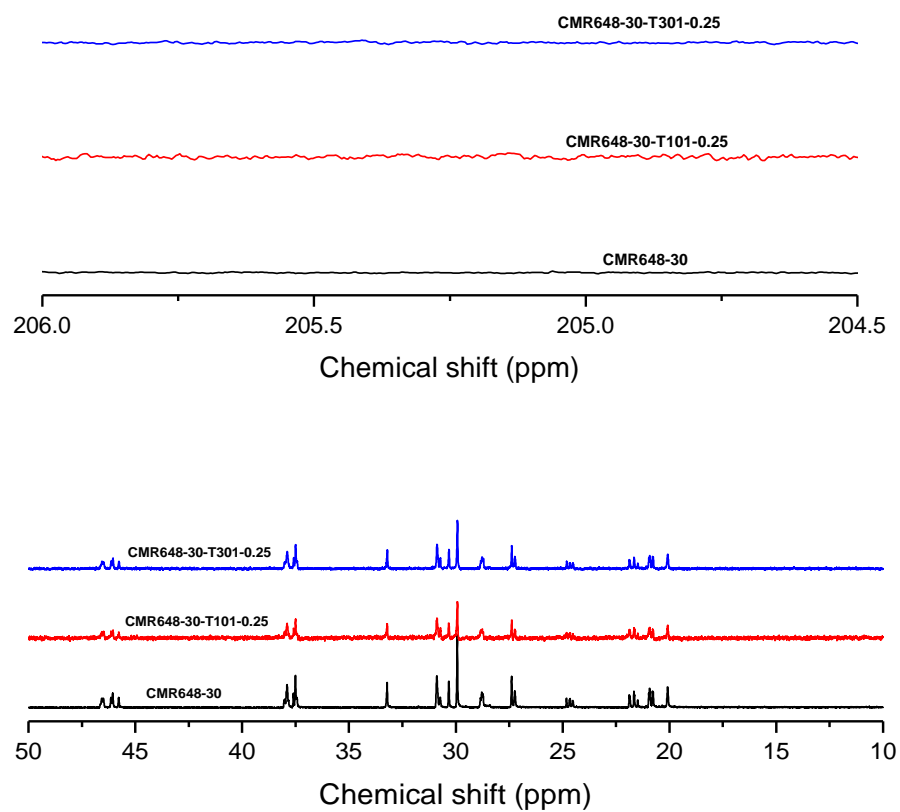


Figure D.1      $^{13}$C NMR spectra of the 30°C fraction belonging to the CMR648 sample, before after treatment with Trigonox®101 and Trigonox®301
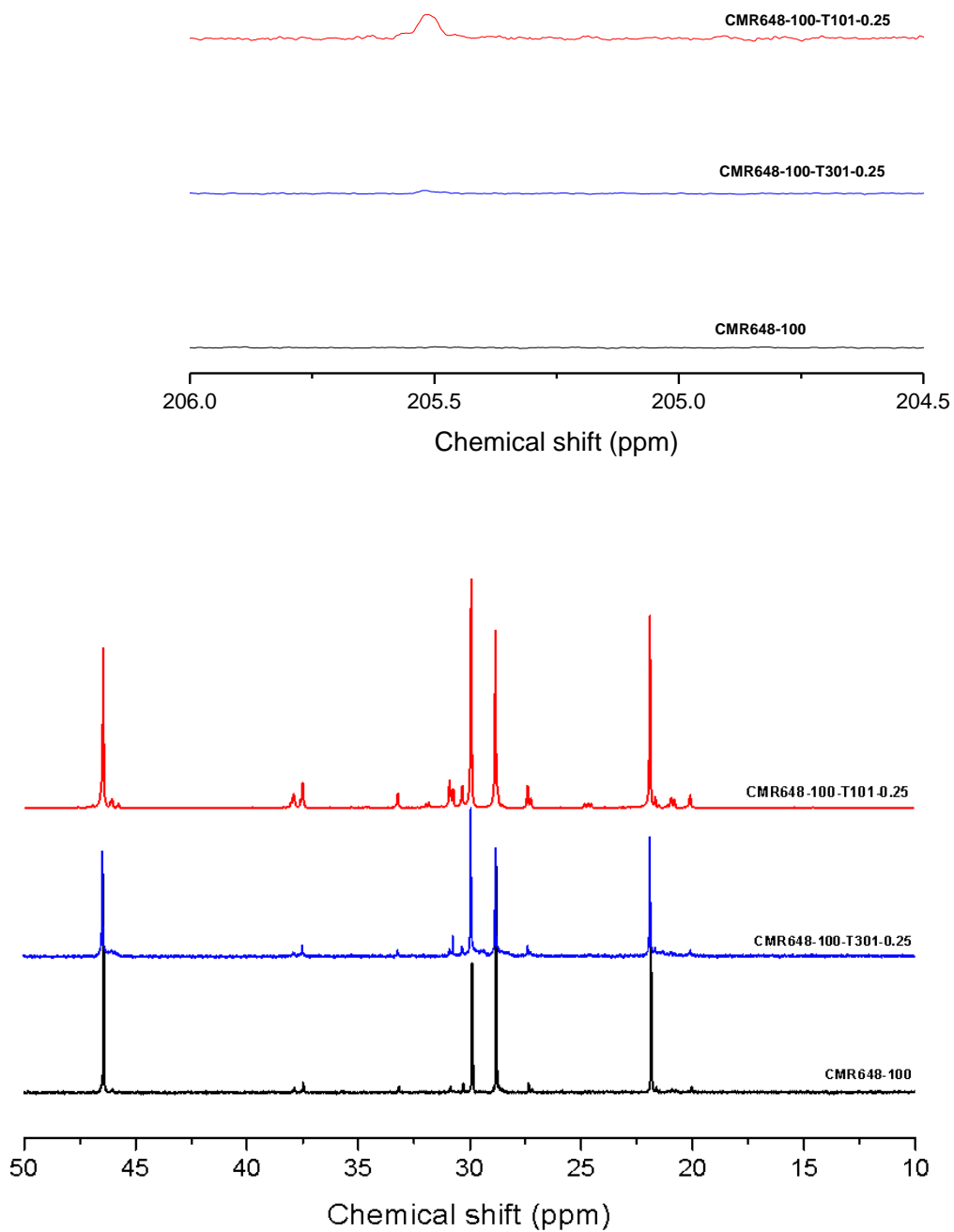
Figure D.2    $^{13}$C NMR spectra of the 100°C fraction belonging to the CMR648 sample, before and after treatment with Trigonox®101 and Trigonox®301
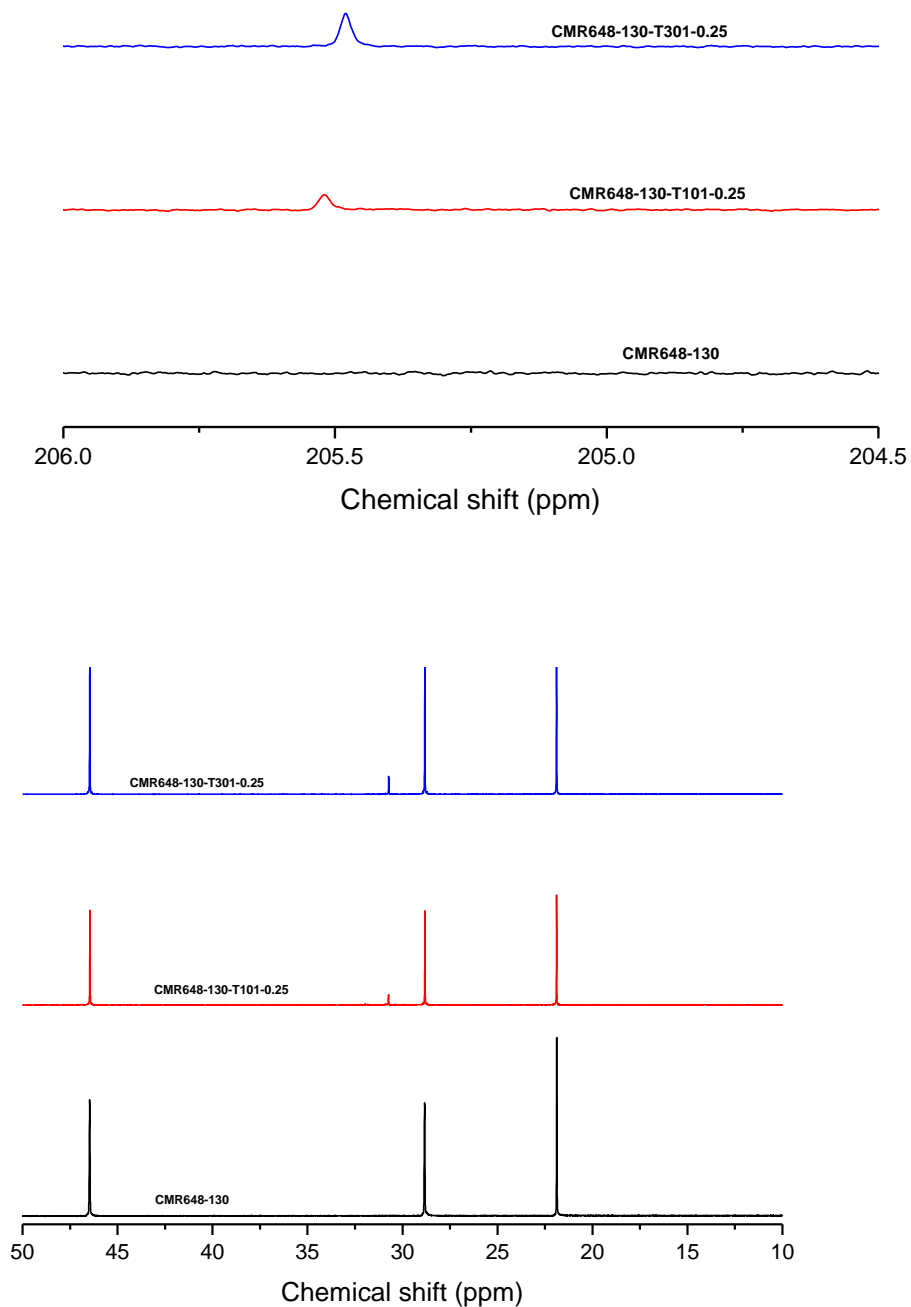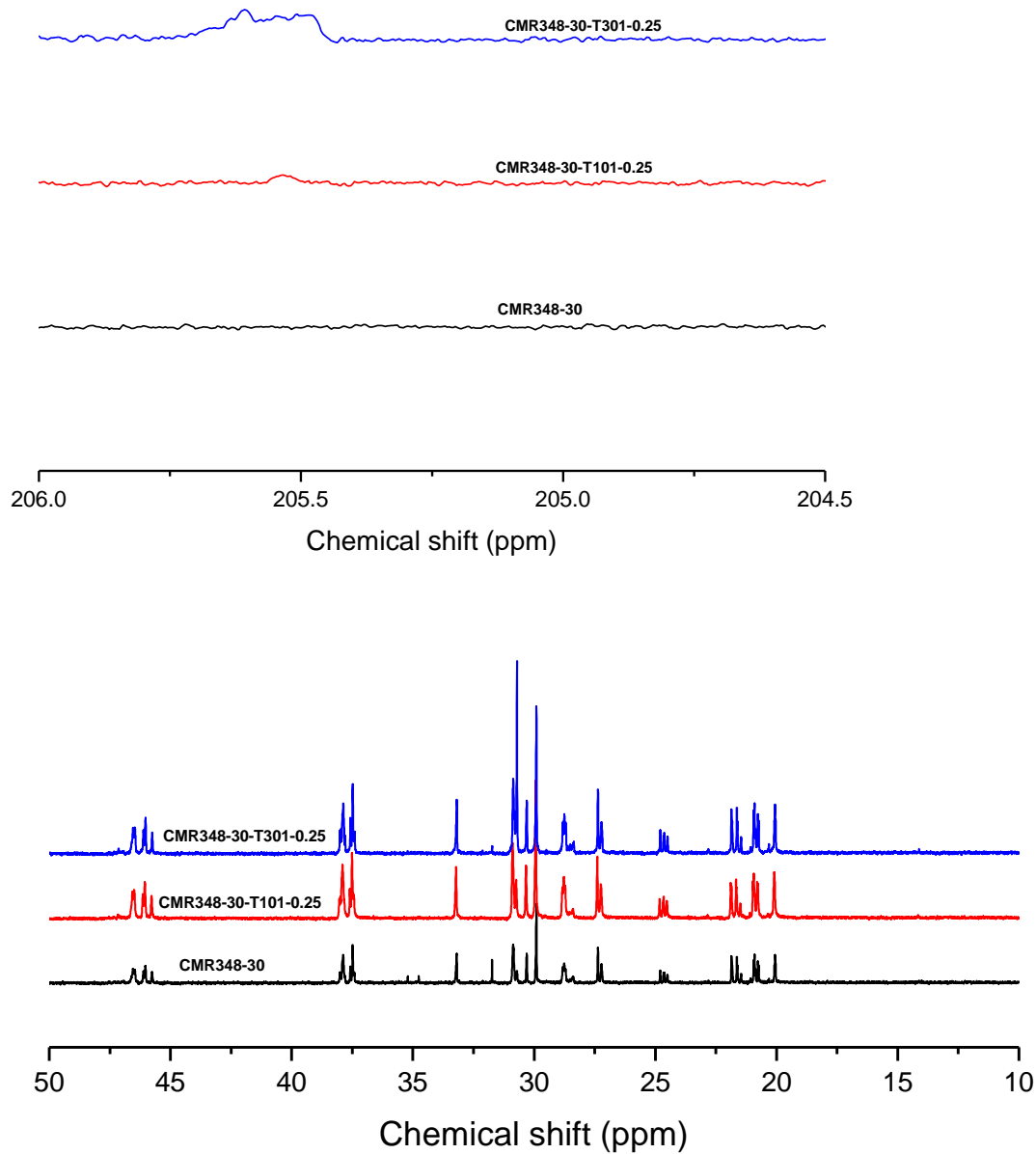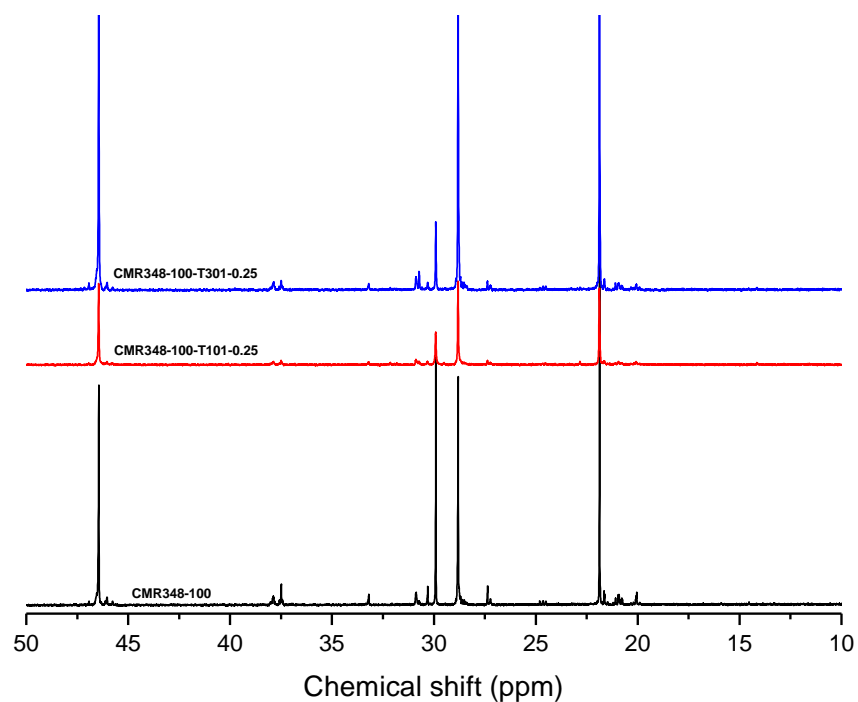
Figure D.3    $^{13}$C NMR spectra of the 130°C fraction belonging to the CMR648 sample, before and after treatment with Trigonox®101 and Trigonox®301

Figure D.4    $^{13}$C NMR spectra of the 30°C fraction belonging to the CMR348 sample, before and after treatment with Trigonox®101 and Trigonox®301
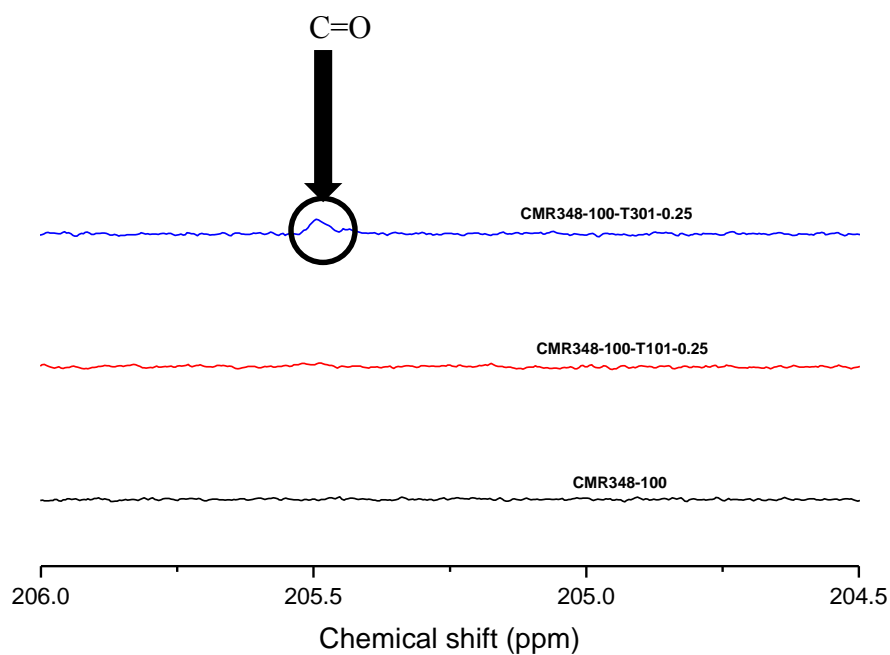
Figure D.5    $^{13}$C NMR spectra of the 100°C fraction belonging to the CMR348 sample, before and after treatment with Trigonox®101 and Trigonox®301

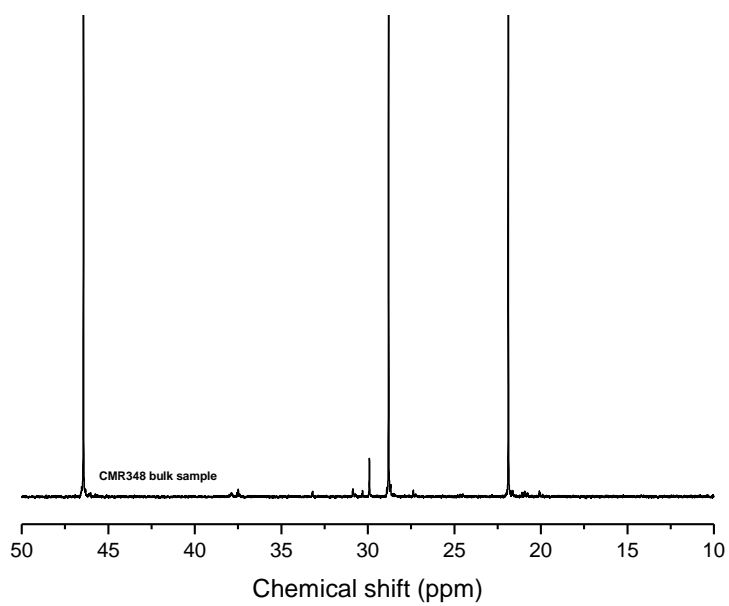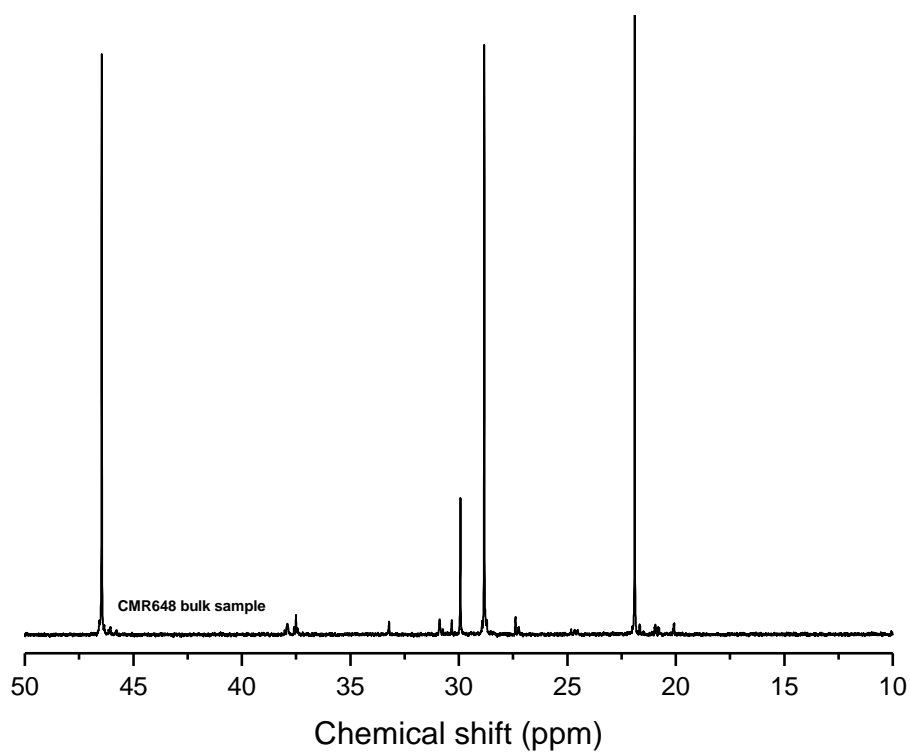Figure D.6        $^{13}$C NMR spectra of the CMR348 bulk sample

Figure D.7        $^{13}$C NMR spectra of the CMR648 bulk sample